

# Spatio-temporal correlations in turbulence from functional renormalisation group

Léonie Canet<sup>1, 2†</sup>

<sup>1</sup>Université Grenoble Alpes, CNRS, LPMMC, 38000 Grenoble, France.

<sup>2</sup>Institut Universitaire de France, 1 rue Descartes, 75005 Paris, France

Space-time correlations are central objects in the statistical theory of turbulence and their modelling plays a crucial role in many applications. Simple phenomenological arguments, such as the Tennekes-Kraichnan random sweeping hypothesis, has proven particularly useful in this respect. However, it remains to be explained how such a simple description can emerge from the highly complex multi-scale nature of turbulence. Recently, the functional renormalisation group (FRG) has rooted important progress in this direction for homogeneous isotropic and stationary turbulence. Indeed, it has allowed for the rigorous derivation, from the Navier-Stokes equation, of an analytical expression for any Eulerian multi-point multi-time correlation function in the limit of large wavenumbers. The corresponding expression for the two-point function confirms the effect of sweeping at small time-delays and yields its precise form, while it unveils a crossover to another regime at large time delays characterised by a slower decay. Moreover, the description of the spatio-temporal behaviour is extended for all  $n$ -point correlation functions. In this paper, we propose an overview of these results and more generally of the FRG method for turbulence. We give a basic introduction to the FRG and emphasise how the field-theoretical framework allows one to systematically and profoundly exploit the symmetries. We show the existence of a fixed-point which controls turbulence for large-scale forcing, which is accessible owing to the non-perturbative nature of the FRG. The major part of the paper is devoted to expounding the spatio-temporal behaviour of correlation functions, and largely illustrating these results through the analysis of direct numerical simulations of homogeneous isotropic turbulence, and also scalar turbulence.

## 1. Introduction

This *JFM Perspectives* proposes a guided tour through the recent achievements and open prospects of Functional Renormalisation Group (FRG) methods applied to the problem of turbulence. The general objective of field-theoretical methods in this field is to build the statistical theory of turbulence “from first principles”, which means from the fundamental hydrodynamical equations, with as little phenomenological inputs as possible. In this respect, focusing on stationary, homogeneous and isotropic turbulence, two unsolved and challenging issues stand out. One of them concerns the spatial (equal-times) properties of turbulence, in particular the calculation of structure functions and their anomalous exponents, the other concerns its temporal properties, through the calculation of multi-(space)point, multi-time

† Email address for correspondence: leonie.canet@grenoble.cnrs.fr

correlation functions. While the FRG has not yet contributed in solving the former, it has brought an important progress for the latter, yielding an explicit expression for  $n$ -point Eulerian correlation functions at large wavenumbers. This result is one of the main topics of this paper. We hence start by a brief overview of spatio-temporal correlations in turbulence.

One of the earliest insights on the temporal behaviour of correlations was provided by Taylor's celebrated analysis of single particle dispersion in an isotropic turbulent flow Taylor (1922). The typical time scale for energy transfers in the turbulent energy cascade can be determined based on Kolmogorov original similarity hypothesis. Assuming a constant energy flux throughout the scales forming the inertial range, one deduces from dimensional analysis that the time for energy transfer from an eddy of size  $k^{-1}$  to smaller eddies scales as  $\tau \sim k^{-2/3}$ , which corresponds to the local eddy turnover time. This scaling is associated with straining, and leads in particular to a frequency spectrum  $E(\omega) \sim \omega^{-2}$ . However, another mechanism, referred to as sweeping, was identified by Heisenberg Heisenberg (1948) and consists in the passive advection of small-scale eddies, without distortion, by the random large-scale eddies, even in the absence of mean flow. This effect introduces a new scale, the root-mean-square velocity  $U_{\text{rms}}$ , related to the large-scale motion, in the dimensional analysis and yields a typical time scale for sweeping  $\tau \sim (U_{\text{rms}}k)^{-1}$ . It then follows that the frequency energy spectrum should scale as  $E(\omega) \sim \omega^{-5/3}$ . The question arises as to which of the two mechanisms dominate the Eulerian correlations, and phenomenological arguments Tennekes (1975) suggest that it is the latter, which means that the small-scale eddies are swept faster than they are distorted by the turbulent energy cascade. This conclusion has been largely confirmed by numerical simulations Orszag & Patterson (1972); Gotoh *et al.* (1993); Kaneda *et al.* (1999); He *et al.* (2004); Favier *et al.* (2010). In particular, the  $\omega^{-5/3}$  frequency spectrum is observed in the Eulerian framework, whereas the  $\omega^{-2}$  spectrum emerges in the Lagrangian framework, which is devoided of sweeping Chevillard *et al.* (2005); L  v  que *et al.* (2007).

Several theoretical attempts were made to calculate the effect of sweeping on the Eulerian spatio-temporal correlations. Kraichnan obtained from a simple model of random advection that the two-point velocity correlations should behave as a Gaussian in the variable  $kt$ , where  $k$  is the wavenumber and  $t$  the time delay Kraichnan (1964). In a nutshell, assuming that the velocity field can be decomposed into a large-scale slowly varying component  $\mathbf{U}$  and a small-scale fluctuating one  $\mathbf{u}$  as  $\mathbf{v} \simeq \mathbf{U} + \mathbf{u}$  with  $|\mathbf{u}| \ll |\mathbf{U}|$ , and assuming that the two components are statistically independent, one arrives at the simplified advection equation  $\partial_t \mathbf{u} + \mathbf{U} \cdot \nabla \mathbf{u} = 0$ , for scales in the inertial range, *i.e.* neglecting forcing and dissipation. This linear equation can be solved in Fourier space and one obtains  $\langle \mathbf{u}(t, \mathbf{k}) \cdot \mathbf{u}(0, -\mathbf{k}) \rangle \propto \exp(-\frac{1}{2}Uk^2t^2)$ , which is the anticipated Gaussian, and corroborates the sweeping time scale  $\tau \sim (Uk)^{-1}$ . However, the previous assumptions cannot be justified for the full Navier-Stokes (NS) equation, so it is not clear a priori whether this should be relevant for real turbulent flows.

Correlation functions were later analyzed using Taylor expansion in time in Ref. Kaneda (1993); Kaneda *et al.* (1999), which yields results compatible with the sweeping time scale  $k^{-1}$  for two-point Eulerian correlations, and the straining time scale  $k^{-2/3}$  for Lagrangian ones. The random sweeping hypothesis has been used in several approaches, such as the modelling of space-time correlations within the elliptic model He & Zhang (2006); Zhao & He (2009) or in models of wavenumber-frequency spectra Wilczek & Narita (2012). Beyond phenomenological arguments, more recently, band-pass filtering techniques were applied to the NS equation, and confirmed the dominant contribution of sweeping in the Eulerian correlations Drivas *et al.* (2017). Very few works were dedicated to the study of multi-point multi-time correlation functions, and only within the quasi-Lagrangian framework L'vov *et al.* (1997); Biferale *et al.* (2011) or within the multifractal approach

Biferale *et al.* (1999). We refer to Wallace (2014) for a general review on space-time correlations in turbulence.

A closely related problem is the nature of space-time correlations of passive scalar fields transported by a turbulent flow. The scalar field can represent temperature or moisture fluctuations, pollutant or virus concentrations, *etc.* . . . , which are transported by a turbulent flow. The scalar is termed passive when it does not affect the carrier flow. This absence of back-reaction is of course an approximation which only holds at small enough concentration and particle size. Understanding the statistical properties of scalar turbulence plays a crucial role in many domains ranging from natural processes to engineering (see e.g. Ref. Shraiman & Siggia (2000); Falkovich *et al.* (2001); Sreenivasan (2019) for reviews). The modelling of the scalar spatio-temporal correlations lies at the basis of many approaches in turbulence diffusion problems Mazzino (1997). Regarding the relevant time scales, the effect of sweeping for the scalar field was early discussed in Ref. Chen & Kraichnan (1989), and its importance was later confirmed in several numerical simulations Yeung & Sawford (2002); O’Gorman & Pullin (2004) and also experiments of Rayleigh-Bénard convection He & Tong (2011).

Of course, one of the major difficulties, which has hindered decisive progress, arises from the non-linear and non-local nature of the hydrodynamical equations. In terms of correlation functions, it implies that the equation for a given  $n$ -point correlation function – *i.e.* the correlation of  $n$  fields evaluated at  $n$  different space-time points – depends on higher-order correlations, and one faces the salient closure problem of turbulence. In order to close this hierarchy, one has to devise some approximation, and many different schemes have been proposed, such as, to mention a few, the Direct Interaction Approximation (DIA) elaborated by Kraichnan (1964), approaches based on quasi-normal hypothesis, in particular the eddy damped quasi-normal Markovian (EDQNM) model Lesieur (2008), or the local energy transfer (LET) theory McComb & Yoffe (2017), we refer to Ref. Zhou (2021) for a recent review. In this context, field-theoretical and Renormalisation Group (RG) approaches offer *a priori* a systematic framework to study correlation functions, allowing one in principles to devise controlled approximation schemes. Although this program has been largely stymied within the standard perturbative RG framework (see Sec. 2), it turned out to be fruitful within the functional and non-perturbative formulation of the RG.

Indeed, the FRG was shown to provide for homogeneous isotropic turbulence the suitable framework to achieve a controlled closure for any  $n$ -point Eulerian correlation function, which becomes asymptotically exact in the limit of large wavenumbers. This closure allows one to establish the explicit analytical expression of the spatio-temporal dependence of any generic  $n$ -point correlation function in this limit. The main merit of this result is to demonstrate on a rigorous basis, from the NS equations, that the sweeping mechanism indeed dominates Eulerian correlations, and moreover to provide its exact form at large wavenumbers. Thereby, the phenomenological evidence for sweeping is endowed with a very general and systematic expression, extended to any  $n$ -point correlation functions. Remarkably, the expression obtained from FRG also carries more information, and predicts in particular a change of behaviour of the Eulerian correlations at large-time delays. In this regime, another time scale emerges, which scales as  $\tau \sim k^{-2}$  and can therefore be called diffusive time scale. The temporal decay of the correlations hence exhibit a crossover from a fast Gaussian decrease at small time delays to a slower exponential one at large time delays. All these results are largely explained and illustrated throughout the paper.

The objective of this *JFM Perspectives* is three-fold: to provide a comprehensive introduction on the basic settings of the FRG for turbulence, and more importantly on the essential ingredients, in particular symmetries, that enter approximation schemes in this framework. The underlying hypotheses are clearly stated to highlight the range of validity of the different

results presented. This more technical part is expounded in Sec. 3 to Sec. 6. The second objective is to explain the physical implications of these results, by comparing them with actual data and observations from experiments and Direct Numerical Simulations (DNS), which is the purpose of Sec. 7 and Sec. 8. The last objective is to point out the main prospects for which FRG methods could provide a valuable tool. Thus, there can be different level of reading of this paper, one can first focus on the concrete outcomes of FRG illustrated in Sec. 7 and Sec. 8, deferring the more technical aspects.

In details, the paper is organised as follows. We start in Sec. 2 by stressing why RG should be useful to study turbulence. We explain in Sec. 3 how one can represent stochastic fluctuations as a path integral, to arrive at the field theories for NS turbulence and passive scalar turbulence. A key advantage of this formulation is that it provides a framework to deeply exploit the symmetries. We show in Sec. 3.3 how one can derive exact identities relating different correlation functions from symmetries, or extended symmetries of the field theory. These identities include well-known relations such as the Kármán-Howarth or Yaglom relations ( Sec. 3.4), but are far more general. The FRG framework is introduced in Sec. 4 with the standard approximation schemes used within this framework. We then present in Sec. 5 a first important result ensuing from this approach, which is the existence of a fixed-point corresponding to the turbulent steady-state for usual forcing concentrated at large scales. The main achievement following from FRG methods is addressed in Sec. 6, namely the derivation of the formal general expression of  $n$ -point spatio-temporal correlation functions at large wavenumbers. The rest of the paper is dedicated to illustrating these results, for NS turbulence in Sec. 7, and for passive scalar turbulence in Sec. 8. Another result, concerning the form of the kinetic energy spectrum in the near-dissipation range of scale is briefly mentioned in Sec. 7.4. Perspectives are discussed in Sec. 9.

## 2. Scale invariance and the Renormalisation Group

### 2.1. Why Renormalisation Group ?

The aim of statistical physics is to determine from a fundamental theory at the microscopic scale the effective behaviour at the macroscopic scale of the system, comprising a large number  $\sim N_A$  of particles (in a broad sense). This requires to average over stochastic fluctuations (thermal, quantum, *etc.* . . ). When the fluctuations are Gaussian, and elementary constituents are non-interacting, central limit theorem applies and allows one to perform the averaging. However, when the system becomes strongly correlated, this procedure fails since the constituents are no longer statistically independent. This problem appeared particularly thorny for critical phenomena, and have impeded for long progress in their theoretical understanding. Indeed, at a second order phase transition, the correlation length of the system diverges, which means that all the degrees of freedom are correlated and fluctuations develop at all scales. The divergence of the correlation length leads to the quintessential property of scale invariance, characterised by universal scaling laws, with anomalous exponents, *i.e.* exponents not complying with dimensional analysis.

The major breakthrough to understand the physical origin of this anomalous behaviour, and primarily to compute it, was achieved with the RG. Although the RG had already been used under other forms in high-energy physics, it acquired its plain physical meaning from the work of K. Wilson & Kogut (1974). The RG provides the tool to perform the average over fluctuations, whatever their nature, even in the presence of strong correlations, and thereby to build the effective theory at large scale from the microscopic one. One of the key feature of the RG is that all the useful information is encoded in the RG flow itself, *i.e.* in the differential equation describing the change of the system under a change of

scale. In particular, a critical point, associated with scale invariance, corresponds by essence to a fixed-point of the RG flow. Let us notice that the notion of large scale is relative to the microscopic one, and it depends on the context. For turbulence, the microscopic scale, denoted  $\Lambda^{-1}$ , refers to the scale at which the continuum description of a fluid, in terms of NS equation, is valid, say the order of the mean-free-path in the fluid (much smaller than the Kolmogorov scale  $\eta$ ). The “large” scale of the RG then refers to typical scales at which the behavior of the fluid is observed, *i.e.* inertial or dissipation ranges, thus including the usual “small” scales of turbulence.

The analogy between critical phenomena and turbulence is striking. Indeed, when turbulence is fully developed, one observes in the inertial range universal behaviours, described by scaling laws with anomalous critical exponents, akin to an equilibrium second-order phase transition. As the RG had been so successful in the latter case, it early arose as the choice candidate to tackle the former. Concomitantly, the RG was extended to study not only the equilibrium but also the dynamics of systems Martin *et al.* (1973); Janssen (1976); de Dominicis (1976), and the first implementations of the “dynamical RG” to study turbulence date back to the early eighties Forster *et al.* (1977); DeDominicis & Martin (1979); Fournier & Frisch (1983). However, the formulation of the RG has remained for long intimately linked with perturbative expansions, relying on the existence of a small parameter. This small parameter is generically chosen as the distance  $\varepsilon = d_c - d$  to an upper critical dimension  $d_c$ , which is the dimension where the fixed-point becomes Gaussian, and the interaction coupling vanishes. In the paradigmatic example of the  $\phi^4$  theory which describes the second-order phase transition in the Ising universality class, the interaction coupling  $g$  has a scaling dimension  $L^{d-4}$ . Thus it vanishes in the  $L \rightarrow \infty$  limit for  $d \geq d_c = 4$ , which means that fluctuations become negligible and the mean-field approximation suffices to provide a reliable description. The Wilson-Fisher fixed-point describing the transition below  $d_c$  can then be captured by a perturbative expansion in  $\varepsilon = d_c - d$  and the coupling  $g$ .

In contrast, in turbulence, the “interaction” is the non-linear advection term, whose “coupling” is unity, *i.e.* it is not small, and does not vanish in any dimension. Thus, one lacks a small parameter to control perturbative expansion. The usual strategy is to introduce an artificial parameter  $\varepsilon$  through a forcing with power-law correlations behaving in wavenumber space as  $p^{4-d-2\varepsilon}$ , *i.e.* applying a forcing on all scales. Fully developed turbulence in  $d = 3$  should then correspond to an infrared (IR) dominated spectrum of the stirring force, as it occurs for  $\varepsilon \geq 2$ , hence for large values for which the extrapolation of the perturbative expansions is fragile. Moreover, one finds an  $\varepsilon$ -dependent fixed-point, with an energy spectrum  $E(p) \propto p^{1-4\varepsilon/3}$ . The K41 value is recovered for  $\varepsilon = 2$ , but this value should somehow freeze for  $\varepsilon$  larger than 2, and such a freezing mechanism can only be invoked within the perturbative analysis Fournier & Frisch (1983). It is worth noting that the perturbative RG analysis allows one to correctly describe the regime  $\varepsilon \leq 3/2$ , which corresponds to a regime dominated by real-space local interactions Mejía-Monasterio & Muratore-Ginanneschi (2012). Not only recovering the K41 spectrum turned out to be difficult within this framework, but the first RG analyses also failed to capture the sweeping effect Yakhot *et al.* (1989); Chen & Kraichnan (1989); Nelkin & Tabor (1990), and led to the conclusion that one should go to a quasi-Lagrangian framework to obtain a reliable description L’vov & Procaccia (1995); L’vov *et al.* (1997). However, the difficulties encountered were severe enough to thwart progress in this direction. We refer to Smith & Woodruff (1998); Adzhemyan *et al.* (1999); Zhou (2010) for reviews of these developments.

In the meantime, a novel formulation of the RG has emerged, which allows for non-perturbative approximation schemes, and thereby bypasses the need of a small parameter. The FRG is a modern implementation of Wilson’s original conception of the RG Wilson & Kogut

(1974). It was formulated in the early nineties Wetterich (1993); Morris (1994); Ellwanger (1994), and widely developed since then Berges *et al.* (2002); Kopietz *et al.* (2010); Delamotte (2012); Dupuis *et al.* (2021). One of the noticeable features of this formalism is its versatility, as testified by its wide range of applications, from high-energy physics (QCD and quantum gravity) to condensed matter (fermionic and bosonic quantum systems) and classical statistical physics, including non-equilibrium classical and quantum systems or disordered ones. We refer the interested reader to Dupuis *et al.* (2021) for a recent review. This led to fertile methodological transfers, borrowing from an area to the other. The FRG was moreover promoted to a high-precision method, since it was shown to yield for the archetypical three-dimensional Ising model results for the critical exponents competing with the best available estimates in the literature Balog *et al.* (2019), and to the most precise ones for the  $O(N)$  models in general De Polsi *et al.* (2020, 2021).

The FRG has been applied to study turbulence in several works Tomassini (1997); Mejía-Monasterio & Muratore-Ginanneschi (2012); Barbi & Münster (2013); Canet *et al.* (2016, 2017); Tarpin *et al.* (2018, 2019); Pagani & Canet (2021), including a study of decaying turbulence within a perturbative implementation of the FRG Fedorenko *et al.* (2013). This method has turned out to be fruitful in this context, which motivates this contribution.

## 2.2. Hydrodynamical equations

The starting point of field-theoretical methods is the fundamental hydrodynamical description of a fluid, given by NS equation

$$\partial_t v_\alpha + v_\beta \partial_\beta v_\alpha = -\frac{1}{\rho} \partial_\alpha p + \nu \nabla^2 v_\alpha + f_\alpha \quad (2.1)$$

where the velocity field  $\mathbf{v}$ , the pressure field  $p$ , and the external force  $\mathbf{f}$  depend on the space-time coordinates  $(t, \mathbf{x})$ , and with  $\nu$  the kinematic viscosity and  $\rho$  the density of the fluid. We focus in this review on incompressible flows, satisfying

$$\partial_\alpha v_\alpha = 0. \quad (2.2)$$

The external stirring force is introduced to maintain a stationary turbulent state. Since the small-scale properties are expected to be universal with respect to the large-scale forcing, it can be chosen as a stochastic force, with a Gaussian distribution, of zero average and covariance

$$\langle f_\alpha(t, \mathbf{x}) f_\beta(t', \mathbf{x}') \rangle = 2\delta(t - t') N_{\alpha\beta} \left( \frac{|\mathbf{x} - \mathbf{x}'|}{L} \right), \quad (2.3)$$

where  $N$  is concentrated around the integral scale  $L$ .

We also consider a passive scalar field  $\theta(t, \mathbf{x})$  advected by a turbulent flow. The dynamics of the scalar is governed by the advection-diffusion equation

$$\partial_t \theta + v_\beta \partial_\beta \theta - \frac{\kappa_\theta}{2} \nabla^2 \theta = f_\theta, \quad (2.4)$$

where  $\kappa_\theta$  is the molecular diffusivity of the scalar, and  $f_\theta$  is an external stirring force acting on the scalar, which can also be chosen Gaussian distributed with zero mean and covariance

$$\langle f_\theta(t, \mathbf{x}) f_\theta(t', \mathbf{x}') \rangle = 2\delta(t - t') M \left( \frac{|\mathbf{x} - \mathbf{x}'|}{L_\theta} \right), \quad (2.5)$$

with  $L_\theta$  the integral scale of the scalar.

Both equations (2.1) and (2.4) yield for some parameters a turbulent regime, where the velocity, pressure, or scalar fields undergo rapid and random variations in space and time.

One must account for these fluctuations to build a statistical theory of turbulence. A natural way to achieve this is via a path integral, which includes all possible trajectories weighted by their respective probability. How to write such a path integral is explained in Sec. 3.1.

### 3. Field theoretical formalism for turbulence

#### 3.1. Path integral representation of a stochastic dynamical equation

The random forcing in the NS equation (2.1) acts as a noise source, and thus the stochastic NS equation is formally equivalent to a Langevin equation. The fundamental difference is that, in usual Langevin description, the origin of the noise lies at the microscopic scale, it is introduced to model some microscopic collision processes, and one is usually interested in the statistical properties of the system at large scales. In the stochastic NS equation, the randomness is introduced at the integral scale, and one is interested in the statistical properties of the system at small scales (but large with respect to the microscopic scale  $\Lambda$ ).

Despite this conceptual difference, in both cases, the dynamical fields are fluctuating ones, and there exists a well-known procedure to encompass all the stochastic trajectories within a path integral, which is the Martin–Siggia–Rose–Janssen–de Dominicis (MSRJD) formalism, Martin *et al.* (1973); Janssen (1976); de Dominicis (1976). The idea is simple, and since it is the starting point of all the subsequent analysis, it is useful to describe the procedure for a scalar field  $\varphi(t, \mathbf{x})$ , following the generic Langevin equation

$$\partial_t \varphi(t, \mathbf{x}) = -\mathcal{F}[\varphi(t, \mathbf{x})] + \eta(t, \mathbf{x}), \quad (3.1)$$

where  $\mathcal{F}$  represents the deterministic forces and  $\eta$  the stochastic noise. This equation can be supplemented by  $m$  additional dynamical constraints of the form

$$C_\ell[\varphi(t, \mathbf{x})] = 0 \quad \ell = 1, \dots, m, \quad (3.2)$$

where  $\mathcal{F}$  and  $C$  are functionals of the fields and their spatial derivatives. The noise has a Gaussian distribution with zero average and a correlator of the form

$$\langle \eta(t, \mathbf{x}) \eta(t', \mathbf{x}') \rangle = 2\delta(t - t') D(|\mathbf{x} - \mathbf{x}'|). \quad (3.3)$$

Note that the derivation we present can be generalised to include temporal correlations, or a field dependence into the noise correlations (3.3). The path integral representation of the stochastic equation is obtained in the following way. The probability distribution of the trajectories of the field follows from an average over the noise as

$$\mathcal{P}[\varphi] = \int \mathcal{D}\eta \mathcal{P}[\eta] \delta(\varphi - \varphi_\eta) \prod_\ell \delta(C_\ell[\varphi]), \quad (3.4)$$

where  $\varphi_\eta$  is a weak solution of (3.1) for a given realisation of  $\eta$ . A change of variable allows one to replace the constraint  $\varphi - \varphi_\eta = 0$  by the explicit equation of motion

$$\mathcal{G}[\varphi(t, \mathbf{x})] = 0 = \partial_t \varphi(t, \mathbf{x}) + \mathcal{F}[\varphi(t, \mathbf{x})] - \eta(t, \mathbf{x}), \quad (3.5)$$

which introduces the functional Jacobian  $\mathcal{J}[\varphi] = \left| \frac{\delta \mathcal{G}}{\delta \varphi} \right|$ , and leads to

$$\mathcal{P}[\varphi] = \int \mathcal{D}\eta \mathcal{P}[\eta] \mathcal{J}[\varphi] \delta(\mathcal{G}[\varphi]) \prod_\ell \delta(C_\ell[\varphi]). \quad (3.6)$$

Two remarks are in order here. First, existence and uniqueness of weak solutions of (3.1) has been implicitly assumed. For the NS equation, this is a subtle issue from a mathematical viewpoint, and uniqueness may not hold in some cases Buckmaster & Vicol (2017). However,

uniqueness is not strictly required in this derivation, in the sense that for a typical set of initial conditions, there may exist a set of non-unique velocity configurations, provided they are of zero measure. Second, the expression of the Jacobian  $\mathcal{J}[\varphi]$  depends on the discretisation of the Langevin equation (3.1). In the Ito's scheme,  $\mathcal{J}$  is independent of the fields and can be absorbed in the normalisation of  $\mathcal{P}[\varphi]$ , while in the Stratonovich's convention, it depends on the fields, and it can be expressed introducing two Grassmann anti-commuting fields  $\psi$  and  $\bar{\psi}$  as

$$\mathcal{J}[\varphi] = \left| \det \frac{\delta \mathcal{G}(t, \mathbf{x})}{\delta \varphi(t', \mathbf{x}')} \right| = \int \mathcal{D}\psi \mathcal{D}\bar{\psi} e^{\int_{t', \mathbf{x}, \mathbf{x}'} \bar{\psi} \frac{\delta \mathcal{G}}{\delta \varphi} \psi}. \quad (3.7)$$

We shall here mostly use the Ito's discretisation and omit the Jacobian contribution henceforth.

One can then use the Fourier representation of the functional Dirac deltas in Eq. (3.6), introducing  $m + 1$  auxiliary fields  $\bar{c}_\ell$  (collectively denoted as  $\bar{c}$ ) and  $\bar{\varphi}$  which yields

$$\mathcal{P}[\varphi] = \int \mathcal{D}\eta \mathcal{P}[\eta] \mathcal{D}\bar{\varphi} \mathcal{D}\bar{c} e^{-i \int_{t, \mathbf{x}} \{ \bar{\varphi} \mathcal{G}[\varphi] + \bar{c}_\ell C_\ell[\varphi] \}} = \int \mathcal{D}\bar{\varphi} \mathcal{D}\bar{c} e^{-S[\varphi, \bar{\varphi}, \bar{c}]}. \quad (3.8)$$

The second equality stems from the integration over the Gaussian noise, resulting in the action

$$S[\varphi, \bar{\varphi}, \bar{c}] = i \int_{t, \mathbf{x}} \left\{ \bar{\varphi} (\partial_t \varphi + \mathcal{F}[\varphi]) + \bar{c}_\ell C_\ell[\varphi] \right\} + \int_{t, \mathbf{x}, \mathbf{x}'} \bar{\varphi}(t, \mathbf{x}) D(|\mathbf{x} - \mathbf{x}'|) \bar{\varphi}(t, \mathbf{x}'). \quad (3.9)$$

One usually absorbs the complex  $i$  into a redefinition of the auxiliary fields  $\bar{\varphi} \rightarrow -i\bar{\varphi}$ ,  $\bar{c} \rightarrow -i\bar{c}$ , which are also called response fields. The action resulting from the MSRJD procedure exhibits a simple structure. The response fields appear linearly as Lagrange multipliers for the equation of motion and dynamical constraints, while the characteristics of the noise, namely its correlator, are encoded in the quadratic term in  $\bar{\varphi}$ .

The path integral formulation offers a simple way to compute all the correlation and response functions of the model. Their generating functional is defined by

$$\begin{aligned} \mathcal{Z}[J, \bar{J}, \bar{j}] &= \left\langle e^{\int_{t, \mathbf{x}} \{ J \varphi + \bar{J} \bar{\varphi} + \bar{j}_\ell \bar{c}_\ell \}} \right\rangle = \int \mathcal{D}\varphi \mathcal{P}[\varphi] e^{\int_{t, \mathbf{x}} \{ J \varphi + \bar{J} \bar{\varphi} + \bar{j}_\ell \bar{c}_\ell \}} \\ &= \int \mathcal{D}\bar{\varphi} \mathcal{D}\bar{c} \mathcal{D}\varphi e^{-S[\varphi, \bar{\varphi}, \bar{c}] + \int_{t, \mathbf{x}} \{ J \varphi + \bar{J} \bar{\varphi} + \bar{j}_\ell \bar{c}_\ell \}}, \end{aligned} \quad (3.10)$$

where  $J, \bar{J}, \bar{j}$  are the sources for the fields  $\varphi, \bar{\varphi}, \bar{c}$  respectively. Correlation functions are obtained by taking functional derivatives of  $\mathcal{Z}$  with respect to the corresponding sources, e.g.

$$\langle \varphi(t, \mathbf{x}) \rangle = \frac{\delta \mathcal{Z}}{\delta J(t, \mathbf{x})}, \quad (3.11)$$

and functional derivatives with respect to response sources generate response functions (*i.e.* response to an external drive), hence the name ‘‘response fields’’. We shall henceforth use ‘‘correlations’’ in a generalised sense including both correlation and response functions. One usually also considers the functional  $\mathcal{W} = \ln \mathcal{Z}$ , which is the analogue of a Helmholtz free energy at equilibrium. It is the generating functional of connected correlation and response functions, *i.e.* cumulants, for instance,

$$\langle \varphi(t, \mathbf{x}) \varphi(t', \mathbf{x}') \rangle_c \equiv \langle \varphi(t, \mathbf{x}) \varphi(t', \mathbf{x}') \rangle - \langle \varphi(t, \mathbf{x}) \rangle \langle \varphi(t', \mathbf{x}') \rangle = \frac{\delta^2 \mathcal{W}}{\delta J(t, \mathbf{x}) \delta J(t', \mathbf{x}')}. \quad (3.12)$$

More generally, one can obtain a  $n$ -point generalised connected correlation function  $\mathcal{W}^{(n)}$  by

taking  $n$  functional derivatives with respect to either  $J$  or  $\bar{J}$  evaluated at  $n$  different space-time points  $(t_i, \mathbf{x}_i)$  as

$$\mathcal{W}^{(n)}(t_1, \mathbf{x}_1, \dots, t_n, \mathbf{x}_n) = \frac{\delta^n \mathcal{W}}{\delta \mathcal{J}_{i_1}(t_1, \mathbf{x}_1) \cdots \delta \mathcal{J}_{i_n}(t_n, \mathbf{x}_n)}. \quad (3.13)$$

where  $\mathcal{J} = (J, \bar{J})$  and hence  $i_k \in \{1, 2\}$ . It is also useful to introduce another notation  $\mathcal{W}^{(\ell, m)}$ , which specifies that the  $\ell$  first derivatives are with respect to  $J$  and the  $m$  last to  $\bar{J}$ , that is

$$\mathcal{W}^{(\ell, m)}(t_1, \mathbf{x}_1, \dots, t_{\ell+m}, \mathbf{x}_{\ell+m}) = \frac{\delta^{\ell+m} \mathcal{W}}{\delta J(t_1, \mathbf{x}_1) \cdots \delta J(t_\ell, \mathbf{x}_\ell) \delta \bar{J}(t_{\ell+1}, \mathbf{x}_{\ell+1}) \cdots \delta \bar{J}(t_{\ell+m}, \mathbf{x}_{\ell+m})}. \quad (3.14)$$

A last generating functional which plays a central role in field theory and in the FRG framework is the Legendre transform of  $\mathcal{W}$ , *i.e.* the analogue of the Gibbs free energy at equilibrium, defined as

$$\Gamma[\langle \varphi \rangle, \langle \bar{\varphi} \rangle, \langle \bar{c} \rangle] = \sup_{\{J, \bar{J}, \bar{j}\}} \left[ \int_{t, \mathbf{x}} \left\{ J \langle \varphi \rangle + \bar{J} \langle \bar{\varphi} \rangle + \bar{j}_\ell \langle \bar{c}_\ell \rangle \right\} - \mathcal{W}[J, \bar{J}, \bar{j}] \right]. \quad (3.15)$$

$\Gamma$  is called the effective action, it is a functional of the average fields, defined with the usual Legendre conjugate relations

$$\langle \varphi(t, \mathbf{x}) \rangle = \frac{\delta \mathcal{W}}{\delta J(t, \mathbf{x})}, \quad J(t, \mathbf{x}) = \frac{\delta \Gamma}{\delta \langle \varphi(t, \mathbf{x}) \rangle}, \quad (3.16)$$

and similarly for the response fields. From a field-theoretical viewpoint,  $\Gamma$  is the generating functional of one-particle-irreducible correlation functions, also called vertices, obtained by taking functional derivatives of  $\Gamma$  with respect to average fields

$$\Gamma^{(n)}(t_1, \mathbf{x}_1, \dots, t_n, \mathbf{x}_n) = \frac{\delta^n \Gamma}{\delta \Psi_{i_1}(t_1, \mathbf{x}_1) \cdots \delta \Psi_{i_n}(t_n, \mathbf{x}_n)}. \quad (3.17)$$

where  $\Psi = (\langle \varphi(t, \mathbf{x}) \rangle, \langle \bar{\varphi}(t, \mathbf{x}) \rangle)$  and  $i_k \in \{1, 2\}$ . They are also denoted  $\Gamma^{(\ell, m)}$  conforming to the definition (3.14). The vertices constitute the main elements in diagrammatic calculations *à la* Feynman. An important point to be highlighted is that both sets of correlation functions  $\Gamma^{(n)}$  and  $\mathcal{W}^{(n)}$  contain the same information on the statistical properties of the model. Each set can be simply reconstructed from the other *via* a sum of tree diagrams.

To conclude these general definitions, we also consider the Fourier transforms in space and time of all these correlation functions. The Fourier convention, used throughout this paper, is

$$f(\omega, \mathbf{q}) = \int_{t, \mathbf{x}} f(t, \mathbf{x}) e^{-i\mathbf{q} \cdot \mathbf{x} + i\omega t}, \quad f(t, \mathbf{x}) = \int_{\omega, \mathbf{q}} f(\omega, \mathbf{q}) e^{i\mathbf{q} \cdot \mathbf{x} - i\omega t}, \quad (3.18)$$

where  $\int_{\omega, \mathbf{q}} \equiv \int \frac{d^d \mathbf{q}}{(2\pi)^d} \frac{d\omega}{2\pi}$ . Because of translational invariance in space and time, the Fourier transform of a  $n$ -point correlation function, *e.g.*  $\Gamma^{(n)}$ , takes the form

$$\Gamma^{(n)}(\omega_1, \mathbf{p}_1, \dots, \omega_n, \mathbf{p}_n) = (2\pi)^{d+1} \delta \left( \sum_i \omega_i \right) \delta^d \left( \sum_i \mathbf{p}_i \right) \bar{\Gamma}^{(n)}(\omega_1, \mathbf{p}_1, \dots, \omega_{n-1}, \mathbf{p}_{n-1}), \quad (3.19)$$

that is, the total momentum and total frequency are conserved, and the last frequency-momentum arguments  $\omega_n, \mathbf{p}_n$  can be omitted since they are fixed as minus the sum of the others.

### 3.2. Action for Navier-Stokes equation and passive scalars

Applying the MSRJD procedure to the NS equation (2.1) and incompressibility constraint (2.2), one obtains the path integral representation

$$\mathcal{Z}[\mathbf{J}, \bar{\mathbf{J}}, K, \bar{K}] = \int \mathcal{D}\mathbf{v} \mathcal{D}\bar{\mathbf{v}} \mathcal{D}p \mathcal{D}\bar{p} e^{-S_{\text{NS}}[\mathbf{v}, \bar{\mathbf{v}}, p, \bar{p}] + \int_{t,\mathbf{x}} \{ \mathbf{J} \cdot \mathbf{v} + \bar{\mathbf{J}} \cdot \bar{\mathbf{v}} + K p + \bar{K} \bar{p} \}}, \quad (3.20)$$

for the fluctuating velocity and pressure fields and their associated response fields, with the NS action

$$\begin{aligned} S_{\text{NS}}[\mathbf{v}, \bar{\mathbf{v}}, p, \bar{p}] = & \int_{t,\mathbf{x}} \left\{ \bar{p} \partial_{\alpha} v_{\alpha} + \bar{v}_{\alpha} \left[ \partial_t v_{\alpha} - \nu \nabla^2 v_{\alpha} + v_{\beta} \partial_{\beta} v_{\alpha} + \frac{1}{\rho} \partial_{\alpha} p \right] \right\} \\ & - \int_{t,\mathbf{x},\mathbf{x}'} \bar{v}_{\alpha}(t,\mathbf{x}) N_{\alpha\beta} \left( \frac{|\mathbf{x} - \mathbf{x}'|}{L} \right) \bar{v}_{\beta}(t,\mathbf{x}'). \end{aligned} \quad (3.21)$$

In this formulation, we have kept the pressure field and introduced a response field  $\bar{p}$  to enforce the incompressibility constraint. Alternatively, the pressure field can be integrated out using the Poisson equation, such that one obtains a path integral in terms of two fields  $\mathbf{v}$  and  $\bar{\mathbf{v}}$  instead of four, at the price of a resulting action which is non-local Barbi & Münster (2013). We here choose to keep the pressure fields since the whole pressure sector turns out to be very simple to handle, as we show in the following.

We now consider a passive scalar field  $\theta$  transported by a turbulent NS velocity flow according to the advection-diffusion equation (2.4). The associated field theory is simply obtained by adding the two fields  $\theta, \bar{\theta}$  and the two corresponding sources  $j, \bar{j}$  to the field multiplet  $\Phi = (\mathbf{v}, \bar{\mathbf{v}}, p, \bar{p}, \theta, \bar{\theta})$  and source multiplet  $\mathcal{J} = (\mathbf{J}, \bar{\mathbf{J}}, K, \bar{K}, j, \bar{j})$  respectively. The generating functional then reads

$$\mathcal{Z}[\mathcal{J}] = \int \mathcal{D}\Phi e^{-S_{\text{NS}}[\mathbf{v}, \bar{\mathbf{v}}, p, \bar{p}] - S_{\theta}[\theta, \bar{\theta}, \mathbf{v}] + \int_{t,\mathbf{x}} \mathcal{J}_i \Phi_i}, \quad (3.22)$$

with the passive scalar action given by

$$S_{\theta}[\theta, \bar{\theta}, \mathbf{v}] = \int_{t,\mathbf{x}} \bar{\theta} \left\{ \partial_t \theta + v_{\beta} \partial_{\beta} \theta - \frac{\kappa_{\theta}}{2} \nabla^2 \theta \right\} - \int_{t,\mathbf{x},\mathbf{x}'} \bar{\theta}(t,\mathbf{x}) M \left( \frac{|\mathbf{x} - \mathbf{x}'|}{L_{\theta}} \right) \bar{\theta}(t,\mathbf{x}'). \quad (3.23)$$

The two actions (3.21) and (3.23) possess fundamental symmetries, some of which only recently identified. They can be used to derive a set of exact identities relating among each others different correlation functions of the system. These identities, which include as particular cases the Kármán-Howarth and Yaglom relations, contain fundamental information on the system. We provide in the next Sec. 3.3 a detailed analysis of these symmetries, and show how the set of exact identities can be inferred from Ward identities.

### 3.3. Symmetries and extended symmetries

We are interested in the stationary state of fully developed homogeneous and isotropic turbulence. We hence assume translational invariance in space and time, as well as rotational invariance. Besides these symmetries, the NS equation possesses other well-known symmetries, such as the Galilean invariance. In the field-theoretical formulation, these symmetries are obviously carried over, but they are moreover endowed with a systematic framework to be fully exploited. Indeed, the path integral formulation provides the natural tool to express the consequences of the symmetries on the correlation functions of the theory, under the form of exact identities which are called Ward identities.

In fact, the field-theoretical formulation is even more far-reaching, in the sense that the

very notion of symmetry can be extended. A symmetry means an invariance of the model (equation of motion or action) under a given transformation of the fields and space-time coordinates. However, it is useful to also consider transformations that do not leave the model strictly invariant, but which lead to a variation which is at most linear in the fields. In this case, exact relations between correlation functions can also be obtained, and they are endowed with a stronger content, *i.e.* they provide additional constraints. The mechanism is very simple, and can be exemplified in the case of the symmetries of the pressure sector.

### 3.3.1. Local shift symmetries of the pressure fields

An evident symmetry of the NS action (3.21) is the invariance under a time-dependent shift of the pressure field  $p(t, \mathbf{x}) \rightarrow p(t, \mathbf{x}) + \varepsilon(t)$  since the latter only appears with a gradient. Let us now consider instead an infinitesimal time- and space-dependent, *i.e.* fully gauged, shift  $p(t, \mathbf{x}) \rightarrow p(t, \mathbf{x}) + \varepsilon(t, \mathbf{x})$ . This field transformation yields a variation of  $\mathcal{S}_{\text{NS}}$  which is linear in  $\bar{\mathbf{v}}$ . A key observation is that this field transformation is a mere affine change of variable in the functional integral  $\mathcal{Z}$ , so it must leave it unaltered. Performing this change of variable in (3.20) and expanding the exponential to first order in  $\varepsilon$ , one obtains

$$0 = \int_{t, \mathbf{x}} \left\langle -\bar{v}_\alpha(t, \mathbf{x}) \partial_\alpha \varepsilon(t, \mathbf{x}) + K(t, \mathbf{x}) \varepsilon(t, \mathbf{x}) \right\rangle, \quad (3.24)$$

where the first term comes from the variation of the action and the second one from the variation of the source term. Since this equality holds for any arbitrary infinitesimal  $\varepsilon(t, \mathbf{x})$ , one deduces the following Ward identity

$$K(t, \mathbf{x}) = \frac{\delta \Gamma}{\delta \langle p(t, \mathbf{x}) \rangle} = -\frac{1}{\rho} \langle \partial_\alpha \bar{v}_\alpha(t, \mathbf{x}) \rangle = \frac{\delta \mathcal{S}_{\text{NS}}}{\delta p(t, \mathbf{x})} \Big|_{\langle \Phi_k \rangle}, \quad (3.25)$$

where the first equality simply stems from the Legendre conjugate relations. This entails that the dependence of the effective action  $\Gamma$  in the pressure field  $p$  remains the same as the one of the original bare action  $\mathcal{S}_{\text{NS}}$ , *i.e.* it keeps the same form in terms of the average fields  $\frac{1}{\rho} \int_{t, \mathbf{x}} \langle \bar{\mathbf{v}} \rangle_\alpha \partial_\alpha \langle p \rangle$ , or otherwise stated, this term is not renormalised.

The same analysis can be carried over for the response pressure field, by considering the infinitesimal gauged field transformation  $\bar{p}(t, \mathbf{x}) \rightarrow \bar{p}(t, \mathbf{x}) + \bar{\varepsilon}(t, \mathbf{x})$ . This yields the Ward identity

$$\bar{K}(t, \mathbf{x}) = \frac{\delta \Gamma}{\delta \langle \bar{p}(t, \mathbf{x}) \rangle} = \langle \partial_\alpha v_\alpha(t, \mathbf{x}) \rangle = \frac{\delta \mathcal{S}_{\text{NS}}}{\delta \bar{p}(t, \mathbf{x})} \Big|_{\langle \Phi_k \rangle}, \quad (3.26)$$

which means that the corresponding term in the effective action is not renormalised either and keeps its bare form  $\int_{t, \mathbf{x}} \langle \bar{p} \rangle \partial_\alpha \langle v_\alpha \rangle$ . Hence the effective action remains linear in the pressure and response pressure fields, and there are no mixed pressure-velocity vertices beyond quadratic order, *i.e.* no vertices for  $n \geq 3$  with a  $p$  or a  $\bar{p}$  leg. As a consequence, the pressure fields only enter in the propagator, and the whole pressure sector essentially decouples, as will be manifest in the FRG framework.

Since the pressure fields are not renormalised, we use in the following the same notation  $p$  for both the pressure and the average pressure, and similarly  $\bar{p}$  for both the response pressure and its average. This is of course not the case for the velocity sector which contains non-trivial fluctuations, and we use the notation  $\mathbf{u} \equiv \langle \mathbf{v} \rangle$  and  $\bar{\mathbf{u}} \equiv \langle \bar{\mathbf{v}} \rangle$  for the average fields, and generically for the field multiplet  $\Psi \equiv \langle \Phi \rangle$ .

### 3.3.2. Time-dependent Galilean symmetry

A fundamental symmetry of the NS equation is the Galilean invariance, which is the invariance under the global transformation  $\mathbf{x} \rightarrow \mathbf{x}' = \mathbf{x} + \mathbf{v}_0 t$ ,  $\mathbf{v}(t, \mathbf{x}) \rightarrow \mathbf{v}(t, \mathbf{x}') - \mathbf{v}_0$ .

In fact, it was early recognised in the field-theoretical context that a time-dependent, or time-gauged, version of this transformation leads to an extended symmetry of the NS action and useful Ward identities (Adzhemyan *et al.* 1994, 1999; Antonov *et al.* 1996). Considering an infinitesimal arbitrary time-dependent vector  $\varepsilon(t)$ , this transformation reads

$$\begin{aligned}\delta v_\alpha(t, \mathbf{x}) &= -\dot{\varepsilon}_\alpha(t) + \varepsilon_\beta(t) \partial_\beta v_\alpha(t, \mathbf{x}) \\ \delta \Phi_k(t, \mathbf{x}) &= \varepsilon_\beta(t) \partial_\beta \Phi_k(t, \mathbf{x})\end{aligned}\quad (3.27)$$

where  $\dot{\varepsilon}_\alpha = \frac{d\varepsilon_\alpha}{dt}$ , and  $\Phi_k$  denotes any other fields  $\bar{v}, p, \bar{p}, \dots$ . The global Galilean transformation is recovered for a constant velocity  $\dot{\varepsilon}(t) = \mathbf{v}_0$ . Let us provide a simple geometrical interpretation of this transformation. The fields  $\Phi_k$  which transform as  $\delta \Phi_k = \varepsilon_\beta(t) \partial_\beta \Phi_k - i.e.$  vary only due to the change of coordinates – can be termed Galilean scalar densities, in the sense that  $\int_{\mathbf{x}} \Phi_k$  is invariant under this transformation. The sum, product, or  $\nabla_i$  operations on such scalar densities preserves this property. However, the time derivative  $\partial_t$  spoils it, whereas it is preserved by the Lagrangian time derivative  $\partial_t + v_\beta \partial_\beta$  which can thus be identified with the covariant derivative for Galilean transformations.

The overall variation of the NS action under the transformation (3.27) is

$$\delta \mathcal{S}_{\text{NS}} = - \int_{t, \mathbf{x}} \varepsilon_\alpha(t) \partial_t^2 \bar{v}_\alpha(t, \mathbf{x}). \quad (3.28)$$

Hence, writing that this transformation, which is simply a change of variable, leaves the functional integral (3.20) unchanged, one deduces the equality

$$\langle \delta \mathcal{S}_{\text{NS}} \rangle = \left\langle \delta \int_{t, \mathbf{x}} \mathcal{J}_\ell \Phi_\ell \right\rangle = \int_{t, \mathbf{x}} \left\{ -\dot{\varepsilon}_\alpha(t) J_\alpha(t, \mathbf{x}) + \varepsilon_\beta(t) \mathcal{J}_\ell(t, \mathbf{x}) \partial_\beta \Psi_\ell(t, \mathbf{x}) \right\}. \quad (3.29)$$

Since this identity is valid for arbitrary  $\varepsilon(t)$ , one obtains

$$\int_{\mathbf{x}} \left\{ \partial_t J_\alpha(t, \mathbf{x}) + \mathcal{J}_\ell(t, \mathbf{x}) \partial_\alpha \Psi_\ell(t, \mathbf{x}) \right\} = - \int_{\mathbf{x}} \partial_t^2 \bar{u}_\alpha(t, \mathbf{x}), \quad (3.30)$$

which is local in time. In contrast, the identity stemming from the usual Galilean invariance with a constant  $\mathbf{v}_0$  is integrated over time, and the r.h.s. is replaced by zero since the action is invariant under global Galilean transformation. One can rewrite this exact identity as the following Ward identity for the functional  $\Gamma$

$$\int_{\mathbf{x}} \left\{ \partial_t \frac{\delta \Gamma}{\delta u_\alpha} + \partial_\alpha \Psi_\ell \frac{\delta \Gamma}{\delta \Psi_\ell} \right\} = - \int_{\mathbf{x}} \partial_t^2 \bar{u}_\alpha, \quad (3.31)$$

or equivalently for the functional  $\mathcal{W}$

$$\int_{\mathbf{x}} \left\{ \partial_t J_\alpha + \mathcal{J}_\ell \partial_\alpha \frac{\delta \mathcal{W}}{\delta \mathcal{J}_\ell} \right\} = - \int_{\mathbf{x}} \partial_t^2 \frac{\delta \mathcal{W}}{\delta \bar{J}_\alpha}. \quad (3.32)$$

The identities (3.31) and (3.32) are functional in the fields. One can deduce from them, by functional differentiation, an infinite set of exact identities amongst the correlation functions  $\Gamma^{(n)}$  or  $\mathcal{W}^{(n)}$ . Let us express them for the vertices. They are obtained by taking functional derivatives of the identity (3.31) with respect to  $\ell$  velocity and  $m$  response velocity fields,

and setting the fields to zero, which yields in Fourier space:

$$\begin{aligned}
\Gamma_{\alpha\alpha_1\dots\alpha_{\ell+m}}^{(\ell+1,m)}(\omega, \mathbf{p} = \mathbf{0}, \omega_1, \mathbf{p}_1, \dots, \omega_{\ell+m}, \mathbf{p}_{\ell+m}) \\
&= - \sum_{k=1}^{\ell+m} \frac{p_k^\alpha}{\omega} \Gamma_{\alpha_1\dots\alpha_{\ell+m}}^{(\ell,m)}(\omega_1, \mathbf{p}_1, \dots, \omega_k + \omega, \mathbf{p}_k, \dots, \omega_{\ell+m}, \mathbf{p}_{\ell+m}) \\
&\equiv \mathcal{D}_\alpha(\omega) \Gamma_{\alpha_1\dots\alpha_{\ell+m}}^{(\ell,m)}(\omega_1, \mathbf{p}_1, \dots, \omega_{\ell+m}, \mathbf{p}_{\ell+m}), \tag{3.33}
\end{aligned}$$

where the  $\alpha_i$  are the space indices of the vector fields. We refer to Tarpin *et al.* (2018) for details on the derivation. The operator  $\mathcal{D}_\alpha(\omega)$  hence successively shifts by  $\omega$  all the frequencies of the function on which it acts. The identities (3.33) exactly relate an arbitrary  $(\ell+m+1)$ -point vertex function with one vanishing wavevector carried by a velocity field  $u_\alpha$  to a lowered-by-one order  $(\ell+m)$ -point vertex function. It is clear that this type of identity can constitute a key asset to address the closure problem of turbulence, since it precisely requires to express higher-order statistical moments in terms of lower-order ones. Of course, this relation only fixes  $\Gamma^{(\ell+m+1)}$  in a specific configuration, namely baring one vanishing wavevector, so it does not allow one to completely eliminate this vertex, and it is not obvious how it can be exploited. In fact, we will show within the FRG framework that this type of configurations play a dominant role at small scales, and the exact identities (3.33) in turn yields the closure of the FRG equations in the corresponding limit.

### 3.3.3. Shift of the response fields

It was also early noticed in the field-theoretical framework that the NS action is invariant under a constant shift of the velocity response field. However, it was not identified until recently that this symmetry could also be promoted to a time-gauged one Canet *et al.* (2015). The latter corresponds to the following infinitesimal coupled transformation of the response fields

$$\begin{aligned}
\delta \bar{v}_\alpha(t, \mathbf{x}) &= \bar{\varepsilon}_\alpha(t) \\
\delta \bar{p}(t, \mathbf{x}) &= v_\beta(t, \mathbf{x}) \bar{\varepsilon}_\beta(t). \tag{3.34}
\end{aligned}$$

This transformation indeed induces a variation of the NS action which is only linear in the fields

$$\delta \mathcal{S}_{\text{NS}} = \int_{t, \mathbf{x}} \bar{\varepsilon}_\beta(t) \partial_t v_\beta(t, \mathbf{x}) + 2 \int_{t, \mathbf{x}, \mathbf{x}'} \bar{\varepsilon}_\alpha(t) N_{\alpha\beta} \left( \frac{|\mathbf{x} - \mathbf{x}'|}{L} \right) \bar{v}_\beta(t, \mathbf{x}'). \tag{3.35}$$

Hence, interpreted as a change of variable in (3.20), this yields the identity  $\langle \delta \mathcal{S}_{\text{NS}} \rangle = \langle \delta \int_{t, \mathbf{x}} \mathcal{J}_\ell \Phi_\ell \rangle$ , which can be written as the following Ward identity for the functional  $\Gamma$

$$\int_{\mathbf{x}} \left\{ \frac{\delta \Gamma}{\delta \bar{u}_\alpha(t, \mathbf{x})} + u_\alpha(t, \mathbf{x}) \frac{\delta \Gamma}{\delta \bar{p}(t, \mathbf{x})} \right\} = \int_{\mathbf{x}} \partial_t u_\alpha(t, \mathbf{x}) + 2 \int_{\mathbf{x}, \mathbf{x}'} N_{\alpha\beta} \left( \frac{|\mathbf{x} - \mathbf{x}'|}{L} \right) \bar{u}_\beta(t, \mathbf{x}'). \tag{3.36}$$

Note that this identity is again local in time. Taking functional derivatives with respect to velocity and response velocity fields and evaluating at zero fields, one can deduce again exact identities for vertex functions Canet *et al.* (2016). They give the expression of any  $\Gamma^{(\ell,m)}$  with one vanishing wavevector carried by a response velocity, which simply reads in Fourier space

$$\Gamma_{\alpha_1\dots\alpha_{\ell+m}}^{(\ell,m)}(\omega_1, \mathbf{p}_1, \dots, \omega_\ell, \mathbf{p}_\ell, \omega_{\ell+1}, \mathbf{p}_{\ell+1} = \mathbf{0}, \dots) = 0, \tag{3.37}$$

for all  $(\ell, m)$  except for the two lower-order ones which keep their bare form:

$$\begin{aligned}\Gamma_{\alpha\beta}^{(1,1)}(\omega_1, \mathbf{p}_1, \omega_2, \mathbf{p}_2 = \mathbf{0}) &= i\omega_1 \delta_{\alpha\beta} (2\pi)^{d+1} \delta(\omega_1 + \omega_2) \delta^d(\mathbf{p}_1 + \mathbf{p}_2), \\ \Gamma_{\alpha\beta\gamma}^{(2,1)}(\omega_1, \mathbf{p}_1, \omega_2, \mathbf{p}_2, \omega_3, \mathbf{p}_3 = \mathbf{0}) &= -i \left( p_2^\alpha \delta_{\beta\gamma} + i p_1^\beta \delta_{\alpha\gamma} \right) \\ &\quad \times (2\pi)^{d+1} \delta(\omega_1 + \omega_2 + \omega_3) \delta^d(\mathbf{p}_1 + \mathbf{p}_2 + \mathbf{p}_3). \quad (3.38)\end{aligned}$$

### 3.3.4. Extended symmetries for the passive scalar fields

Let us now consider the symmetries and extended symmetries of the passive scalar action (3.23). This action possesses two extended symmetries related to time-dependent shifts of the scalar field :  $\theta(t, \mathbf{x}) \rightarrow \theta(t, \mathbf{x}) + \varepsilon(t)$  and the joint transformation for the response field

$$\begin{aligned}\bar{\theta}(t, \mathbf{x}) &\rightarrow \bar{\theta}(t, \mathbf{x}) + \bar{\varepsilon}(t) \\ \bar{p}(t, \mathbf{x}) &\rightarrow \bar{p}(t, \mathbf{x}) + \bar{\varepsilon}(t)\theta(t, \mathbf{x}).\end{aligned} \quad (3.39)$$

Each of these transformations leads to a variation of the action which is linear in the fields. The corresponding functional Ward identities are straightforward to derive and read respectively Pagani & Canet (2021).

$$\begin{aligned}\int_{\mathbf{x}} \frac{\delta\Gamma}{\delta\theta(t, \mathbf{x})} &= - \int_{\mathbf{x}} \partial_t \bar{\theta}(t, \mathbf{x}) \\ \int_{\mathbf{x}} \frac{\delta\Gamma}{\delta\bar{\theta}(t, \mathbf{x})} &= \int_{\mathbf{x}} \left\{ \partial_t \theta(t, \mathbf{x}) + v_\beta(t, \mathbf{x}) \partial_\beta \theta(t, \mathbf{x}) \right\}.\end{aligned} \quad (3.40)$$

These identities imply that the two terms  $\int \bar{\theta} \partial_t \theta$  and  $\int \bar{\theta} v_\beta \partial_\beta \theta$  are not renormalised, and they entail that any vertex bearing one vanishing wavevector carried either by a  $\theta$  or a  $\bar{\theta}$  field vanishes – except for  $\Gamma^{\theta\bar{\theta}}$  which keeps its bare form – *i.e.*

$$\begin{aligned}\Gamma^{(n_\nu, n_{\bar{\nu}}, n_\theta \geq 1, n_{\bar{\theta}})}(\dots, \omega_\theta, \mathbf{p}_\theta = 0, \dots) &= 0 \\ \Gamma^{(n_\nu, n_{\bar{\nu}}, n_\theta, n_{\bar{\theta}} \geq 1)}(\dots, \omega_{\bar{\theta}}, \mathbf{p}_{\bar{\theta}} = 0, \dots) &= 0 \\ \Gamma^{(0,0,1,1)}(\omega_\theta, \mathbf{p}_\theta = \mathbf{0}, \omega_{\bar{\theta}}, \mathbf{p}_{\bar{\theta}}) &= i\omega_\theta (2\pi)^{d+1} \delta(\omega_\theta + \omega_{\bar{\theta}}) \delta^d(\mathbf{p}_\theta + \mathbf{p}_{\bar{\theta}}).\end{aligned} \quad (3.41)$$

These identities are very similar to Eqs. (3.37,3.38) ensuing from the time-gauged shift of the response fields.

Moreover, the time-dependent Galilean symmetry is also an extended symmetry of the total action  $\mathcal{S}_{\text{NS}} + \mathcal{S}_\theta$ . Indeed, the passive scalar and its response field behave as Galilean scalar densities under time-gauged Galilean transformations (3.27), *i.e.*  $\delta\theta(t, \mathbf{x}) = \varepsilon_\beta(t) \partial_\beta \theta(t, \mathbf{x})$  and  $\delta\bar{\theta}(t, \mathbf{x}) = \varepsilon_\beta(t) \partial_\beta \bar{\theta}(t, \mathbf{x})$ , which yield a variation of the total action linear in the field. The associated Ward identity constrains the vertices for which one of the velocity has a zero wavenumber,

$$\begin{aligned}\Gamma_{\alpha_1 \dots \alpha_{n_\nu + n_{\bar{\nu}} + 1}}^{(n_\nu + 1, n_{\bar{\nu}}, n_\theta, n_{\bar{\theta}})} \left( \dots, \underbrace{\omega_\ell, \mathbf{p}_\ell = 0}_{\ell = \text{velocity index}}, \dots \right) &= - \sum_{i=1}^n \frac{p_i^{\alpha_\ell}}{\omega_\ell} \Gamma_{\alpha_1 \dots \alpha_{n_\nu + n_{\bar{\nu}}}}^{(n_\nu, n_{\bar{\nu}}, n_\theta, n_{\bar{\theta}})} \left( \dots, \underbrace{\omega_i + \omega_\ell, \mathbf{p}_i}_{i^{\text{th}} \text{ field}}, \dots \right), \\ &= \mathcal{D}_{\alpha_1}(\omega_\ell) \Gamma_{\alpha_1 \dots \alpha_{n_\nu + n_{\bar{\nu}}}}^{(n_\nu, n_{\bar{\nu}}, n_\theta, n_{\bar{\theta}})} \left( \dots, \omega_i, \mathbf{p}_i, \dots \right)\end{aligned} \quad (3.42)$$

where  $\alpha_1 \dots \alpha_{n_\nu + n_{\bar{\nu}} + 1}$  are the spatial indices of the velocity (and response velocity) fields,  $n = n_\theta + n_{\bar{\theta}} + n_\nu + n_{\bar{\nu}}$ , and  $\mathcal{D}_\alpha$  is the same operator as in Eq. (3.33).

To summarise, the key point is that the Ward identities for the scalar advected by the NS flow share essentially the same structure as the ones for the NS action. They have a strong

implication: when at least one wavevector of any vertex is set to zero, then it vanishes, except if the wavevector is carried by a velocity field, in which case it is controlled by (3.33) or (3.42), *i.e.* given in terms of a linear combination of lower-order vertices through the operator  $\mathcal{D}_\alpha$ . This constitutes the cornerstone of the large wavenumber closure expounded in Sec. 6.

Let us emphasise that this program can still be completed. First, for 2D turbulence, additional extended symmetries have recently been unveiled, which are reported in Appendix B. One of them is also realised in 3D turbulence but has not been exploited yet in the FRG formalism. Second, another important symmetry of the Euler or NS equation is the scaling or dilatation symmetry, which amounts to the transformation  $\mathbf{v}(t, \mathbf{x}) \rightarrow b^h \mathbf{v}(b^z t, b\mathbf{x})$  Frisch (1995); Dubrulle (2019). One can also derive from this symmetry, possibly extended, functional Ward identities. This route has not been explored either. Both could lead to future fruitful developments.

### 3.4. Kármán-Howarth and Yaglom relations

The path integral formulation conveys an interesting viewpoint on well-known exact identities such as the Kármán-Howarth relation von Kármán & Howarth (1938) or the equivalent Yaglom relation for passive scalars. The Kármán-Howarth relation stems from the energy budget equation associated with the NS equation, and imposing stationarity, homogeneity and isotropy. From this relation, one can derive the exact four-fifths Kolmogorov law for the third order structure function  $S^{(3)}$  Frisch (1995). It turns out that the Kármán-Howarth relation also emerges as the Ward identity associated with a fully-gauged shift of the response fields (which is a generalisation of the time-gauged shift discussed in Sec. 3.3.3), and can thus be obtained in the path integral formulation as a consequence of symmetries Canet *et al.* (2015).

To show this, let us consider the NS action (3.21) with an additional source  $L_{\alpha\beta}$  in (3.20) coupled to the local quadratic term  $v_\alpha(t, \mathbf{x})v_\beta(t, \mathbf{x})$  (which is a composite operator in the field-theoretical language), *i.e.* the term  $\int_{t, \mathbf{x}} v_\alpha L_{\alpha\beta} v_\beta$  is added in  $\mathcal{J}$ . This implies that a local, *i.e.* at coinciding space-time points, quadratic average in velocities, can then be simply obtained by taking a functional derivative with respect to this new source

$$\langle v_\alpha(t, \mathbf{x})v_\beta(t, \mathbf{x}) \rangle = \frac{\delta \mathcal{W}}{\delta L_{\alpha\beta}(t, \mathbf{x})} = -\frac{\delta \Gamma}{\delta L_{\alpha\beta}(t, \mathbf{x})}. \quad (3.43)$$

Note that to define  $\Gamma$ , the Legendre transform is not taken with respect to the source  $L_{\alpha\beta}$ , *i.e.* both functional  $\mathcal{W}$  and  $\Gamma$  depend on  $L_{\alpha\beta}$ , and hence (3.43) ensues.

The introduction of the source for the composite operator  $v_\alpha v_\beta$  allows one to consider a further extended symmetry of the NS action, namely the time *and space* dependent version of the field transformation (3.34), which amounts to  $\bar{\varepsilon}_\alpha(t) \rightarrow \bar{\varepsilon}_\alpha(t, \mathbf{x})$ . The variation of the NS action under this gauged transformation

$$\langle \delta \mathcal{S}_{\text{NS}} \rangle = \left\langle \partial_t v_\alpha + \frac{1}{\rho} \partial_\alpha p - \nu \nabla^2 v_\alpha + \partial_\beta (v_\alpha v_\beta) - 2 \int_{\mathbf{x}'} \left( N_{\alpha\beta} \left( \frac{|\mathbf{x} - \mathbf{x}'|}{L} \right) \bar{v}_\beta(t, \mathbf{x}') \right) \right\rangle, \quad (3.44)$$

is linear in the fields, but for the local quadratic term, which can nonetheless be expressed as a derivative with respect to  $L_{\alpha\beta}$ . The resulting Ward identity can be written equivalently in terms of  $\Gamma$  or  $\mathcal{W}$ . We give it for  $\mathcal{W}$  since it renders more direct the connection with the Kármán-Howarth relation

$$-\partial_t \frac{\delta \mathcal{W}}{\delta J_\alpha} - \frac{1}{\rho} \partial_\alpha \frac{\delta \mathcal{W}}{\delta K} + \nu \nabla^2 \frac{\delta \mathcal{W}}{\delta J_\alpha} + \bar{J}_\alpha + \bar{K} \frac{\delta \mathcal{W}}{\delta J_\alpha} - \partial_\beta \frac{\delta \mathcal{W}}{\delta L_{\alpha\beta}} + 2 \int_{\mathbf{x}'} N_{\alpha\beta} \left( \frac{|\mathbf{x} - \mathbf{x}'|}{L} \right) \frac{\delta \mathcal{W}}{\delta \bar{J}_\beta(t, \mathbf{x}')} = 0. \quad (3.45)$$

We emphasise that, compared to (3.36), this identity is now *fully local*, in space as well as in

time, *i.e.* it is no longer integrated over space. It is also an exact identity for the generating functional  $\mathcal{W}$  itself, which means that it entails an infinite set of exact identities amongst correlation functions. The Kármán-Howarth relation embodies the lowest order one, which is obtained by differentiating (3.45) with respect to  $J_\gamma(t_y, \mathbf{y})$ , and evaluating the resulting identity at zero external sources. Note that in the MSRJD formalism, the term proportional to  $N_{\alpha\beta}$  is simply equal to a force-velocity correlation  $\langle f_\alpha(t, \mathbf{x})v_\gamma(t_y, \mathbf{y}) \rangle$  Canet *et al.* (2015). Summing over  $\gamma = \alpha$  and specialising to equal time  $t_y = t$ , one deduces

$$\begin{aligned} & -\partial_t \langle v_\alpha(t, \mathbf{x})v_\alpha(t, \mathbf{y}) \rangle + \nu(\Delta_x + \Delta_y) \langle v_\alpha(t, \mathbf{x})v_\alpha(t, \mathbf{y}) \rangle \\ & -\partial_\beta^x \langle v_\alpha(t, \mathbf{x})v_\beta(t, \mathbf{x})v_\alpha(t, \mathbf{y}) \rangle - \partial_\beta^y \langle v_\alpha(t, \mathbf{y})v_\beta(t, \mathbf{y})v_\alpha(t, \mathbf{x}) \rangle \\ & + \langle f_\alpha(t, \mathbf{x})v_\alpha(t, \mathbf{y}) \rangle + \langle f_\alpha(t, \mathbf{y})v_\alpha(t, \mathbf{x}) \rangle = 0, \end{aligned} \quad (3.46)$$

which is the well-known Kármán-Howarth relation.

Once again, taking other functional derivatives with respect to arbitrary sources yields infinitely many exact relations. To give another example, by differentiating twice Eq. (3.45) with respect to  $L_{\mu\nu}(t_y, \mathbf{y})$  and  $J_\gamma(t_z, \mathbf{z})$ , one obtains the exact relation for a pressure-velocity correlation Canet *et al.* (2015)

$$\begin{aligned} & \nu \langle v_\alpha(t, \mathbf{x})\Delta_x v_\alpha(t, \mathbf{x})v^2(t, \mathbf{y}) \rangle - \frac{1}{\rho} \partial_\alpha^x \langle v^2(t, \mathbf{y})v_\alpha(t, \mathbf{x})p(t, \mathbf{x}) \rangle \\ & + \langle f_\alpha(t, \mathbf{x})v_\alpha(t, \mathbf{x})v^2(t, \mathbf{y}) \rangle - \frac{1}{2} \partial_\alpha^x \langle v_\alpha(t, \mathbf{x})v^2(t, \mathbf{x})v^2(t, \mathbf{y}) \rangle = 0, \end{aligned} \quad (3.47)$$

which was first derived in Ref. Falkovich *et al.* (2010).

Shortly after Kolmogorov's derivation of the exact relation for the third-order structure function, Yaglom established the analogous formula for scalar turbulence Yaglom (1949). It was shown in Pagani & Canet (2021) that this relation can also be simply inferred from symmetries of the passive scalar action (3.23). More precisely, it ensues from the spacetime-dependent (*i.e.* fully gauged) shift of the response fields

$$\bar{\theta}(t, \mathbf{x}) \rightarrow \bar{\theta}(t, \mathbf{x}) + \bar{\varepsilon}(t, \mathbf{x}), \quad \bar{p}(t, \mathbf{x}) \rightarrow \bar{p}(t, \mathbf{x}) + \bar{\varepsilon}(t, \mathbf{x})\theta(t, \mathbf{x}) \quad (3.48)$$

in the path integral (3.22), in the presence of the additional source term  $\int_{t, \mathbf{x}} L_\alpha v_\alpha \theta$  where  $L_\alpha$  is the source coupled to the composite operator  $v_\alpha \theta$ . Following the same reasoning, one deduces an exact functional Ward identity for the passive scalar, which writes in term of  $\mathcal{W}$

$$\left( \partial_t - \frac{\kappa_\theta}{2} \nabla^2 \right) \frac{\delta W}{\delta j(t, \mathbf{x})} + \partial_\beta \frac{\delta W}{\delta L_\beta(t, \mathbf{x})} - \int_{\mathbf{y}} M \left( \frac{|\mathbf{x} - \mathbf{y}|}{L_\theta} \right) \frac{\delta W}{\delta \bar{j}(t, \mathbf{y})} = 0. \quad (3.49)$$

The lowest order relation stemming from it is the Yaglom relation

$$-\frac{1}{2} \frac{\partial}{\partial(x-y)_\alpha} \left\langle |\theta(t, \mathbf{x}) - \theta(t, \mathbf{y})|^2 (v_\alpha(t, \mathbf{x}) - v_\alpha(t, \mathbf{y})) \right\rangle = 2\epsilon_\theta, \quad (3.50)$$

where  $\epsilon_\theta$  is the mean dissipation rate of the scalar. This relation hence also follows from symmetries in the path integral formulation.

#### 4. The functional renormalisation group

As mentioned in Sec. 2, the idea underlying the FRG is Wilson's original idea of progressive averaging of fluctuations in order to build up the effective description of a system from its microscopic model. This progressive averaging is organised scale by scale, in general in wavenumber space, and thus leads to a sequence of scale-dependent models, embodied in

Wilson’s formulation in a scale-dependent Hamiltonian or action Wilson & Kogut (1974). In the FRG formalism, one rather considers a scale-dependent effective action  $\Gamma_\kappa$ , called effective average action, where  $\kappa$  denotes the RG scale. It is a wavenumber scale, which runs from the microscopic ultraviolet (UV) scale  $\Lambda$  to a macroscopic IR scale (e.g. the integral scale). The key in the RG procedure is that the information about many properties of the system can be captured by the *flow* of these models, *i.e.* their evolution with the RG scale, without requiring to explicitly carry out the integration of the fluctuations. The RG flow is governed by an exact very general equation, which can take different forms depending on the precise RG used (Wilson Wilson & Kogut (1974) or Polchinski flow equation Polchinski (1984), Callan-Symanzik flow equation Callan (1970); Symanzik (1970), . . .). The one at the basis of the FRG formalism is usually called the Wetterich’s equation Wetterich (1993). We briefly introduce it in the next sections on the example of the generic scalar field theory of Sec. 3.1, denoting generically  $\Phi(t, \mathbf{x})$  the field multiplet, e.g.  $\Phi = (\varphi, \bar{\varphi}, \bar{c}_\ell)$ ,  $\Psi = \langle \Phi \rangle$  the multiplet of average fields, and  $\mathcal{J}$  the multiplet of corresponding sources.

#### 4.1. Progressive integration of fluctuations

The core of the RG procedure is to turn the global integration over fluctuations in the path integral (3.10) into a progressive integration, organised by wavenumber shells. To achieve this, one introduces in the path integral a scale-dependent weight  $e^{-\Delta S_\kappa}$  whose role is to suppress fluctuations below the RG scale  $\kappa$ , giving rise to a new, scale-dependent generating functional

$$\mathcal{Z}_\kappa[\mathcal{J}] = \int \mathcal{D}\Phi e^{-S[\Phi] - \Delta S_\kappa[\Phi] + \int_{t,\mathbf{x}} \mathcal{J}_\ell \Phi_\ell}. \quad (4.1)$$

The new term  $\Delta S_\kappa$  is chosen quadratic in the fields

$$\Delta S_\kappa[\Phi] = \frac{1}{2} \int_{t,\mathbf{x},\mathbf{x}'} \Phi_m(t, \mathbf{x}) \mathcal{R}_{\kappa,mm'}(|\mathbf{x} - \mathbf{x}'|) \Phi_{m'}(t, \mathbf{x}'), \quad (4.2)$$

where  $\mathcal{R}_\kappa$  is called the regulator, or cut-off, matrix. Note that it has been chosen here proportional to  $\delta(t - t')$ , or equivalently independent of frequencies. This means that the selection of fluctuations is operated in space, and not in time, as in equilibrium. †

The precise form of the non-vanishing elements  $[\mathcal{R}]_{\kappa,ij}$  of the cutoff matrix is not important, provided they satisfy the following requirements, simply denoting  $R_\kappa$  a given non-vanishing element

$$\begin{aligned} R_\kappa(p^2) &\sim \kappa^2 && \text{for } |\mathbf{p}| \lesssim \kappa \\ R_\kappa(p^2) &\longrightarrow 0 && \text{for } |\mathbf{p}| \gtrsim \kappa. \end{aligned} \quad (4.3)$$

The first one endows the low wavenumber modes with a large “mass”, such that these modes are damped, or filtered out, for their contribution in the functional integral to be suppressed. The second one ensures that the cutoff vanishes for large wavenumber modes, which are thus unaffected. Hence, only these modes are integrated over, thus achieving the progressive averaging. Moreover,  $R_{\kappa=\Lambda}$  are required to be very large such that all fluctuations are frozen at the microscopic scale, and  $R_{\kappa=0}$  to vanish such that all fluctuations are averaged over in this limit.

It follows that the free energy functional  $\mathcal{W}'_\kappa = \ln \mathcal{Z}_\kappa$  also becomes scale-dependent. One

† The selection can in principle be operated also in time, although it poses some technical difficulties, not to violate causality Canet *et al.* (2011a) and symmetries involving time – typically the Galilean invariance. A spacetime cutoff was implemented only in Duclut & Delamotte (2017) for Model A, which is a simple, purely dissipative, dynamical extension of the Ising model. In the following, we restrict ourselves to frequency-independent regulators.

defines the scale-dependent effective average action through the modified Legendre transform

$$\Gamma_\kappa[\Psi] + \Delta\mathcal{S}_\kappa[\Psi] = \sup_{\mathcal{J}} \left[ \int_{t,x} \mathcal{J}_\ell \Psi_\ell - \mathcal{W}_\kappa[\mathcal{J}] \right]. \quad (4.4)$$

The regulator term is added in the relation in order to enforce that, at scale  $\kappa = \Lambda$ , the effective average action coincides with the microscopic action  $\Gamma_{\kappa=\Lambda} = \mathcal{S}$ . In the opposite limit  $\kappa \rightarrow 0$ , the standard effective action  $\Gamma$ , encompassing all the fluctuations, is recovered since the regulator is removed in this limit, and  $\Delta\mathcal{S}_{\kappa=0} = 0$ . Thus, the sequence of  $\Gamma_\kappa$  provides an interpolation between the microscopic bare action and the full effective action.

#### 4.2. Exact flow equation for the effective average action

The evolution of the generating functionals  $\mathcal{W}_\kappa$  and  $\Gamma_\kappa$  with the RG scale  $\kappa$  obeys an exact differential equation, which can be simply inferred from (4.1) and (4.4) since the dependence on  $\kappa$  only comes from the regulator term  $\Delta\mathcal{S}_\kappa$ . This yields for  $\mathcal{W}_\kappa$  the flow equation

$$\partial_s \mathcal{W}_\kappa[\mathcal{J}] = -\frac{1}{2} \text{Tr} \left[ \partial_s \mathcal{R}_{\kappa, mn} \left( \frac{\delta^2 \mathcal{W}_\kappa[\mathcal{J}]}{\delta \mathcal{J}_m \delta \mathcal{J}_n} + \frac{\delta \mathcal{W}_\kappa[\mathcal{J}]}{\delta \mathcal{J}_m} \frac{\delta \mathcal{W}_\kappa[\mathcal{J}]}{\delta \mathcal{J}_n} \right) \right], \quad (4.5)$$

where  $s \equiv \log(\kappa/\Lambda)$ . This equation is very similar to Polchinski equation Polchinski (1984). Some simple algebra then leads to Wetterich equation for  $\Gamma_\kappa$  Delamotte (2012)

$$\partial_s \Gamma_\kappa[\Psi] = \frac{1}{2} \text{Tr} \left[ \partial_s \mathcal{R}_{\kappa, mn} G_{\kappa, mn} \right] \equiv \frac{1}{2} \text{Tr} \left[ \partial_s \mathcal{R}_{\kappa, mn} \left( \Gamma_\kappa^{(2)}[\Psi] + \mathcal{R}_\kappa \right)_{mn}^{-1} \right], \quad (4.6)$$

where  $G_\kappa \equiv \mathcal{W}_\kappa^{(2)}$  denotes the inverse of  $(\Gamma_\kappa^{(2)} + \mathcal{R}_\kappa)$ , *i.e.* the propagator. To alleviate notations, the indices  $m, n$  refer to the field indices within the multiplet, as well as other possible indices (e.g. vector component) and space-time coordinates. Accordingly, the trace includes the summation over all internal indices as well as the integration over all spacial and temporal coordinates (deWitt notation, integrals are implicit).

While Eq. (4.6) or (4.5) are exact, they are functional partial differential equations which cannot be solved exactly in general. Their functional nature implies that they encompass an infinite set of flow equations for the associated correlation functions. For instance, taking one functional derivative of (4.6) with respect to a given field and evaluating the resulting expression at a fixed background field configuration (say  $\Psi(t, \mathbf{x}) = 0$ ) yields the flow equation for the one-point function  $\Gamma^{(1)}$ . This equation depends on the three-point vertex  $\Gamma^{(3)}$ . More generally, the flow equation for the  $n$ -point vertex  $\Gamma^{(n)}$  involves  $\Gamma^{(n+1)}$  and  $\Gamma^{(n+2)}$ , such that one has to consider an infinite hierarchy of flow equations. This pertains to the very common closure problem of non-linear systems. It means that one has to devise some approximations.

#### 4.3. Non-perturbative approximation schemes

This part may appear technical for readers not familiar with RG methods. Its objective is to explain the rationale behind the approximation schemes in the study of turbulence, which are detailed in the rest of the paper.

In the FRG context, several approximation schemes have been developed and are commonly used Dupuis *et al.* (2021). Of course one can implement a perturbative expansion, in any available small parameter, such as a small coupling or an infinitesimal distance to a critical dimension  $\varepsilon = d - d_c$ . One then retrieves results obtained from standard perturbative RG techniques. However, the key advantage of the FRG formalism is that it is suited to the implementation of non-perturbative approximation schemes. The most commonly used is the derivative expansion, which consists in expanding the effective average action  $\Gamma_\kappa$  in

powers of gradients and time derivatives. This is equivalent to an expansion around zero external wavenumbers  $|\mathbf{p}_i| = 0$  and frequencies  $\omega_i = 0$  and is thus adapted to describe the long-distance long-time properties of a system. One can in particular obtain universal properties of a system at criticality (e.g. critical exponents), but also non-universal properties, such as phase diagrams. Even though it is non-perturbative in the sense that it does not rely on an explicit small parameter, it is nonetheless controlled. It can be systematically improved, order by order (adding higher-order derivatives), and an error can be estimated at each order, due to the existence of an effective small parameter related to the cutoff. The convergence and accuracy of the derivative expansion have been studied in depth for archetypal models, namely the Ising model and  $O(N)$  models Dupuis *et al.* (2021). The outcome is that the convergence is fast, and most importantly that the results obtained for instance for the critical exponents are very precise. For the 3D Ising model, the derivative expansion has been pushed up to the sixth order  $O(\partial^6)$  and the results for the critical exponents compete in accuracy with the best available estimates in the literature (from conformal bootstrap methods) Balog *et al.* (2019). For the  $O(N)$  models, the results are the most accurate ones De Polsi *et al.* (2020, 2021).

The derivative expansion is by construction restricted to describe the zero wavenumber and frequency sector, it does not allow one to access the full space-time dependence of generic correlation functions. To overcome this limitation, another approximation scheme, called the Blaizot-Méndez-Galain-Wschebor (BMW) scheme Blaizot *et al.* (2006, 2007); Benitez *et al.* (2008), was proposed and now stands as the other commonly used approximation scheme within the FRG. It lies at the basis of all the FRG studies dedicated to turbulence. The BMW scheme essentially exploits an intrinsic property of the Wetterich flow equation conveyed by the presence of the regulator. Wetterich equation has a one-loop structure. To avoid any confusion, let us emphasise that this does not mean that it is equivalent to a one-loop perturbative expansion: the propagator entering Eq. (4.6) is the full (functional) renormalised propagator of the theory, not the bare one. This simply means that there is only one internal, or loop, (*i.e.* integrated over) wavevector  $\mathbf{q}$  and frequency  $\omega$ . This holds true for the flow equation of any vertex  $\Gamma^{(n)}$ , which depends on the  $n$  external wavevectors  $\mathbf{p}_i$  and frequencies  $\varpi_i$ , but involves only on one internal wavevector and frequency  $(\omega, \mathbf{q})$ .

The key feature of Wetterich equation is that the internal wavevector  $\mathbf{q}$  is controlled by the scale-derivative of the regulator. Because of the requirement (4.3),  $\partial_s \mathcal{R}_\kappa(\mathbf{q})$  is exponentially vanishing for  $q \equiv |\mathbf{q}| \gtrsim \kappa$ , which implies that the loop integral is effectively cut to  $q \simeq \kappa$ . This points to a specific limit where this property can be exploited efficiently, namely the large wavenumber limit. Indeed, if one considers large external wavenumbers  $p_i \equiv |\mathbf{p}_i| \gg \kappa$ , then  $|\mathbf{q}| \ll |\mathbf{p}_i|$  is automatically satisfied. One may thus expand the vertices entering the flow equation around  $\mathbf{q} \simeq 0$ , which can be interpreted as an expansion in powers of  $q/p_i$ . This expansion becomes formally exact in the limit where all  $p_i \rightarrow \infty$ . Moreover, a generic  $\Gamma^{(n)}$  vertex with one zero wavevector can be expressed as a derivative with respect to a constant field of the corresponding  $\Gamma^{(n-1)}$ . This allows one in the original BMW approximation scheme to close the flow equation at a given order (say for the two-point function), at the price of keeping a dependence in a background constant field  $\Psi_0$ , *i.e.*  $\bar{\Gamma}_\kappa^{(2)}(\varpi, \mathbf{p}; \Psi_0)$ , which can be cumbersome. This approximation can also in principles be improved order by order, by achieving the  $\mathbf{q}$  expansion in the flow equation for the next order  $(n + 1)$  vertex instead of the  $n$ th one, although it becomes increasingly difficult.

In the context of non-equilibrium statistical physics, the BMW approximation scheme was implemented successfully to study the Kardar-Parisi-Zhang equation describing kinetic roughening of stochastically growing interfaces Kardar *et al.* (1986). The KPZ equation exactly maps to the Burgers equation for randomly stirred fluids Bec & Khanin (2007),

which highlights its connection with turbulence. The KPZ equation offers a striking example where the perturbative RG flow equations have been re-summed to all orders in perturbation theory, but fails in  $d \geq 2$  to find the strong-coupling fixed-point expected to govern the KPZ critical rough phase Wiese (1998). In contrast, the FRG framework allows one to access this fixed point in all dimensions even at the lowest order of the derivative expansion Canet *et al.* (2010). This fixed-point turns out to be genuinely non-perturbative, *i.e.* not connected to the Gaussian (non-interacting) fixed-point in any dimension, hence explaining the failure of perturbation theory, to all orders. However, in order to obtain a quantitative description of the statistical properties of the rough phase, the derivative expansion is not sufficient, and one needs to resort to the BMW scheme, which indeed yields very accurate results for the KPZ equation Canet *et al.* (2011*b*); Kloss *et al.* (2012).

For the NS equation, the BMW approximation scheme turns out to be remarkably efficient in two respects which will become clear in the following: technically, the symmetries and extended symmetries allow one to get rid of the background field dependence, which is also the case for the KPZ problem. Moreover, physically, the large wavenumber limit is not trivial for turbulence, which is unusual. In critical phenomena exhibiting standard scale invariance, the large wavenumbers simply decouple from the IR properties and this limit carries no independent information.

## 5. Fixed-point for Navier-Stokes turbulence

As mentioned in Sec. 2, perturbative RG approaches to turbulence have been hindered by the need to define a small parameter. The introduction of a forcing with power-law correlations  $p^{4-d-2\varepsilon}$  leads to a fixed-point with an  $\varepsilon$ -dependent energy spectrum, which is not easily linked to the expected Kolmogorov one. In this respect, the first achievement of FRG was to find the fixed-point corresponding to fully-developed turbulence, both in  $d = 3$  and  $d = 2$ , obtained for a physical forcing concentrated at the integral scale. As explained in Sec. 4.3, the crux is that one can devise in the FRG framework approximation schemes which are not based on a small parameter, thereby circumventing the previous difficulty. This fixed point was first obtained in a pioneering work by Tomassini Tomassini (1997), which has been largely overlooked at the time. He developed an approximation close in spirit to what is now called the Blaizot–Mendez–Wschebor (BMW) approximation, although it was not yet invented at the time. In the meantime, the FRG framework was successfully developed to study the KPZ equation where it yielded the strong-coupling fixed-point Canet *et al.* (2010). Inspired by the KPZ example, the stochastic NS equation was revisited using similar FRG approximations in Refs. Mejía-Monasterio & Muratore-Ginanneschi (2012); Canet *et al.* (2016). We now present the resulting fixed-point for fully developed turbulence.

To show the existence of the fixed point and characterise the associated energy spectrum, one can focus on the two-point correlation functions. The general FRG flow equation for the two-point functions is obtained by differentiating twice the exact flow equation (4.6) for the effective average action  $\Gamma_\kappa$ . It reads

$$\begin{aligned} \partial_\kappa \bar{\Gamma}_{\kappa, \ell m}^{(2)}(\varpi, \mathbf{p}) = & \text{Tr} \int_{\omega, \mathbf{q}} \partial_\kappa \mathcal{R}_\kappa(\mathbf{q}) \cdot \bar{G}_\kappa(\omega, \mathbf{q}) \cdot \left( -\frac{1}{2} \bar{\Gamma}_{\kappa, \ell m}^{(4)}(\varpi, \mathbf{p}, -\varpi, -\mathbf{p}, \omega, \mathbf{q}) \right. \\ & \left. + \bar{\Gamma}_{\kappa, \ell}^{(3)}(\varpi, \mathbf{p}, \omega, \mathbf{q}) \cdot \bar{G}_\kappa(\varpi + \omega, \mathbf{p} + \mathbf{q}) \cdot \bar{\Gamma}_{\kappa, m}^{(3)}(-\varpi, -\mathbf{p}, \varpi + \omega, \mathbf{p} + \mathbf{q}) \right) \cdot G_\kappa(\omega, \mathbf{q}) \end{aligned} \quad (5.1)$$

where the background field dependencies are implicit, as well as the last arguments of the  $\bar{\Gamma}_\kappa^{(n)}$  which are determined by frequency and wavevector conservation according to (3.19). We used a matrix notation, where only the external field index  $\ell$  and  $m$  are specified, e.g.

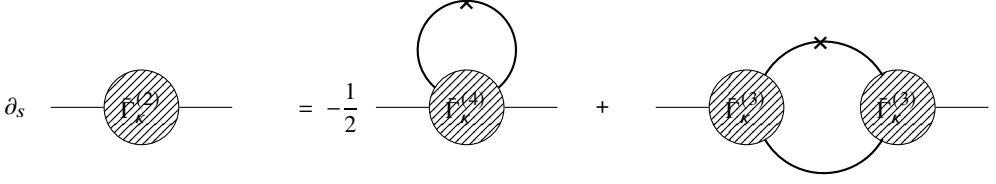


Figure 1: Diagrammatic representation of the flow of  $\bar{\Gamma}_\kappa^{(2)}$ . The bold lines represent the propagator  $\bar{G}_\kappa$  and the crosses the derivative of the regulator  $\partial_\kappa \mathcal{R}_\kappa$ .

$\bar{\Gamma}_{\kappa,\ell}^{(3)}$  is the  $4 \times 4$  matrix of all three-point vertices with one leg fixed at  $(\ell, \vec{w}, \mathbf{p})$  and the other two spanning all fields, and similarly for  $\bar{\Gamma}_{\kappa,\ell m}^{(4)}$ . It can be represented diagrammatically as in Fig. 1. In order to make explicit calculations, we follow in this part the same strategy as for the KPZ problem, that is we resort to an ansatz for the effective average action  $\Gamma_\kappa$  to close the flow equations.

### 5.1. Ansatz for the effective average action

One can first infer the general structure of  $\Gamma_\kappa$  stemming from the symmetry constraints analysed in Sec. 3.3, and in particular the non-renormalisation theorems. It endows the following form

$$\Gamma_\kappa[\mathbf{u}, \bar{\mathbf{u}}, p, \bar{p}] = \int_{t,\mathbf{x}} \left\{ \bar{u}_\alpha \left( \partial_t u_\alpha + u_\beta \partial_\beta u_\alpha + \frac{\partial_\alpha p}{\rho} \right) + \bar{p} \partial_\alpha u_\alpha \right\} + \tilde{\Gamma}_\kappa[\mathbf{u}, \bar{\mathbf{u}}] \quad (5.2)$$

where the explicit terms are the ones which vary linearly under the time-gauged Galilean and shift symmetries. Therefore, they are not renormalised and keep their bare forms, while the functional  $\tilde{\Gamma}_\kappa$  is fully invariant under the time-gauged Galilean and shift transformations.

We now turn to the regulator. It should be quadratic in the fields, satisfy the general constraints (4.3), and preserve the symmetries. A suitable choice is

$$\Delta S_\kappa[\mathbf{u}, \bar{\mathbf{u}}] = - \int_{t,\mathbf{x},\mathbf{x}'} \left\{ \bar{u}_\alpha(t, \mathbf{x}) N_{\kappa,\alpha\beta}(|\mathbf{x}-\mathbf{x}'|) \bar{u}_\beta(t, \mathbf{x}') + \bar{u}_\alpha(t, \mathbf{x}) R_{\kappa,\alpha\beta}(|\mathbf{x}-\mathbf{x}'|) u_\beta(t, \mathbf{x}') \right\}. \quad (5.3)$$

The first term is simply the original forcing term, promoted to a regulator by replacing the integral scale  $L$  by the RG scale  $\kappa^{-1}$ , since it naturally satisfy all the requirements. The forcing thus builds up with the RG flow, and the physical forcing scale is restored when  $\kappa = L^{-1}$ . The additional  $R_\kappa$  term can be interpreted as an Ekman friction term in the NS equation. Its presence is fundamental in  $d = 2$  to damp energy transfer towards larger and larger scales. Within the FRG formalism, this manifests itself as an IR divergence in the flow equation when the  $R_\kappa$  term is absent, which is removed by its presence. This term is thus mandatory to properly regularise the RG flow in  $d = 2$ . Its effect is to introduce an effective energy dissipation at the boundary of the effective volume  $\kappa^{-d}$ , which is negligible in  $d = 3$  compared to the dissipation at the Kolmogorov scale.

These two terms can be parametrised introducing a scale-dependent forcing amplitude  $D_\kappa$  and viscosity  $\nu_\kappa$  as

$$N_{\kappa,\alpha\beta}(\mathbf{q}) = \delta_{\alpha\beta} D_\kappa \hat{n}(\mathbf{q}/\kappa), \quad R_{\kappa,\alpha\beta}(\mathbf{q}) = \delta_{\alpha\beta} \nu_\kappa \mathbf{q}^2 \hat{r}(\mathbf{q}/\kappa). \quad (5.4)$$

They are chosen diagonal in components without loss of generality since the propagators are transverse due to incompressibility, and thus the component  $\propto q_\alpha q_\beta$  plays no role in the flow equations. The general structure of the propagator matrix  $\bar{G}_\kappa$ , *i.e.* the inverse of the Hessian

of  $\Gamma_\kappa + \Delta S_\kappa$  is given in Appendix A. One can show in particular that the propagator in the velocity sector is purely transverse

$$\bar{G}_{\kappa,\alpha\beta}(\omega, \mathbf{q}) = P_{\alpha\beta}^\perp(\mathbf{q})\bar{G}_{\kappa,\perp}(\omega, \mathbf{q}), \quad P_{\alpha\beta}^\perp(\mathbf{q}) = \delta_{\alpha\beta} - \frac{q_\alpha q_\beta}{q^2}. \quad (5.5)$$

Let us now devise an ansatz for  $\tilde{\Gamma}$ . The ansatz which has been used for turbulence is similar in spirit to the one considered for the KPZ problem. It realises an implementation of the BMW approximation adapted to preserve the symmetries. At lowest order, it consists in keeping the most general wavevector (but not frequency) dependence for the two-point functions, while neglecting all higher-order vertices but the bare one. The corresponding ansatz is called LO (leading order) ansatz, and reads

$$\tilde{\Gamma}_\kappa[\mathbf{u}, \bar{\mathbf{u}}] = \int_{t,\mathbf{x},\mathbf{x}'} \left\{ \bar{u}_\alpha(t, \mathbf{x}) f_{\kappa,\alpha\beta}^\nu(\mathbf{x} - \mathbf{x}') u_\beta(t, \mathbf{x}') - \bar{u}_\alpha(t, \mathbf{x}) f_{\kappa,\alpha\beta}^D(\mathbf{x} - \mathbf{x}') \bar{u}_\beta(t, \mathbf{x}') \right\}. \quad (5.6)$$

Note that higher-order approximations have been implemented in the context of the KPZ equation, keeping in particular the most general frequency dependence of the two-point functions and an arbitrary dependence in the field, *i.e.* taking into account the flow of higher-order vertices as well. At LO, the flow is hence projected onto two renormalisation functions  $f_\kappa^\nu$  and  $f_\kappa^D$  which can be interpreted as an effective viscosity and an effective forcing, and induces a renormalisation of the two-point correlation and response functions. The renormalisation of multi-point interactions is neglected in this ansatz, which is a rather simple approximation.

The initial condition of the flow at scale  $\kappa = \Lambda$  corresponds to

$$f_{\Lambda,\alpha\beta}^D(\mathbf{x} - \mathbf{x}') = 0 \quad , \quad f_{\Lambda,\alpha\beta}^\nu(\mathbf{x} - \mathbf{x}') = -\nu \delta_{\alpha\beta} \nabla_x^2 \delta^{(d)}(\mathbf{x} - \mathbf{x}') \quad (5.7)$$

such that one recovers the original NS action (3.21).

The calculation of the two-point functions from the LO ansatz is straightforward. At vanishing fields and in Fourier space, one obtains

$$\begin{aligned} \tilde{\Gamma}_{\kappa,\alpha\beta}^{(1,1)}(\omega, \mathbf{p}) &= f_{\kappa,\alpha\beta}^\nu(\mathbf{p}) \\ \tilde{\Gamma}_{\kappa,\alpha\beta}^{(0,2)}(\omega, \mathbf{p}) &= -2f_{\kappa,\alpha\beta}^D(\mathbf{p}). \end{aligned} \quad (5.8)$$

Within the LO approximation, the only non-zero vertex function is the bare one, which reads in Fourier space

$$\bar{\Gamma}_{\kappa,\alpha\beta\gamma}^{(2,1)}(\omega_1, \mathbf{p}_1, \omega_2, \mathbf{p}_2) = -i(p_2^\alpha \delta_{\beta\gamma} + p_1^\beta \delta_{\alpha\gamma}). \quad (5.9)$$

One can then compute the flow equations for the two-point functions  $\tilde{\Gamma}_{\kappa,\alpha\beta}^{(1,1)}$  and  $\tilde{\Gamma}_{\kappa,\alpha\beta}^{(0,2)}$  from (5.1). They are purely transverse, and lead to the flows for  $f_{\kappa,\perp}^\nu$  and  $f_{\kappa,\perp}^D$ , see Appendix A for details and their explicit expressions. These equations are first-order differential equation in the RG scale  $\kappa$ , they can be integrated numerically, from the initial condition (5.7) down to  $\kappa \rightarrow 0$ . Since we are interested in the existence of a fixed point, it is convenient, prior to performing this integration, to non-dimensionalise all quantities by the RG scale.

## 5.2. Scaling dimensions

First, one defines running anomalous dimensions from the coefficients  $D_\kappa$  and  $\nu_\kappa$  as

$$\eta_\kappa^D = -\partial_s \ln D_\kappa \quad , \quad \eta_\kappa^\nu = -\partial_s \ln \nu_\kappa. \quad (5.10)$$

Indeed, one expects that if a fixed point is reached, these coefficients behave as power laws  $D_\kappa \sim \kappa^{-\eta^D}$  and  $\nu_\kappa \sim \kappa^{-\eta^\nu}$ . The physical anomalous dimensions are then related to the

fixed point values  $\eta_*^D$  and  $\eta_*^\nu$ . Let us determine the scaling dimensions of the fields from Eqs. (5.2,5.3). Since  $\Gamma_\kappa$  and  $\Delta\mathcal{S}_\kappa$  have no dimension, one deduces from the first term in  $\Gamma_\kappa$  that  $[u_\alpha \bar{u}_\beta] = \kappa^d$  and from the  $R_\kappa$  term in  $\Delta\mathcal{S}_\kappa$  that  $[u_\alpha \bar{u}_\beta] = \nu_\kappa \omega \kappa^{-2} \nu_\kappa^{-1}$ . This implies that the scaling dimension of the frequency is  $[\omega] = \nu_\kappa \kappa^2 \equiv \kappa^z$ , which defines the critical dynamical exponent as  $z = 2 - \eta_*^\nu$ . The scaling dimensions of the fields can be deduced from the other terms of  $\Gamma_\kappa$  as

$$[u_\alpha] = (\kappa^{d-2} D_\kappa \nu_\kappa^{-1})^{1/2}, \quad [\bar{u}_\alpha] = (\kappa^{d+2} \nu_\kappa D_\kappa^{-1})^{1/2}. \quad (5.11)$$

One may then measure wavenumbers in units of  $\kappa$ , e.g.  $\mathbf{p} = \kappa \hat{\mathbf{p}}$  and frequencies in units of  $\nu_\kappa \kappa^2$ , e.g.  $\varpi = \nu_\kappa \kappa^2 \hat{\varpi}$ , where hat symbols denote dimensionless variables. As one expects a power-law behaviour for the coefficient  $\nu_\kappa$  beyond a certain scale, e.g. the Kolmogorov scale  $\eta^{-1}$ , one can relate it to the bare viscosity  $\nu_\Lambda$  as

$$\nu_\kappa = \nu_{\eta^{-1}} (\kappa \eta)^{-\eta^\nu} \simeq \nu_\Lambda (\kappa \eta)^{-\eta^\nu}, \quad (5.12)$$

assuming that the evolution of the viscosity from the microscopic scale  $\Lambda$  up to the inverse of the Kolmogorov scale is negligible.

The non-dimensionalisation of the fields introduce a scaling dimension for the coupling of the advection term – let us denote it  $\lambda$  ( $\lambda = 1$ ). We thus define the corresponding dimensionless coupling as  $\hat{\lambda}_\kappa = (\kappa^{d-4} D_\kappa \nu_\kappa^{-3})^{1/2} \lambda$ . The Ward identities yield that  $\lambda$  is not renormalised ( $\lambda$  stays equal to one), which means that the loop contribution to its flow vanishes, *i.e.*  $\partial_s \lambda = 0$ . One thus obtains for the flow of  $\hat{\lambda}_\kappa$

$$\partial_s \hat{\lambda}_\kappa = \frac{\hat{\lambda}_\kappa}{2} (d - 4 + 3\eta_*^\nu - \eta_\kappa^D), \quad (5.13)$$

which has also been obtained in other RG approaches. One can deduce from this equation that if a non-trivial fixed-point exists ( $\hat{\lambda}_* \neq 0$ ), then it is characterised by a single independent anomalous dimension  $\eta_\kappa^D$ , as the other one can be expressed as

$$\eta_\kappa^\nu = (4 - d + \eta_\kappa^D)/3. \quad (5.14)$$

The running anomalous dimension  $\eta_\kappa^D$  should be determined by computing the flow equation for  $D_\kappa$ , which has to be integrated along with the flow equations for  $f_\kappa^\nu(\mathbf{p})$  and  $f_\kappa^\nu(\mathbf{p})$ . In the case of fully developed turbulence, the value of  $\eta_\kappa^D$  can be inferred by requiring a stationary state, that is that the mean injection rate balances the mean dissipation rate all along the flow. The average injected power by unit mass at the scale  $\kappa$  can be expressed as Canet *et al.* (2016)

$$\begin{aligned} \bar{\epsilon} &= \langle \epsilon_{\text{inj}} \rangle = \langle f_\alpha(t, \mathbf{x}) v_\alpha(t, \mathbf{x}) \rangle = \lim_{\delta t \rightarrow 0^+} \int_{\mathbf{x}'} N_{\kappa, \alpha\beta}(|\mathbf{x} - \mathbf{x}'|) G_{\kappa, \alpha\beta}^{u\bar{u}}(t + \delta t, \mathbf{x}; t, \mathbf{x}') \\ &= D_\kappa \kappa^d \lim_{\delta t \rightarrow 0^+} \left[ (d-1) \int_{\hat{\omega}, \hat{\mathbf{q}}} \hat{n}(\hat{\mathbf{q}}) e^{-i\hat{\omega}\delta t} \hat{G}_{\kappa, \perp}^{u\bar{u}}(\hat{\omega}, \hat{\mathbf{q}}) \right] \\ &\equiv D_\kappa \kappa^d \hat{\gamma}, \end{aligned} \quad (5.15)$$

where  $\hat{\gamma}$  depends only on the forcing profile since the frequency integral of the response function is one because of causality. It is given by

$$\hat{\gamma} = (d-1) \int \frac{d^d \hat{\mathbf{q}}}{(2\pi)^d} \hat{n}(\hat{\mathbf{q}}) = (d-1) \frac{2\pi^{d/2}}{(2\pi)^d \Gamma(d/2)} \int_0^\infty d\hat{q} \hat{q}^{d-1} \hat{n}(\hat{q}) \quad (5.16)$$

where the last identity holds for an isotropic forcing.

The conditions for stationarity depend on the dimension, and in particular on the main

form of energy dissipation, which differs in  $d = 3$  and  $d = 2$ . Let us focus in the following in  $d = 3$ . One can show that in this dimension, the dissipation at the Kolmogorov scale prevails on the dissipation at the boundary mediated by the regulator  $R_\kappa$ , and that it does not depend on  $\kappa$  (it is given through an integral dominated by its UV bound  $\propto \eta^{-1}$ ). One concludes that to obtain a steady state, the mean injection should balance the mean dissipation and thus it should not depend on  $\kappa$  either. This requires  $D_\kappa \sim \kappa^{-d}$ , that is

$$\eta_\kappa^D = d = 3.$$

The value of  $\eta^\nu$  is then fixed by (5.14) to  $\eta^\nu = 4/3$ .

Thus, one may express the running coefficient  $\nu_\kappa$  using (5.12) and the coefficient  $D_\kappa$  in term of the injection rate using (5.15) as

$$D_\kappa = \frac{\bar{\epsilon}}{\hat{\gamma}} \kappa^{-3} \quad \nu_\kappa = \bar{\epsilon}^{1/3} \kappa^{-4/3}, \quad (5.17)$$

where we used the definition of the Kolmogorov scale as  $\nu = \bar{\epsilon}^{1/3} \eta^{4/3}$ .

Finally, the scaling dimension of any correlation or vertex function can be deduced from the scaling dimensions of the fields. This yields for instance for the two-point correlation function

$$\bar{G}_{\kappa,\perp}^{uu}(\omega, \mathbf{p}) = \frac{\bar{\epsilon}^{1/3}}{\hat{\gamma} \kappa^{13/3}} \hat{G}_{\kappa,\perp}^{uu} \left( \hat{\omega} = \frac{\omega}{\bar{\epsilon}^{1/3} \kappa^{2/3}}, \hat{\mathbf{p}} = \frac{\mathbf{p}}{\kappa} \right). \quad (5.18)$$

We present in Sec. 5.4 the results stemming from the numerical integration of the dimensionless flow equations.

### 5.3. Fixed-point renormalisation functions

Using the analysis of Sec. 5.2, we define the dimensionless functions  $\hat{h}_\kappa^\nu$  and  $\hat{h}_\kappa^D$  as

$$f_{\kappa,\perp}^\nu(\mathbf{p}) = \nu_\kappa \kappa^2 \hat{p}^2 \hat{h}_\kappa^\nu(\hat{\mathbf{p}}) \quad \text{and} \quad f_{\kappa,\perp}^D(\mathbf{p}) = D_\kappa \hat{p}^2 \hat{h}_\kappa^D(\hat{\mathbf{p}}). \quad (5.19)$$

Their flow equations are given by

$$\begin{aligned} \partial_s \hat{h}_\kappa^\nu(\hat{\mathbf{p}}) &= \eta_\kappa^\nu \hat{h}_\kappa^\nu(\hat{\mathbf{p}}) + \hat{\mathbf{p}} \partial_{\hat{\mathbf{p}}} \hat{h}_\kappa^\nu(\hat{\mathbf{p}}) + \nu_\kappa^{-1} \frac{\partial_s f_{\kappa,\perp}^\nu(\mathbf{p})}{\hat{p}^2} \\ \partial_s \hat{h}_\kappa^D(\hat{\mathbf{p}}) &= (\eta_\kappa^D + 2) \hat{h}_\kappa^D(\hat{\mathbf{p}}) + \hat{\mathbf{p}} \partial_{\hat{\mathbf{p}}} \hat{h}_\kappa^D(\hat{\mathbf{p}}) + D_\kappa^{-1} \frac{\partial_s f_{\kappa,\perp}^D(\mathbf{p})}{\hat{p}^2} \end{aligned} \quad (5.20)$$

with the substitutions for dimensionless quantities in the flow equations (A 8) and (A 9) for  $\partial_s f_{\kappa,\perp}^\nu(\mathbf{p})$  and  $\partial_s f_{\kappa,\perp}^D(\mathbf{p})$ .

These flow equations can be integrated numerically from the initial condition (5.7) which corresponds to  $\hat{h}_\kappa^\nu(\hat{\mathbf{p}}) = 1$  and  $\hat{h}_\kappa^D(\hat{\mathbf{p}}) = 0$ . The wavevectors are discretised on a (modulus, angle) grid. At each RG time step  $s$ , the derivatives are computed using 5-point finite differences, the integrals are computed using Gauss-Legendre quadrature, with both interpolation and extrapolation procedures to evaluate combinations  $\mathbf{p} + \mathbf{q}$  outside of the mesh points. One observes that the functions  $\hat{h}_\kappa^\nu$  and  $\hat{h}_\kappa^D$  smoothly deform from their constant initial condition to reach a fixed point where they stop evolving after a typical RG time  $s \lesssim -10$ . This is illustrated on Fig. 2, where the fixed-point functions recorded at  $s = -25$  are highlighted with a thick line. This result shows that the fully developed turbulent state corresponds to a fixed point of the RG flow, which means that it is scale invariant. However, this fixed-point exhibits a very peculiar feature.

Indeed, the fixed point functions are found to behave as power laws at large wavenumbers as expected. However, the corresponding exponents differ from their K41 values. The functions

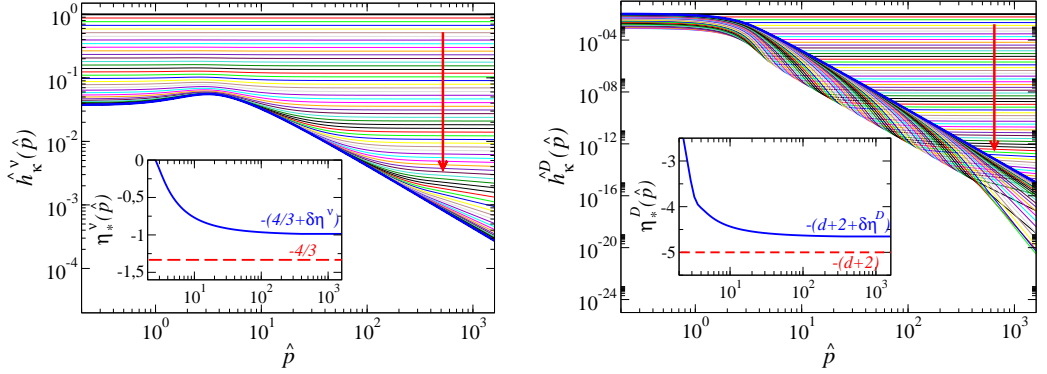


Figure 2: RG evolution of the renormalisation functions  $\hat{h}_\kappa^\nu$  and  $\hat{h}_\kappa^D$  with the RG scale, from constant initial conditions (black horizontal lines) to their fixed-point shape (bold blue lines). The red arrows indicate the RG flow, decreasing the RG time from  $s = 0$  to  $s = -25$ . *Insets*: local exponents, defined by (5.22), at the fixed-point, with the corresponding K41 values indicated as dashed lines.

can be described at large  $\hat{p}$  as

$$\hat{h}_\kappa^\nu(\hat{p}) \sim \hat{p}^{-\eta^\nu + \delta\eta^\nu} \quad \text{and} \quad \hat{h}_\kappa^D(\hat{p}) \sim \hat{p}^{-(\eta^D + 2) + \delta\eta^D} \quad (5.21)$$

where  $\delta\eta^\nu$  and  $\delta\eta^D$  are the deviations from K41 scaling. The insets of Fig. 2 show the actual local exponents  $\eta_{\text{loc}}^\nu$  and  $\eta_{\text{loc}}^D$  at the fixed-point defined as

$$\eta_{\text{loc}}^D = \frac{d \ln \hat{h}_*^D(\hat{p})}{d \ln \hat{p}} \quad \eta_{\text{loc}}^\nu = \frac{d \ln \hat{h}_*^\nu(\hat{p})}{d \ln \hat{p}}. \quad (5.22)$$

When a function  $f(x)$  behaves as a power law  $f(x) \sim x^\alpha$  in some range, the local exponent defined by this logarithmic derivative identifies with  $\alpha$  on this range. It is clear that  $\eta_{\text{loc}}^\nu$  differs from its expected K41 value  $\eta^\nu = 4/3$ , and similarly for  $\eta_{\text{loc}}^D$ . The deviations are estimated numerically as  $\delta\eta^\nu \simeq \delta\eta^D \simeq 0.33$ .

The very existence of these deviations originates in an unusual property of the flow equations, which is termed non-decoupling. It will be explained in details in Sec. 6, we here simply give a brief account. Non-decoupling means that the loop contributions  $\frac{\partial_s f_{\kappa, \perp}^D(\mathbf{p})}{\hat{p}^2}$  and  $\frac{\partial_s f_{\kappa, \perp}^\nu(\mathbf{p})}{p^2}$  in the flow equations (5.20) do not become negligible in the limit of large wavenumbers compared to the other terms. Intuitively, a large wavenumber is equivalent to a large mass, and degrees of freedom with a large mass are damped and do not contribute in the dynamics at large (non-microscopic) scale. This means that the IR (effective) properties are not affected by the UV (microscopic) details, and this pertains to the mechanism for universality. For turbulence, it is not the case, and it leads to an explicit breaking of scale invariance (see Sec. 6). Within the simple LO approximation, the signature of this non-decoupling is that the exponent of the power-laws at large  $p$  are not fixed by the scaling dimensions  $\eta_*^\nu$  and  $\eta_*^D$ , but exhibit anomalous scaling, carried by the deviations  $\delta\eta^\nu$  and  $\delta\eta^D$ . However, it turns out that this peculiar feature plays no role for *equal-time* quantities. The LO approximation leads to Kolmogorov scaling for the energy spectrum and the structure functions, as we now show.

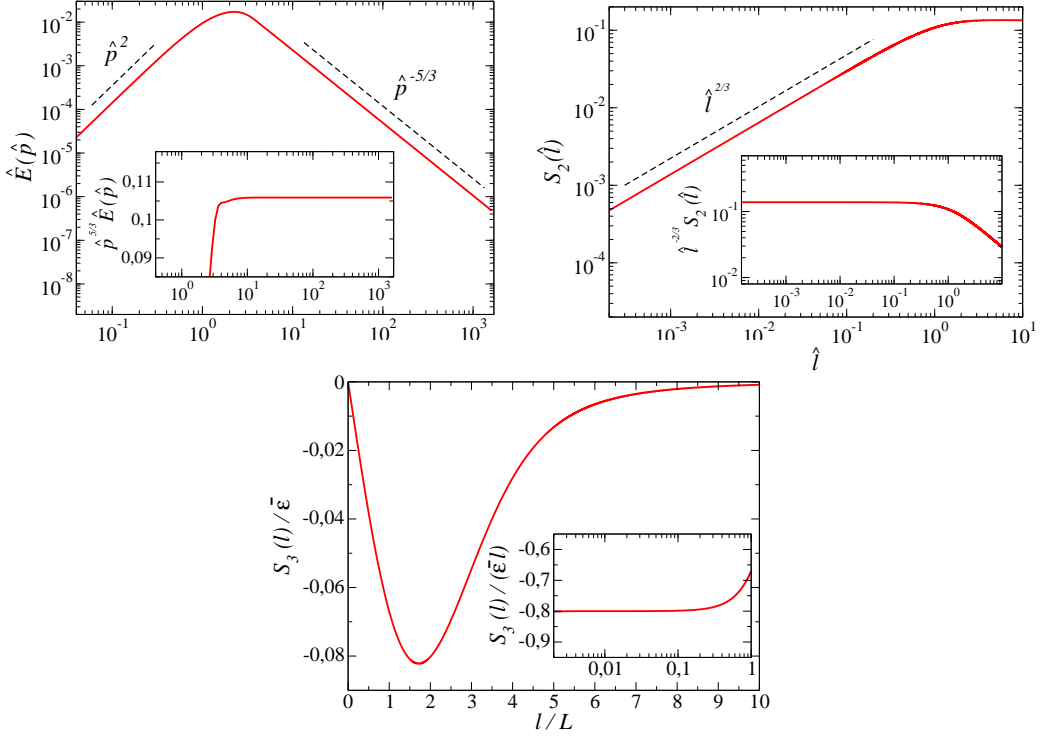


Figure 3: *Top left panel*: Kinetic energy spectrum (*main plot*) and compensated one (*inset*); *Top right panel*: Second order structure function (*main plot*) and compensated one (*inset*); *Bottom panel*: Third order structure function (*main plot*) and compensated one (*inset*). All functions are calculated from the fixed-point obtained within the LO approximation in  $d = 3$ .

#### 5.4. Kinetic energy spectrum and second order structure function

Let us now compute from this fixed point physical observables, such as the kinetic energy spectrum and the second-order structure function. The mean total energy per unit mass is given by

$$\frac{1}{2} \langle \mathbf{v}(t, \mathbf{x})^2 \rangle = \frac{1}{2} G_{\alpha\alpha}^{uu}(0, 0) = \frac{1}{2} \int \frac{d^d \mathbf{p}}{(2\pi)^d} \int \frac{d\omega}{2\pi} G_{\alpha\alpha}^{uu}(\omega, \mathbf{p}). \quad (5.23)$$

The kinetic energy spectrum, defined as the energy density at wavenumber  $p$ , is hence given for an isotropic flow by

$$\mathcal{E}(p) = \frac{1}{2} \frac{2\pi^{d/2}}{(2\pi)^d \Gamma(d/2)} p^{d-1} (d-1) \int \frac{d\omega}{2\pi} G_{\perp}^{uu}(\omega, p). \quad (5.24)$$

The statistical properties of the system are obtained once all fluctuations have been integrated over, *i.e.* in the limit  $\kappa \rightarrow 0$ . Since the RG flow reaches a fixed-point, the limit  $\kappa \rightarrow 0$  simply amounts to evaluating at the fixed-point. Within the LO approximation, and in  $d = 3$ , one finds

$$\mathcal{E}(p) = \frac{\bar{\epsilon}^{2/3}}{\hat{\gamma} \kappa^{5/3}} \hat{E}(\hat{p}), \quad \text{with} \quad \hat{E}(\hat{p}) = \frac{1}{2\pi^2} \hat{p}^2 \frac{\hat{h}_*^D(\hat{p})}{\hat{h}_*^V(\hat{p})}. \quad (5.25)$$

The function  $\hat{E}(\hat{p})$  is represented in Fig. 3, with in the inset the compensated spectrum  $\hat{p}^{5/3} \hat{E}(\hat{p})$ . At small  $\hat{p}$ , it behaves as  $\hat{p}^2$ , which reflects equipartition of energy. At large  $\hat{p}$ ,

the two corrections  $\delta\eta^\nu$  and  $\delta\eta^D$  turn out to compensate in (5.25), such that one accurately recovers the Kolmogorov spectrum  $\hat{\mathcal{E}}(\hat{p}) \simeq a\hat{p}^{-5/3}$ , with  $a$  a numerical factor, and thus one obtains

$$\mathcal{E}(p) \sim \frac{a}{\hat{\gamma}} \bar{\epsilon}^{2/3} p^{-5/3} \equiv C_K \bar{\epsilon}^{2/3} p^{-5/3}. \quad (5.26)$$

The Kolmogorov constant  $C_K$  is given by the ratio  $a/\hat{\gamma}$ . The value of  $a$  can be read off from the plateau value of the compensated spectrum  $\hat{p}^{5/3}\hat{\mathcal{E}}(\hat{p})$  shown in the inset of Fig. 3, which yields  $a \simeq 0.106$ . For the present choice of forcing profile, which is  $\hat{h}(\hat{x}) = \hat{x}^2 e^{-\hat{x}^2}$ , one obtains from (5.16)  $\hat{\gamma} = \frac{3}{8}\pi^{-3/2}$ , and thus  $C_K \simeq 1.572$ , which is in agreement with typical measured experimental values. Note that  $C_K$  is a priori non-universal since it explicitly depends on the forcing profile through  $\hat{\gamma}$ . However, it was shown in Tomassini (1997) within a similar approximation that the numerical value of  $C_K$  varies very mildly when changing the forcing profile.

The  $n$ th order structure function is defined as

$$\mathcal{S}_n(\ell) = \left\langle [(\mathbf{v}(t, \mathbf{z} + \boldsymbol{\ell}) - \mathbf{v}(t, \mathbf{z})) \cdot \hat{\boldsymbol{\ell}}]^n \right\rangle. \quad (5.27)$$

The second order is thus given by

$$\begin{aligned} \mathcal{S}_2(\ell) &= -2\hat{\ell}_\alpha \hat{\ell}_\beta \left\langle v_\beta(t, \mathbf{z} + \boldsymbol{\ell}) v_\alpha(t, \mathbf{z}) - v_\beta(t, \mathbf{z}) v_\alpha(t, \mathbf{z}) \right\rangle \\ &= -2 \int_{\omega, \mathbf{q}} G_\perp^{uu}(\omega, \mathbf{q}) \left[ e^{i\mathbf{q} \cdot \boldsymbol{\ell}} - 1 \right] \left[ 1 - \frac{(\hat{\boldsymbol{\ell}} \cdot \mathbf{q})^2}{q^2} \right]. \end{aligned} \quad (5.28)$$

Within the LO approximation and in  $d = 3$ , one obtains

$$\mathcal{S}_2(\ell) = \frac{\bar{\epsilon}^{2/3}}{\hat{\gamma}} \kappa^{-2/3} \hat{S}_2(\hat{\ell}) \quad \text{with} \quad \hat{S}_2(\hat{\ell}) = -\frac{1}{2\pi^2} \int_0^\infty d\hat{q} \hat{q}^2 \frac{\hat{h}_*^D(\hat{p})}{\hat{h}_*^\nu(\hat{p})} I_2(\hat{q}\hat{\ell}) \quad (5.29)$$

and  $I_2$  given by the integral

$$I_2(x) = \frac{4}{x^3} \left[ \sin x - x \cos x - \frac{x^3}{3} \right]. \quad (5.30)$$

The function  $\hat{S}_2(\hat{\ell})$  is plotted in Fig. 3. Again, for small  $\hat{\ell}$ , the corrections  $\delta\eta^\nu$  and  $\delta\eta^D$  precisely compensate such that the second order structure function behaves as the power law  $\hat{S}_2(\hat{\ell}) = b\hat{\ell}^{2/3}$  with Kolmogorov exponent, and one has

$$\mathcal{S}_2(\ell) = \bar{\epsilon}^{2/3} \frac{b}{\hat{\gamma}} \ell^{2/3}. \quad (5.31)$$

Finally, let us emphasise that the third-order structure function is fixed by the gauged-shift symmetry of the response fields (or equivalently by the Kármán-Howarth relation), and thus one recovers the exact result for  $\mathcal{S}_3$  for any approximation of the form (5.2) which automatically preserves the symmetries, and in particular already at LO. Indeed, the third-order structure function can be expressed, using translational invariance and incompressibility as Tarpin (2018)

$$\begin{aligned} \mathcal{S}_3(\ell) &= 6\hat{\ell}_\alpha \hat{\ell}_\beta \hat{\ell}_\gamma \langle v_\alpha(t, 0) v_\beta(t, 0) v_\gamma(t, \boldsymbol{\ell}) \rangle \\ &= 6\hat{\ell}_\alpha \hat{\ell}_\beta \hat{\ell}_\gamma \int_{\omega, \mathbf{q}} \left[ q^2 (\delta_{\beta\gamma} q_\alpha + \delta_{\alpha\gamma} q_\beta) - 2q_\alpha q_\beta q_\delta \right] \frac{K(\omega, \mathbf{q})}{iq^4} e^{i(\mathbf{q} \cdot \boldsymbol{\ell})} \\ &= \frac{6}{(2\pi)^2} \int_0^\infty dq q I_3(q\ell) \int_{-\infty}^\infty \frac{d\omega}{2\pi} K(\omega, \mathbf{q}) \end{aligned} \quad (5.32)$$

where  $I_3$  is given by the integral

$$I_3(x) = -\frac{8}{x^4} \left[ (x^3 - 3) \sin x + 3x \cos x \right]. \quad (5.33)$$

The function  $K$  is related to the scalar part of the correlation function  $\frac{\delta \mathcal{W}}{\delta L_{\alpha\beta}(t,0) \delta J_\gamma(t,\ell)}$ , which can be expressed in terms of the two-point functions. Indeed, taking one functional derivative of the Ward identity Eq. (3.45) with respect to  $J_\gamma$ , and evaluating at zero sources, one obtains in Fourier space

$$K(\omega, \mathbf{q}) = (i\omega - \nu q^2) G_\perp^{uu}(\omega, \mathbf{q}) + 2D_L \hat{n}(L\mathbf{q}) G_\perp^{u\bar{u}}(-\omega, \mathbf{q}), \quad (5.34)$$

where  $D_L$  is the forcing amplitude at the integral scale, related to the mean energy injection as  $\bar{\epsilon} = D_L L^{-3} \hat{\gamma}$  according to Eq. (5.15) Tarpin (2018). The first contribution to  $S_3$ , proportional to  $G_\perp^{uu}$ , can be evaluated within the LO approximation. One obtains that it behaves at small  $\ell$  as  $(\ell/\eta)^{-1/3}$ , which implies that it is negligible in the inertial range. In this range,  $S_3$  is hence dominated by the second contribution, proportional to  $G_\perp^{u\bar{u}}$ , which writes,

$$S_3(\ell) = -\frac{6}{(2\pi)^2} \frac{\bar{\epsilon}}{\hat{\gamma}} L \int_0^\infty dy y I_3\left(y \frac{\ell}{L}\right) \hat{n}(y) \quad (5.35)$$

The result is represented in Fig. 3, for the choice  $\hat{n}(x) = x^2 e^{-x^2}$ . one observes that the 4/5th law is recovered for scales  $\ell$  in the inertial range  $\ell \gg L$ . It can also be shown analytically from (5.35) since in the inertial range,  $I_3$  is dominated by the small values of its argument, and  $I_3(x) \sim \frac{8}{15}x$  for  $x \rightarrow 0$ . The remaining integral on  $y$  can then be identified with  $\hat{\gamma}$  defined in Eq. (5.16), which yields

$$S_3(\ell) = -\frac{4}{5} \bar{\epsilon} \ell. \quad (5.36)$$

To conclude, the merits of this approach are to unambiguously establish the existence of the fixed-point with K41 scaling associated with fully developed turbulence, for a realistic large-scale forcing, which was out of reach of standard perturbative RG approaches. The approximation used here, in the form of the LO ansatz (5.6), is rather simple, since it completely neglects the frequency dependence of the two-point functions, as well as any renormalisation of the vertices. While it is sufficient to recover the exact result for  $S_3$  and K41 scaling, it does not yield an anomalous exponent for  $S_2$ . Hence, both the frequency and field dependences are bound to be important to generate possible intermittency corrections to K41 exponents. However, more refined approximations including these aspects (such as the ones implemented for KPZ) have not been studied yet in the context of turbulence, and remain a promising but challenging route to explore in the quest of the computation of intermittency effects from first principles.

## 6. Closure in the large wavenumber limit of the FRG flow equations

This section stresses the second main achievement stemming from FRG methods in turbulence, which is the general expression for the space-time dependence of any correlation function (at any order  $n$ ) of the velocity field in the turbulent stationary state in the limit of large wavenumbers. This expression can be extended to other fields (pressure field, response fields), as well as to correlations of passive scalars transported by a turbulent flow (see Sec. 8), and it is exact in the limit of infinite wavenumbers.

The ensuing form for the two-point velocity-velocity correlation at small time delays is a Gaussian in the variable  $kt$ , where  $k$  is the wavenumber and  $t$  the time delay. As stated in the introduction, this Gaussian decay was early predicted based on a simplified model

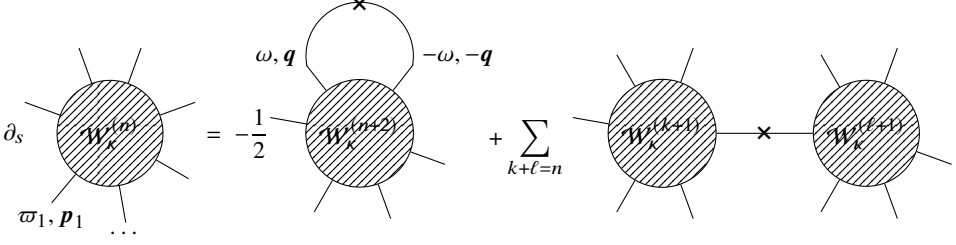


Figure 4: Diagrammatic representation of the flow of an arbitrary  $n$ -point generalised correlation function  $\mathcal{W}_\kappa^{(n)}$ . The crosses represent the derivative of the regulator  $\partial_\kappa \mathcal{R}_\kappa$  and the lines the propagator  $\bar{G}_\kappa$ .

for random advection Kraichnan (1964), although the corresponding assumptions cannot be justified for NS equations. The FRG framework allows to rigorously establish, from the full NS equation, that such a Gaussian form is indeed realised in turbulent flow but only at small time delays. Moreover, the results derived from FRG are much more general in two respects: first, they describe the behaviour of the correlations at any time delays, and unveil a crossover at large time to a regime of slower decorrelation, as an exponential in  $k^2 t$ ; second, they are not restricted to the two-point correlation but provide the expression for any order  $n$ -point correlation and response functions.

In the following, the principles of the derivation are first briefly reviewed in Sec. 6.1, and Sec. 6.2, before providing a simple heuristic explanation of the large time regime in Sec. 6.3. Thorough comparisons with DNS are reported in Sec. 7 and Sec. 8.

### 6.1. Exact leading order term of the flow of a $n$ -point correlation function

The derivation is based on the large wavenumber expansion, which is inspired by the BMW approximation scheme described in Sec. 4.3. Its unique feature for turbulence is that the flow equation for any correlation function can be closed without further approximation than the  $p_i \rightarrow \infty$  limit, and becomes exact in this limit.

The starting point is the exact flow equation (4.5) for the generating functional  $\mathcal{W}_\kappa$ . A  $n$ -point correlation function  $\mathcal{W}_\kappa^{(n)}$  is defined according to (3.13) as the  $n$ th functional derivative of  $\mathcal{W}_\kappa$  with respect to the corresponding sources  $\mathcal{J}_1, \dots, \mathcal{J}_n$ . The flow equation for  $\mathcal{W}_\kappa^{(n)}$  is thus obtained by taking  $n$  functional derivatives of Eq. (4.5), which yields

$$\partial_s \frac{\delta^n \mathcal{W}_\kappa[\mathcal{J}]}{\delta \mathcal{J}_1 \cdots \delta \mathcal{J}_n} = -\frac{1}{2} \partial_s \mathcal{R}_{\kappa, \alpha\beta} \left[ \frac{\delta^{n+2} \mathcal{W}_\kappa[\mathcal{J}]}{\delta \mathcal{J}_\alpha \delta \mathcal{J}_\beta \delta \mathcal{J}_1 \cdots \delta \mathcal{J}_n} + \sum_{\substack{(\{a_k\}, \{a_\ell\}) \\ k+\ell=n}} \frac{\delta^{k+1} \mathcal{W}_\kappa[\mathcal{J}]}{\delta \mathcal{J}_\alpha \delta \mathcal{J}_{a_1} \cdots \delta \mathcal{J}_{a_k}} \frac{\delta^{\ell+1} \mathcal{W}_\kappa[\mathcal{J}]}{\delta \mathcal{J}_\beta \delta \mathcal{J}_{a_{k+1}} \cdots \delta \mathcal{J}_{a_{k+\ell}}} \right], \quad (6.1)$$

where  $(\{a_k\}, \{a_\ell\})$  indicates all possible bipartitions of the indices  $1, \dots, n$ . This equation can be represented diagrammatically as in Fig. 4, where the cross stands for  $\partial_s \mathcal{R}_\kappa$ . It is clear that in the second diagram, the internal line carries a partial sum of external wavenectors  $\sum_{i=1}^{k+1} \mathbf{p}_i$ , which enters the derivative of the regulator. If one considers the large wavenumber limit, defined as the limit where all external wavenectors and all their partial sums are large with respect to the RG scale  $\kappa$ , then this diagram is exponentially suppressed, and can be neglected in this limit.

Let us now consider the first diagram. In this diagram, the derivative of the regulator

carries a loop wavevector  $\mathbf{q}$ , which enters two of the legs of  $\mathcal{W}_\kappa^{(n+2)}$ . The idea is then to apply the BMW expansion on these two legs. Technically, within the FRG framework, approximations are justified and performed on the  $\Gamma_\kappa^{(n)}$ , not directly on the  $\mathcal{W}_\kappa^{(n)}$ , because the flow equation of the formers ensures that they remain analytic at any finite scale  $\kappa$  in wavevectors and frequencies (both in the UV and in the IR) thanks to the presence of the regulator. In particular, they can be Taylor expanded. However, any  $\mathcal{W}_\kappa^{(n)}$  can be expressed in terms of the  $\Gamma_\kappa^{(n)}$ , as a sum of tree diagrams whose vertices are the  $\Gamma_\kappa^{(k)}$ ,  $k \leq n$ , and the edges the propagators. Hence,  $\mathcal{W}_\kappa^{(n+2)}$  can be thought of, in its  $\Gamma$  representation, as a functional of the average field  $\Psi$ , leading to

$$\partial_s \frac{\delta^n \mathcal{W}_\kappa [\mathcal{J}]}{\delta \mathcal{J}_1 \cdots \delta \mathcal{J}_n} = -\frac{1}{2} \partial_s \mathcal{R}_{\kappa, \alpha\beta} \frac{\delta \Psi_\gamma}{\delta \mathcal{J}_\alpha} \frac{\delta \Psi_\delta}{\delta \mathcal{J}_\beta} \frac{\delta^2}{\delta \Psi_\gamma \delta \Psi_\delta} \frac{\delta^n \mathcal{W}_\kappa [\mathcal{J}]}{\delta \mathcal{J}_1 \cdots \delta \mathcal{J}_n}, \quad (6.2)$$

where  $\frac{\delta \Psi_\gamma}{\delta \mathcal{J}_\alpha} = \mathcal{W}_{\kappa, \gamma\alpha}^{(2)} \equiv G_{\kappa, \gamma\alpha}$  are simply propagators. The loop wavevector  $\mathbf{q}$  then enters either a propagator  $G_\kappa$  or a vertex  $\Gamma_\kappa^{(k)}$ , which can be evaluated in the limit  $\mathbf{q} \rightarrow 0$ . At this stage, the symmetries, through the set of associated Ward identities for the  $\Gamma_\kappa^{(n)}$ , play a crucial role. Indeed, the analysis of Sec. 3.3 has established that any vertex  $\Gamma_\kappa^{(n)}$  with one wavevector set to zero can be expressed exactly in a very simple way: if the  $\mathbf{q} = 0$  is carried by a velocity field, then it is given in terms of lower-order vertices  $\Gamma_\kappa^{(n-1)}$  through the  $\mathcal{D}_\alpha$  operator Eq. (3.33), or it vanishes if it is carried by any other fields. This has a stringent consequence, which is that only contributions where  $\Psi_\gamma$  and  $\Psi_\delta$  are velocity fields survive in Eq. (6.2), yielding

$$\partial_s \mathcal{W}_{\kappa, \alpha_1 \cdots \alpha_n}^{(n)} = -\frac{1}{2} \int_{\omega, \mathbf{q}} \left( \bar{G}_{u_\gamma u_\alpha} \partial_s \mathcal{R}_{\kappa, u_\alpha u_\beta} \bar{G}_{u_\beta u_\delta} \right) (\omega, \mathbf{q}) \frac{\delta}{\delta u_\gamma(-\omega, -\mathbf{q})} \frac{\delta}{\delta u_\delta(\omega, \mathbf{q})} \mathcal{W}_{\kappa, \alpha_1 \cdots \alpha_n}^{(n)}, \quad (6.3)$$

where the  $\alpha_k$ 's denote both the field indices and their space components. One can then prove, after some algebra, the following identity

$$\frac{\delta}{\delta u_\gamma(-\omega, -\mathbf{q})} \frac{\delta}{\delta u_\delta(\omega, \mathbf{q})} \mathcal{W}_{\kappa, \alpha_1 \cdots \alpha_n}^{(n)}(\omega_1, \mathbf{p}_1, \cdots) \Big|_{\mathbf{q}=0} = \mathcal{D}_\gamma(-\omega) \mathcal{D}_\delta(\omega) \mathcal{W}_{\kappa, \alpha_1 \cdots \alpha_n}^{(n)}(\omega_1, \mathbf{p}_1, \cdots). \quad (6.4)$$

The proof relies on expressing the  $\mathcal{W}_\kappa^{(n)}$  in terms of the  $\Gamma_\kappa^{(n)}$  for which the wavenumber expansions are justified and then on using the Ward identities. We refer the interested reader to Tarpin *et al.* (2018); Tarpin (2018) for the complete proof. One thus obtains the explicit flow equation

$$\begin{aligned} \partial_s \mathcal{W}_{\kappa, \alpha_1 \cdots \alpha_n}^{(n)}(\cdots, \varpi_i, \mathbf{p}_i, \cdots) &= \frac{1}{2} \int_{\omega, \mathbf{q}} \left( \bar{G}_{u_\gamma u_\alpha} \partial_s \mathcal{R}_{\kappa, u_\alpha u_\beta} \bar{G}_{u_\beta u_\delta} \right) (\omega, \mathbf{q}) \\ &\quad \sum_{k, \ell=1}^n \frac{p_k^\gamma p_\ell^\delta}{\omega^2} \mathcal{W}_{\kappa, \alpha_1 \cdots \alpha_n}^{(n)}(\cdots, \varpi_k + \omega, \mathbf{p}_k, \cdots, \varpi_\ell - \omega, \mathbf{p}_\ell, \cdots) + \mathcal{O}(p_{\max}), \end{aligned} \quad (6.5)$$

which constitutes one of the most important results obtained with FRG methods. The flow equation for an arbitrary  $n$ -point connected correlation function  $\mathcal{W}_\kappa^{(n)}$  (of any fields, velocity, pressure, response fields, ...) is closed in the large wavenumber limit, in the sense that it no longer involves higher-order vertices. Remarkably, it does not depend on the whole hierarchy of  $\mathcal{W}_\kappa^{(m)}$  with  $m \leq n$ , but only on the  $n$ -point function itself and propagators (*i.e.* two-point

functions), and it is a linear equation in  $\mathcal{W}_\kappa^{(n)}$ . Once the two-point functions are determined (within some approximation scheme), any  $n$ -point correlations can be simply obtained. The term on the r.h.s. is calculated exactly, *i.e.* it is the exact leading term in the large wavenumber expansion. Subleading corrections are at most of order  $p_{\max}$  where  $p_{\max}$  indicates the largest external wavevector at which the function is evaluated.

This equation can be further simplified, by noting that  $\mathcal{W}_\kappa^{(n)}$  in the r.h.s. does not enter the integral over  $\mathbf{q}$ , but only the integral over the internal frequency  $\omega$ . Moreover,  $\mathcal{W}_\kappa^{(n)}$  depends on the latter only through local shifts of the external frequencies. Hence, let us denote by  $H_{\kappa,\gamma\delta}$  the term containing the propagators and the regulator

$$H_{\kappa,\gamma\delta}(\omega, \mathbf{q}) = \left( \bar{G}_{u_\gamma u_\alpha} \partial_s \mathcal{R}_{\kappa, u_\alpha u_\beta} \bar{G}_{u_\beta u_\delta} \right) (\omega, \mathbf{q}). \quad (6.6)$$

One can show that because of incompressibility, the propagators are transverse, hence  $H_{\kappa,\gamma\delta}(\omega, \mathbf{q}) = P_{\gamma\delta}^\perp(\mathbf{q}) H_{\kappa,\perp}(\omega, \mathbf{q})$ . Finally, by Fourier transforming back in time variables, the shifts in frequency can be transferred to the Fourier exponentials, such that the function  $\mathcal{W}_\kappa^{(n)}$  in the mixed time-wavevector coordinates  $(t_i, \mathbf{p}_i)$  can be pulled out of the frequency integral also, yielding

$$\begin{aligned} \partial_s \mathcal{W}_{\kappa, \alpha_1 \dots \alpha_n}^{(n)}(\dots, t_i, \mathbf{p}_i, \dots) &= \frac{d-1}{2d} \mathcal{W}_{\kappa, \alpha_1 \dots \alpha_n}^{(n)}(\dots, t_i, \mathbf{p}_i, \dots) \\ &\times \sum_{k, \ell=1}^n \mathbf{p}_k \cdot \mathbf{p}_\ell \int_{\omega, \mathbf{q}} H_{\kappa, \perp}(\omega, \mathbf{q}) \frac{e^{i\omega(t_k - t_\ell)} - e^{i\omega t_k} - e^{-i\omega t_\ell} + 1}{\omega^2} + O(p_{\max}). \end{aligned} \quad (6.7)$$

Thus, one is left with a linear ordinary differential equation, which can be solved explicitly, as detailed in Sec. 6.2. Again, the detailed proof of this expression can be found in Tarpin *et al.* (2018); Tarpin (2018). We discuss in Appendix B the next-to-leading order in the large wavenumber expansion, which has been computed for 2D turbulence in Tarpin *et al.* (2019).

## 6.2. General expression of the time-dependence of $n$ -point correlation functions

Let us now discuss the form of the general solution of the flow equation (6.7) for a generalised correlation function  $\mathcal{W}_\kappa^{(n)}$ . As emphasised in Sec. 6.1, Eq. (6.7) is very special in many respects: i) it is closed as it depends only on  $\mathcal{W}_\kappa^{(n)}$  (besides the propagators) and not on higher-order correlation functions, ii) it is linear in  $\mathcal{W}_\kappa^{(n)}$ , iii) the leading order in the large  $p$  expansion is exact, and iv) it does not decouple, which implies that the large wavenumber limit contains non-trivial information. This information is related to the breaking of standard scale invariance, and reflects the fact that the small-scale properties of turbulence are affected by the large scales.

We have shown in Sec. 5 that the FRG flow for NS equation, in some reasonable approximation, with a physical large-scale forcing, reaches a fixed point. This means that the flow essentially stops when  $\kappa$  crosses the integral scale  $L^{-1}$ . However, because of the non-decoupling, the large scale remains imprinted in the solution. It is instructive to uncover the underlying mechanism. At a fixed-point of a RG flow, the system does not depend any longer on the RG scale  $\kappa$  by definition, which leads to scale invariance. The usual way to evidence such a behaviour is to introduce as in Sec. 5 non-dimensionalised quantities, denoted with a hat symbol. Wavevectors are measured in units of  $\kappa$ , e.g.  $\hat{\mathbf{p}} = \mathbf{p}/\kappa$ , frequencies in units of  $\nu_\kappa \kappa^2$ , e.g.  $\hat{\omega} = \omega/(\nu_\kappa \kappa^2)$ . Denoting generically  $d_n$  the scaling dimension of a given correlation function  $\mathcal{W}_\kappa^{(n)}$ , one also defines  $\hat{\mathcal{W}}_{\kappa, \alpha_1 \dots \alpha_n}^{(n)}(\dots, \hat{t}_i, \hat{\mathbf{p}}_i, \dots) = \frac{\mathcal{W}_{\kappa, \alpha_1 \dots \alpha_n}^{(n)}(\dots, \nu_\kappa \kappa^2 t_i, \mathbf{p}_i/\kappa, \dots)}{\kappa^{d_n}}$ . For a generalised correlation function of  $m$  velocity fields

and  $\bar{m}$  response fields with  $m + \bar{m} = n$  in mixed time-wavevector coordinates, one has  $d_n = 3(m - 1) + (m - \bar{m}/3)$  in  $d = 3$ . The flow equation for the dimensionless correlation function then writes

$$\left\{ \partial_s - d_n - \hat{\mathbf{p}}_i \cdot \partial_{\hat{\mathbf{p}}_i} + z \hat{t}_i \partial_{\hat{t}_i} \right\} \hat{\mathcal{W}}_{\kappa, \alpha_1 \dots \alpha_n}^{(n)}(\dots, \hat{t}_i, \hat{\mathbf{p}}_i, \dots) = \hat{\mathcal{F}}_{\text{loop}}(\dots, \hat{t}_i, \hat{\mathbf{p}}_i, \dots), \quad (6.8)$$

where  $\hat{\mathcal{F}}_{\text{loop}}$  denotes the non-linear part of the flow, corresponding to the contribution of the loop (6.7), expressed in dimensionless quantities.

Scale invariance, as encountered in usual critical phenomena (say at a second order phase transition), emerges if two conditions are fulfilled: existence of a fixed-point, and decoupling. Indeed, let us assume that the flow reaches a fixed-point, which means  $\partial_s \hat{\mathcal{W}}_{\kappa}^{(n)} = 0$  and that decoupling occurs, which means that the loop contribution of the flow is negligible in the limit of large wavenumber, *i.e.*

$$\frac{\hat{\mathcal{F}}_{\text{loop}}}{\hat{\mathcal{W}}_{\kappa}^{(n)}} \xrightarrow{\hat{\mathbf{p}}_i \rightarrow \infty} 0. \quad (6.9)$$

One can easily show, using some elementary changes of variables, that the general form of the solution to the remaining homogeneous equation is a scaling form

$$\hat{\mathcal{W}}_{*, \alpha_1 \dots \alpha_n}^{(n)}(\dots, \hat{t}_i, \hat{\mathbf{p}}_i, \dots) = \frac{1}{\hat{p}_{\text{tot}}^{d_n}} \hat{w}_{\alpha_1 \dots \alpha_n}^{(n)}\left(\dots, \hat{t}_i \hat{p}_i^z, \frac{\hat{\mathbf{p}}_i}{\hat{p}_i}, \dots\right), \quad (6.10)$$

where  $\hat{p}_{\text{tot}} = \sum_{i=1}^{n-1} \hat{p}_i$  and  $\hat{w}^{(n)}$  is a universal scaling function which form is not known, and could be determined by explicitly integrating the flow equation.

If there is no decoupling, *i.e.* if the condition (6.9) does not hold, the solution to (6.8) is no longer a scaling form, but is modified by the loop contribution. The explicit expression of this solution can be obtained as an integral expression, which can be simplified in two limits, the limits of small and large time delays, that we study separately.

### 6.2.1. Small time regime

The limit of small time delays corresponds to the limit where all  $\hat{t}_i \rightarrow 0$ . In this limit, one can expand the exponential in the second line of (6.7)

$$\int_{\omega, \mathbf{q}} H_{\kappa, \pm}(\omega, \mathbf{q}) \frac{e^{i\omega(t_k - t_\ell)} - e^{i\omega t_k} - e^{-i\omega t_\ell} + 1}{\omega^2} \xrightarrow{t_i \rightarrow 0} I_{\kappa} t_k t_\ell \quad \text{with} \quad I_{\kappa} \equiv \int_{\omega, \mathbf{q}} H_{\kappa, \pm}(\omega, \mathbf{q}). \quad (6.11)$$

Note that the explicit expression of  $H_{\kappa}$  is not needed in the following, one only demands that the frequency integral converges. The flow equation for the dimensionless  $\hat{\mathcal{W}}_{\kappa}^{(n)}$  then simplifies to

$$\left\{ \partial_s - d_n - \hat{\mathbf{p}}_i \cdot \partial_{\hat{\mathbf{p}}_i} + z \hat{t}_i \partial_{\hat{t}_i} \right\} \hat{\mathcal{W}}_{\kappa, \alpha_1 \dots \alpha_n}^{(n)}(\dots, \hat{t}_i, \hat{\mathbf{p}}_i, \dots) = \frac{\hat{I}_{\kappa}}{3} |\hat{t}_\ell \hat{\mathbf{p}}_\ell|^2 \hat{\mathcal{W}}_{\kappa, \alpha_1 \dots \alpha_n}^{(n)}(\dots, \hat{t}_i, \hat{\mathbf{p}}_i, \dots). \quad (6.12)$$

Since the flow reaches a fixed-point, one can focus on the fixed-point equation as previously ( $\partial_s \cdot = 0$ ). At the fixed-point,  $\hat{I}_{\kappa} \rightarrow \hat{I}_*$  which is just a number. To solve the fixed-point equation, one can introduce a  $(n - 1) \times (n - 1)$  rotation matrix  $\mathcal{R}$  in wavevector space such that  $\mathcal{R}_{i1} = \frac{t_i}{\sqrt{t_\ell t_\ell}}$  and define new variables  $\boldsymbol{\rho}_k$  such that  $\mathbf{p}_i = \mathcal{R}_{ij} \boldsymbol{\rho}_j$ . This transforms the sum  $|t_\ell \mathbf{p}_\ell|^2$  into  $t_\ell t_\ell |\boldsymbol{\rho}_1|^2$ , and allows one to obtain the explicit solution, which reads in physical

units Tarpin *et al.* (2018)

$$\begin{aligned} \log \left[ \bar{\epsilon}^{\frac{\bar{m}-m}{3}} L^{-d_n} \mathcal{W}_{\alpha_1 \dots \alpha_n}^{(m, \bar{m})}(t_1, \mathbf{p}_1, \dots, t_{n-1}, \mathbf{p}_{n-1}) \right] &= -\alpha_0 \bar{\epsilon}^{2/3} L^{2/3} t_\ell t_\ell \rho_1^2 \\ -d_n \log(\rho_1 L) + w_0^{(m, \bar{m})} \alpha_1 \dots \alpha_n \left( \rho_1^{2/3} \bar{\epsilon}^{1/3} t_1, \frac{\rho_1}{\rho_1}, \dots, \rho_1^{2/3} \bar{\epsilon}^{1/3} t_{n-1}, \frac{\rho_{n-1}}{\rho_1} \right) &+ \mathcal{O}(p_{\max} L), \end{aligned} \quad (6.13)$$

where  $w_0^{(m, \bar{m})}$  is a universal scaling function, which explicit form is not given by the fixed point equation only, but can be computed numerically by integrating the flow equation in some approximation. The constant  $\alpha_0 = \hat{\gamma}_*/2$  is non-universal since it depends on the forcing profile through  $\hat{\gamma}$ , but it does not depend on the order  $n$  of the correlation, nor on the specific fields involved (velocity, response velocity). It is thus the same number for all correlation functions of a given flow.

All the terms in the second line of (6.13) correspond to the K41 scaling form obtained in (6.10). However, these terms are subdominant, that is of the same order as the indicated neglected terms  $\mathcal{O}(p_{\max} L)$  in the flow equation. Hence, they should be consistently discarded (included in  $\mathcal{O}(p_{\max} L)$ ), and were kept here only for the sake of the discussion. As they are of the same order as the neglected terms, it means that they could receive corrections, *i.e.* be modified by these terms. In particular, at equal time, the leading term in the first line of (6.13) vanishes, and one is left with only these subdominant contributions, which are of the form K41 plus possible corrections. In other words, the FRG calculation says nothing at this order about intermittency corrections on the scaling exponents of the structure functions, which are equal-time quantities.

However, at unequal times, the important part of the result is the term in the first line of (6.13), which is the exact leading term at large wavenumber. For this reason, the most meaningful way to write this result is under the form

$$\mathcal{W}_{\alpha_1 \dots \alpha_n}^{(m, \bar{m})}(t_1, \mathbf{p}_1, \dots, t_{n-1}, \mathbf{p}_{n-1}) \propto \exp \left[ -\alpha_0 (L/\tau)^2 |t_\ell \mathbf{p}_\ell|^2 + \mathcal{O}(p_{\max} L) \right], \quad (6.14)$$

where  $\tau = (L^2/\bar{\epsilon}^{1/3})$  is the eddy turnover time at the integral scale, and  $(L/\tau)$  identifies with  $U_{\text{rms}}$ , yielding the sweeping time scale  $(U_{\text{rms}} p)^{-1}$  expected from phenomenological arguments. The salient feature of this result is that it breaks standard scale invariance, which directly originates in the non-decoupling. As stressed before, if there were decoupling, *i.e.* if the fixed point conformed with a standard critical point, a time variable could only appear through the scaling combination  $p^z t$  with  $z = 2/3$  in K41 theory. Instead, time enters in (6.14) through the combination  $pt$ , which can be interpreted as an effective dynamical exponent  $z = 1$ . This is a large correction, which can be attributed to the effect of random sweeping. As a consequence, the argument in the exponential explicitly depends on a scale, the integral scale  $L$ . This residual dependence in the integral scale of the statistical properties of turbulence in the inertial range is well-known, and crucially distinguishes turbulence from standard critical phenomena.

### 6.2.2. Large time regime

Let us now consider the large time limit of (6.7), corresponding to  $t_i \rightarrow \infty$ . One can show that in this limit

$$\begin{aligned} \int_{\omega, \mathbf{q}} H_{K, \pm}(\omega, \mathbf{q}) \frac{e^{i\omega(t_k - t_\ell)} - e^{i\omega t_k} - e^{-i\omega t_\ell} + 1}{\omega^2} \Big|_{t_i \rightarrow \infty} &\simeq \frac{J_K}{2} (|t_k| + |t_\ell| - |t_\ell - t_k|) \\ \text{with } J_K &= \int_{\mathbf{q}} H_{K, \pm}(0, \mathbf{q}), \end{aligned} \quad (6.15)$$

and thus the dimensionless flow equation for  $\mathcal{W}_\kappa^{(n)}$  becomes in this limit

$$\left\{ \partial_s - d_n - \hat{\mathbf{p}}_i \cdot \partial_{\hat{\mathbf{p}}_i} + z \hat{t}_i \partial_{\hat{t}_i} \right\} \mathcal{W}_{\kappa, \alpha_1 \dots \alpha_n}^{(n)}(\dots, \hat{t}_i, \hat{\mathbf{p}}_i, \dots) = \frac{\hat{J}_\kappa}{6} \sum_{k, \ell} \hat{\mathbf{p}}_k \cdot \hat{\mathbf{p}}_\ell \left( |\hat{t}_k| + |\hat{t}_\ell| - |\hat{t}_k - \hat{t}_\ell| \right) \mathcal{W}_{\kappa, \alpha_1 \dots \alpha_n}^{(n)}(\dots, \hat{t}_i, \hat{\mathbf{p}}_i, \dots). \quad (6.16)$$

This equation can be solved at the fixed-point in an analogous way as for the small time limit, introducing another rotation matrix such that in the new wavevector variables  $\mathbf{q}_1 = \sum_k \mathbf{p}_k$ . Specifying to equal time lags  $t_i = t$  for simplicity, the solution reads Tarpin *et al.* (2018)

$$\log \left( \bar{\epsilon}^{\frac{\bar{m}-m}{3}} L^{-d_n} \mathcal{W}_{\alpha_1 \dots \alpha_n}^{(m, \bar{m})}(t, \mathbf{p}_1, \dots, \mathbf{p}_{n-1}) \right) = -\alpha_\infty \bar{\epsilon}^{1/3} L^{4/3} |t| \varrho_1^2 - d_n \log(\varrho_1 L) + w_\infty^{(m, \bar{m})}(\alpha_1 \dots \alpha_n) \left( \varrho_1^{2/3} \bar{\epsilon}^{1/3} t, \frac{\mathbf{q}_1}{\varrho_1}, \dots, \frac{\mathbf{q}_{n-1}}{\varrho_1} \right) + \mathcal{O}(p_{\max} L). \quad (6.17)$$

The non-universal constant  $\alpha_\infty = \hat{\gamma} \hat{J}_*/4$  is again the same for any generalised correlation function, irrespective of its order or fields content. Moreover, the same comments apply for the subleading terms in the second line of (6.17): they merely represent K41 scaling, with possible corrections induced by the neglected terms. The main feature of this solution is thus captured by the expression

$$\mathcal{W}_{\alpha_1 \dots \alpha_n}^{(m, \bar{m})}(t_1, \mathbf{p}_1, \dots, t_{n-1}, \mathbf{p}_{n-1}) \propto \exp \left( -\alpha_\infty (L^2/\tau) \left| \sum_{\ell} \mathbf{p}_\ell \right|^2 |t| + \mathcal{O}(p_{\max} L) \right). \quad (6.18)$$

At large time delays, the temporal decay of correlation functions is also sensitive to the large scale and thus explicitly breaks scale invariance as in the small time regime. However, the decay drastically slows down, since it crosses over for all wavenumbers from a Gaussian at small time delays to an exponential at large ones. Note that the dependence in the wavenumbers is quadratic in both regime. This large time regime had not been predicted before. However, it was already in germ in early studies of sweeping, as was noted in Gorbunova *et al.* (2021a). This allows one to provide a simple physical interpretation of these two regimes, see Sec. 6.3. Let us first summarise for later comparisons the explicit forms of the two-point correlation function of the velocity fields:

$$\begin{aligned} C_{\alpha\beta}^{(2)}(t, \mathbf{k}) &\equiv \text{FT} \left[ \left\langle v_\alpha(t_0, \mathbf{r}_0) v_\beta(t_0 + t, \mathbf{r}_0 + \mathbf{r}) \right\rangle \right] \\ &= C_{\alpha\beta}^{(2)}(0, \mathbf{k}) \begin{cases} \exp \left( -\alpha_0 (L/\tau)^2 t^2 k^2 \right) & t \ll \tau \\ \exp \left( -\alpha_\infty (L^2/\tau) |t| k^2 \right) & t \gg \tau \end{cases} \end{aligned} \quad (6.19)$$

and of the three-point correlation function at small time delays  $t_1, t_2 \ll \tau$

$$\begin{aligned} C_{\alpha\beta\gamma}^{(3)}(t_1, \mathbf{k}_1, t_2, \mathbf{k}_2) &\equiv \text{FT} \left[ \left\langle v_\alpha(t_0 + t_1, \mathbf{r}_0 + \mathbf{r}_1) v_\beta(t_0 + t_2, \mathbf{r}_0 + \mathbf{r}_2) v_\gamma(t_0, \mathbf{r}_0) \right\rangle \right] \\ &= C_{\alpha\beta\gamma}^{(3)}(0, \mathbf{k}_1, 0, \mathbf{k}_2) \exp \left( -\alpha_0 (L/\tau)^2 |\mathbf{k}_1 t_1 + \mathbf{k}_2 t_2|^2 \right). \end{aligned} \quad (6.20)$$

### 6.3. Intuitive physical interpretation

Let us now provide an heuristic derivation of these results, proposed in Gorbunova *et al.* (2021a). The early analysis of Eulerian sweeping effects by Kraichnan Kraichnan (1964) was

based on the Lagrangian expression for the Eulerian velocity field as

$$u_i(t, \mathbf{r}) = \exp_{\rightarrow}[-\boldsymbol{\xi}(t, \mathbf{r}|t_0) \cdot \nabla] u_i(t_0, \mathbf{r}) + \int_{t_0}^t ds \exp_{\rightarrow}[-\boldsymbol{\xi}(t, \mathbf{r}|s) \cdot \nabla] [v \nabla^2 u_i(s, \mathbf{r}) - \nabla_i p(s, \mathbf{r})]. \quad (6.21)$$

In this equation,  $\boldsymbol{\xi}(t, \mathbf{r}|s) = \mathbf{r} - \mathbf{X}(t, \mathbf{r}|s)$  is the Lagrangian displacement vector, where  $\mathbf{X}(t, \mathbf{r}|s)$  denotes the position at time  $s$  of the Lagrangian fluid particle located at position  $\mathbf{r}$  at time  $t$ , which satisfies

$$\frac{d}{ds} \mathbf{X}(t, \mathbf{r}|s) = \mathbf{u}(s, \mathbf{X}(t, \mathbf{r}|s)), \quad \mathbf{X}(t, \mathbf{r}|t) = \mathbf{r}. \quad (6.22)$$

One can write using (6.21) the expression of the two-point correlation function. This expression can be simplified under some general assumptions, namely slow variations in space and time of the displacement field, and its statistical independence from the initial velocities at sufficiently long time  $t$ . Moreover, since the displacements are dominated by the large scales of the flow, whose statistics are nearly Gaussian Corrsin (1959, 1962), one may plausibly further assume a normal distribution for  $\boldsymbol{\xi}$ , resulting in the following expression

$$C^{(2)}(t, \mathbf{k}) = \exp \left[ -\frac{1}{2} \langle |\boldsymbol{\xi}(t, \mathbf{r}|0)|^2 \rangle k^2 \right] C^{(2)}(0, \mathbf{k}) \left\{ 1 + O(v k^2 |t|, k U_{rms}(k) |t|) \right\}. \quad (6.23)$$

According to these arguments, the two-point velocity correlation undergoes a rapid decay in the time-difference  $t$  which arises from an average over rapid oscillations in the phases of Fourier modes due to sweeping, or ‘‘convective dephasing’’ Kraichnan (1964).

The connection with the FRG results (6.19) stems from exploiting the results of the classical study by Taylor Taylor (1922) on one-particle turbulent dispersion. In this study, the Lagrangian displacement field was shown to exhibit two regimes

$$\langle |\boldsymbol{\xi}(t, \mathbf{r}|0)|^2 \rangle \sim \begin{cases} U_{rms}^2 t^2 & |t| \ll \tau \\ 2D|t| & |t| \gg \tau \end{cases} \quad (6.24)$$

where the early-time regime corresponds to ballistic motion with the rms velocity  $U_{rms}$  and the long-time regime corresponds to diffusion with a turbulent diffusivity  $D \propto U_{rms}^2 \tau$ . Inserting these results in (6.23) then yields the FRG expressions (6.19). This argument can be generalised in principles to multi-point correlation functions, which, under the same kind of assumptions, would also lead to similar expressions as the ones derived from FRG. Of course, the FRG derivation is far more systematic and rigorous than these heuristic arguments, but the latter provide an intuitive physical interpretation of these results.

The FRG results have been tested in extensive DNS, focused on the temporal dependence of two- and three-point correlation functions. We report in Sec. 7 and Sec. 8 the main results.

## 7. Comparison with Direct Numerical Simulations

Extensive DNS were performed on high-performance computational clusters to quantitatively test the FRG results. The DNS consist of direct numerical integration of the NS equation with a stochastic forcing using standard pseudo-spectral methods and Runge-Kutta scheme for time advancement, with typical spatial resolution conforming the standard criterion  $k_{max} \eta \simeq 1.5$ , and Taylor based Reynolds numbers  $R_\lambda$  from 40 to 250 for corresponding grid sizes from  $64^3$  to  $1024^3$ . Details can be found, e.g. in Gorbunova (2021). The analysis focused on the two-point and three-point correlation function of the velocity field, which were computed in the stationary state, using averages over spherical shells in wavenumber and over successive

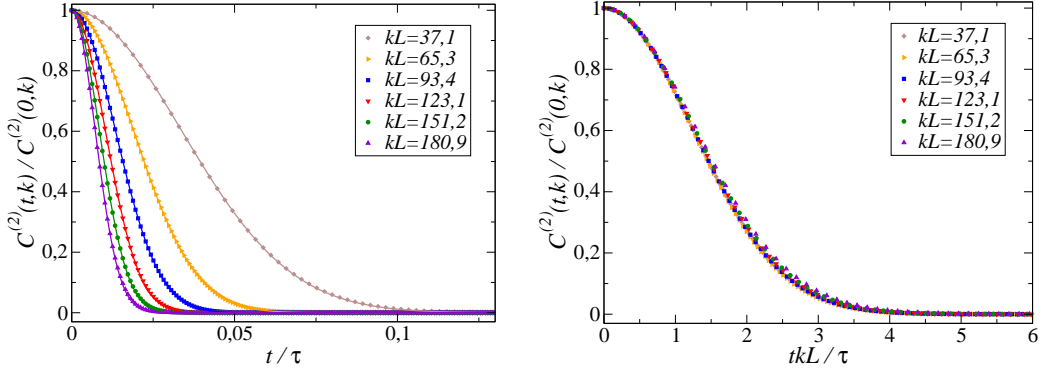


Figure 5: *Left panel*: Time dependence of the normalised two-point correlation function  $C^{(2)}(t, k)$  at different wavenumbers  $k$  for a simulation at  $R_\lambda = 90$ . Data from the simulation are represented with symbols, and their Gaussian fits with plain lines. *Right panel*: Same data plotted as a function of  $kt$ , which leads to their collapse as expected from the FRG result (6.19).

time windows, typically

$$C^{(2)}(t, \mathbf{k}) = \frac{1}{N_t} \sum_{j=1}^{N_t} \frac{1}{M_n} \sum_{\mathbf{k} \in S_n} \Re [u_i(t_{0j}, \mathbf{k}) u_i^*(t_{0j} + t, \mathbf{k})], \quad (7.1)$$

where  $N_t$  is the number of time windows in the simulation,  $M_n$  is the number of modes in the spectral spherical shell  $S_n$ , and  $k = n\Delta k$ ,  $n \in \mathbb{Z}$ .

### 7.1. Small time regime and sweeping

We first present the result for the two-point correlation function at small time delays, whose theoretical expression is given by Eq. (6.19). The time dependence of  $C^{(2)}(t, k)$  is displayed in the left panel of Fig. 5 for a sample of different wavenumbers  $k$ . The larger ones exhibit a faster decorrelation as expected. For each  $k$ , the normalised curve  $C^{(2)}(t, k)/C^{(2)}(0, k)$  is fitted with a two-parameter Gaussian function  $f_{\text{Gaus}}(t) = c \exp(-(t/\tau_0)^2)$ , which provides a very accurate model for all curves, as illustrated in the figure. Moreover, all curves collapse into a single Gaussian function when plotted as a function of  $kt$ , as expected from the theory (6.19). The fine quality of the collapse is shown in the right panel of Fig. 5.

The fitting parameter  $\tau_0$  is plotted as a function of  $kL$  in the left panel of Fig. 6, which clearly confirms that it is proportional to  $k^{-1}$  at large enough  $k$ , and not to the K41 time scale  $k^{-2/3}$ , in plain agreement with the FRG result. Similar results were also obtained in Ref. Sanada & Shanmugasundaram (1992); Favier *et al.* (2010), where the characteristic decorrelation time is estimated by integrating the correlation function, as well as in the work of Kaneda *et al.* (1999), where the characteristic time is measured through the second derivative of the correlation function.

The non-universal constant  $\alpha_0$  can be deduced from  $\tau_0$  as  $\alpha_0 = \tau^2/(\tau_0 kL)^2$ . As can be observed in the right panel of Fig. 6, this quantity reaches a plateau, which value corresponds to the theoretical  $\alpha_0$  at large  $k$ . The physical origin of the departure from the plateau at intermediate and small wavenumbers can be clearly identified in the simulations as a ‘‘contamination’’ from the forcing Gorbunova *et al.* (2021a). Indeed, by analyzing the modal energy transfers, one observes that the plateau is reached when the energy transfer to a mode  $k$  is local, *i.e.* mediated by neighbouring modes only through the cascade process. The modes at intermediate and small  $k$  also receive energy via direct non-local transfers from the forcing

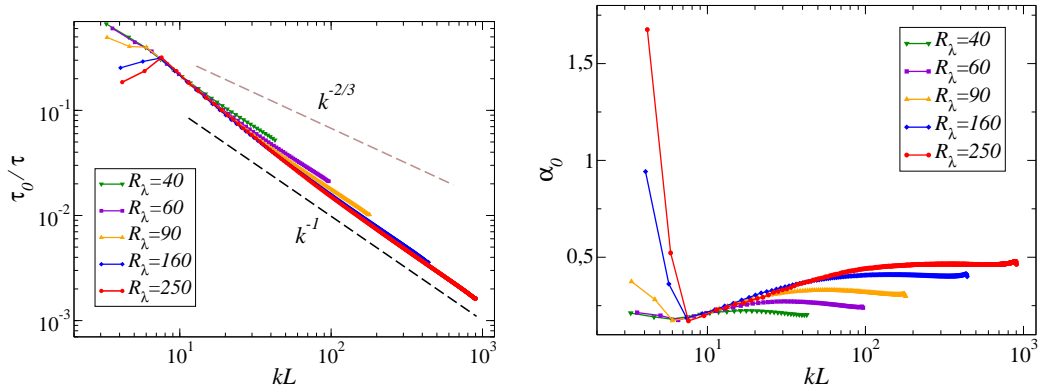


Figure 6: *Left panel*: Decorrelation time  $\tau_0$  extracted from the Gaussian fit as a function of the wavenumber for various  $R_\lambda$ . *Right panel*: Non-universal constant  $\alpha_0$  obtained as  $\alpha_0 = \tau^2/(\tau_0 kL)^2$ . It reaches a plateau at large wavenumber, which extends with increasing  $R_\lambda$ .

range in the simulations. This means that the large wavenumber limit underlying the FRG derivation corresponds to the modes  $k$  in the inertial range with negligible direct energy transfer from the forcing range. Of course, the “large wavenumber” domain extends with the Reynolds number, as visible in Fig. 6.

### 7.2. Three-point correlation function

Let us now present the results for the three-point correlation function. The general expression of this correlation (6.20) involves a product of velocities which is not local in  $\mathbf{k}$ . This is unpracticable in DNS heavily relying on parallel computation and memory distribution. To overcome this difficulty, one can focus on a particular configuration, which corresponds to an advection-velocity correlation. This correlation is defined as

$$T(t, \mathbf{k}) \equiv \left\langle N_\ell(t_0 + t, \mathbf{k}) u_\ell^*(t_0, \mathbf{k}) \right\rangle \quad (7.2)$$

$$N_\ell(t, \mathbf{k}) = -ik_n P_{\ell m}^\perp(\mathbf{k}) \sum_{\mathbf{k}'} \left\langle u_m(t, \mathbf{k}') u_n(t, \mathbf{k} - \mathbf{k}') \right\rangle,$$

where  $N$  is simply the Fourier transform of the advection and pressure term appearing in the NS equation expressed in spectral space

$$\partial_t u_\ell(t, \mathbf{k}) = N_\ell(t, \mathbf{k}) - \nu k^2 u_\ell(t, \mathbf{k}) + f_\ell(t, \mathbf{k}). \quad (7.3)$$

At equal times,  $T(0, \mathbf{k})$  is thus the usual energy transfer, and (7.2) represents its time-dependent generalisation. Let us note that  $T(t, \mathbf{k})$  is still a statistical moment of order three, although evaluated in a specific configuration involving only two space-time points. It is proportional to a linear combination of three-point correlation function  $C^{(3)}$  as

$$T(t, \mathbf{k}) \sim \sum_{\mathbf{k}'} C_{m n \ell}^{(3)}(t, \mathbf{k}', t, \mathbf{k} - \mathbf{k}') \quad \text{all } |\mathbf{k}| \gg L^{-1} \quad \exp\left(-\alpha_0 (L/\tau)^2 k^2 t^2\right) \quad (7.4)$$

and according to the FRG result, it should behave in the limit where all wavenumbers  $|\mathbf{k}|$ ,  $|\mathbf{k}'|$  and  $|\mathbf{k} - \mathbf{k}'|$  are large compared to  $L^{-1}$ , as the indicated Gaussian in  $kt$ .

However, the sum in (7.4) involves all possible wavenumber  $\mathbf{k}'$ , and not only large ones. Hence, in order to compare it with the FRG prediction, one needs to perform a scale decomposition, as defined e.g. in Refs. Frisch (1995); Verma (2019). Each velocity field  $\mathbf{u}(\mathbf{k})$  can be decomposed into a small-scale component  $\mathbf{u}^S(\mathbf{k})$  for  $|\mathbf{k}| > K_c$  and a large-scale

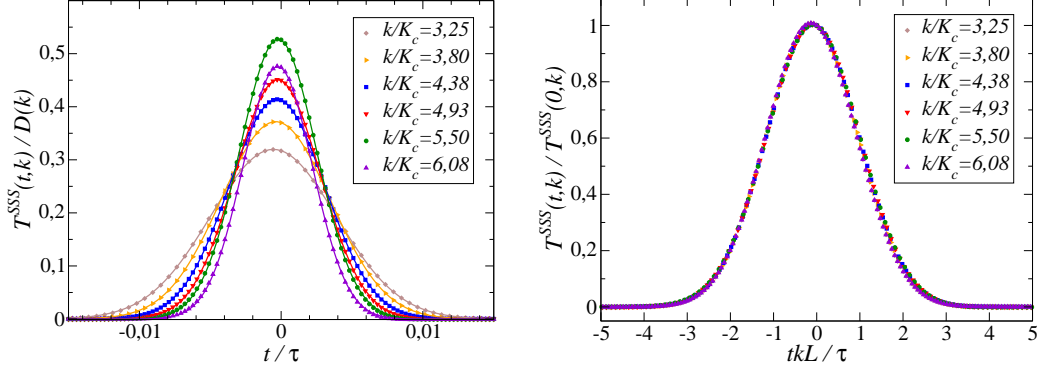


Figure 7: *Left panel*: Advection-velocity spatio-temporal correlation function  $T^{SSS}(t, k)$  from DNS at  $R_\lambda = 90$ , normalised by the dissipation spectrum  $\hat{D}(k) = \nu k^2 C^{(2)}(0, k)$ . Data from the simulation are represented with symbols, and their Gaussian fits with plain lines. *Right panel*: same curves  $T^{SSS}(t, k)$  normalised by  $T^{SSS}(0, k)$  and plotted as a function of  $kt$ , which induces their collapse.

one  $\mathbf{u}^L(\mathbf{k})$  for  $|\mathbf{k}| \leq K_c$  as  $\mathbf{u}(\mathbf{k}) = \mathbf{u}^S(\mathbf{k}) + \mathbf{u}^L(\mathbf{k})$ , where  $K_c$  is a cutoff wavenumber. This cutoff is chosen such that the direct energy transfers from the forcing range to the modes  $|\mathbf{k}| > K_c$  are negligible, which coincides with the regime of validity of the large wavenumber limit of the FRG identified on the basis of the two-point correlation function. This scale decomposition then leads for  $T$  to the following expression

$$T(t, \mathbf{k}) = [T^{SSS} + T^{SLS} + T^{SSL} + T^{SLL}] (t, \mathbf{k}) \quad (7.5)$$

with  $T^{XYZ}(t, \mathbf{k}) = -[u_i^X]^*(\mathbf{k}, t_0) \text{FT}[u_j^Y \partial_j u_i^Z](\mathbf{k}, t_0 + t)$  where  $X, Y, Z$  stand for  $S$  or  $L$ . Using the terminology of Ref. Verma (2019) for instantaneous energy transfers (*i.e.* for  $t = 0$ ), the first superscript of  $T^{XYZ}$  is related to the mode receiving energy in a triadic interaction process (it is actually the mode  $\mathbf{k}$  for which the equation (7.5) is written setting  $t = 0$ ), the intermediate superscript denotes the mediator mode and the last superscript is related to the giver mode that sends the energy to the receiver. The mediator mode does not loose nor receive energy in the interaction, it corresponds to the advecting velocity field, which comes as prefactor of the operator  $\nabla$  in the non-linear term of the Navier-Stokes equation. We focus on the term  $T^{SSS}$ , which gathers all triadic interactions where the three modes belong to the small scales (all wavenumbers are large). This term constitutes with  $T^{SLS}$  the turbulent energy cascade.

We show in Fig. 7 the results for  $T^{SSS}(t, \mathbf{k})$  computed from DNS. All the curves for  $T(t, \mathbf{k})$  and  $T^{SSS}(t, \mathbf{k})$  for the different wavenumbers  $k$  are fitted with the function  $g_{\text{Gaus}}(t) = c(1 - t/\tau_l) \exp(-(t/\tau_0)^2)$ , where  $c$ ,  $\tau_l$  and  $\tau_0$  are the fit parameters. This function provides a very accurate modellisation of the data both for  $T$  and  $T^{SSS}$  for all  $k$ . However, only the curves  $T^{SSS}$  are well approximated by pure Gaussians ( $\tau_l \ll \tau_0$ ), whereas without scale decomposition the curves for  $T$  are in general not symmetric and can take negative values (see Gorbunova *et al.* (2021a) for details).

The Gaussian form of  $T^{SSS}$  is in agreement with the FRG result (7.4). As shown in Fig. 7, all the curves for different wavenumbers collapse onto a single Gaussian when plotted as a function of the variable  $kt$ , as expected from Eq. (7.4). Moreover, let us emphasise that the non-universal parameter  $\alpha_0$  in this equation is predicted to be the same as the one for the two-point correlation function in Eq. (6.19). The decorrelation time  $\tau_0$  extracted from the fit with  $g_{\text{Gaus}}$  is displayed in Fig. 8, together with the value obtained from  $C^{(2)}$  and also the one from the full correlation  $T$ . They show as expected a  $k^{-1}$  dependence. The non-universal

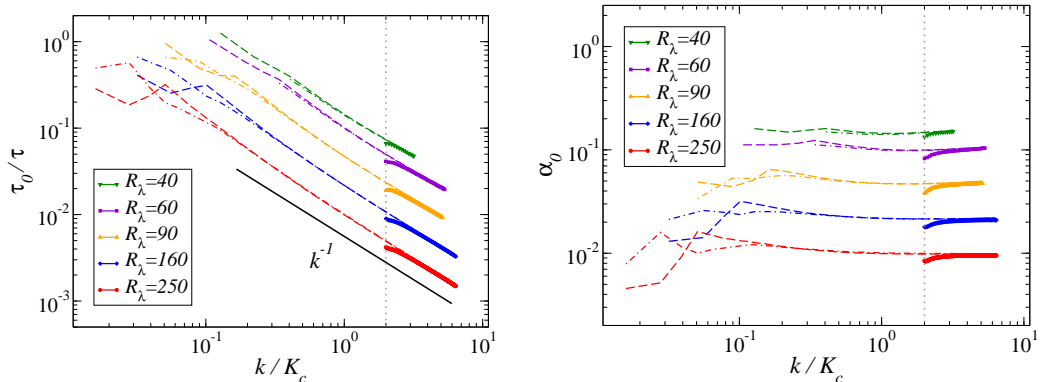


Figure 8: *Left panel*: Decorrelation time  $\tau_0$  extracted from the Gaussian fits of the purely small-scale advection-velocity correlation  $T^{SSS}$  (plain lines), the two-point correlation function  $C^{(2)}$  (dashed lines) and the full advection-velocity correlation  $T$  (dashed-dotted lines). *Right panel*: non-universal parameter  $\alpha_0$  obtained as  $\alpha_0 = \tau^2/(\tau_0 k L)^2$ . The data for the different  $R_\lambda$  in both panels have been shifted vertically for clarity.

parameter can be obtained as  $\alpha_0 = \tau^2/(\tau_0 k L)^2$ , and is shown in Fig. 8. At sufficiently large wavenumbers, corresponding to the regime of validity of FRG, the three values coincide with very good precision. At smaller wavenumbers, they are also in good agreement for  $C^{(2)}$  and for  $T$ , although in this regime  $\tau_l$  can be large. The detailed analysis of these results can be found in Ref. Gorbunova *et al.* (2021a).

To summarise this part, the results for the spatio-temporal dependence of the two-point and the specific configuration of the three-point correlation function studied in DNS hence confirm with accuracy the FRG prediction in the small-time regime, including the equality of the non-universal prefactors in the exponentials. This regime corresponds to a fast decorrelation on a time scale  $\tau \sim k^{-1}$  related to sweeping. Because of this fast initial decay, the observation in the DNS of the crossover to another slower regime at large-time is very challenging for NS turbulence, as we now briefly discuss.

### 7.3. Large time regime

The initial Gaussian decay of the two-point correlation function leads to a fast decrease of the amplitude of the signal within a short time interval. In all the simulations of NS equation, the correlation function falls to a level comparable with the numerical noise while it is still in the Gaussian regime, which prevents from detecting the crossover to an exponential and resolving the large time regime.

Interestingly, although this crossover could not be accessed for the real part of the correlation function, it was observed for a different quantity, namely the correlation function of the modulus of the velocity, defined as

$$C_{mod}^{(2)}(t, k) = \langle \|\hat{\mathbf{u}}(t_0, \mathbf{k})\| \|\hat{\mathbf{u}}(t_0 + t, \mathbf{k})\| \rangle - \langle \|\hat{\mathbf{u}}(t_0, \mathbf{k})\| \rangle \langle \|\hat{\mathbf{u}}(t_0 + t, \mathbf{k})\| \rangle. \quad (7.6)$$

The result obtained in DNS for this quantity is displayed in Fig. 9, which clearly shows the existence of a Gaussian regime at short time followed by an exponential regime at large time, analogous to the one expected for the real part of the two-point correlation function. Remarkably, very comparable results were obtained in air jet experiments where a similar correlation is measured Poulain, C. *et al.* (2006). Of course, this is a quite different object, and there is no theoretical understanding so far of its behaviour, neither from FRG nor from a heuristic argument. Indeed, in the latter argument, the decorrelation stems for a rapid

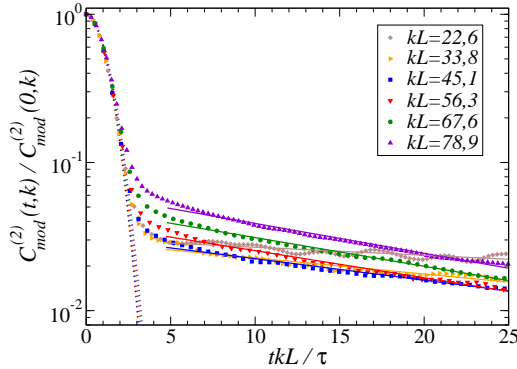


Figure 9: Time dependence of the normalised two-point correlation function of the velocity modulus  $C_{mod}^{(2)}(t, k)$  at  $R_\lambda = 60$  for different wavenumbers  $k$ . The numerical data is represented with dots, the dashed lines correspond to Gaussian fits and the plain lines to exponential fits.

random dephasing of the Fourier modes, while the phases obviously cannot play a role for the decorrelation of the modulus. We mention it here as an interesting puzzle, which deserves further work to be explained.

Although the large time regime appears difficult to access in DNS of NS equation, it can be unraveled in the case of scalar turbulence, which we present in Sec. 8. Prior to this, let us briefly mention another result which concerns the kinetic energy spectrum in the near-dissipation range.

#### 7.4. Kinetic energy spectrum in the near-dissipation range

The expression for the two-point correlation function of the velocity obtained from FRG can also be used to study the kinetic energy spectrum beyond the inertial range, that is beyond the Kolmogorov scale  $\eta = \nu^{3/4} \bar{\epsilon}^{-1/3}$ . Based on Kolmogorov hypotheses and dimensional analysis, the kinetic energy spectrum is expected to endow the universal form

$$E(k) = \bar{\epsilon}^{2/3} k^{-5/3} F(\eta k) \quad (7.7)$$

where  $F(x) \rightarrow C_K$  for  $x \lesssim 1$  since viscous effects are negligible in the inertial range, and  $F(x)$  fastly decays for  $x \gtrsim 1$  in the dissipation range. Although  $F$  is expected to be universal, its analytical expression is not known. Many empirical expressions of the form  $F(x) \sim x^{-\beta} \exp(-\mu x^\gamma)$  with different values for  $\gamma$  ranging from 1/2 to 2 were proposed Monin & Yaglom (2007). We refer to e.g. Khurshid *et al.* (2018); Gorbunova *et al.* (2020); Buaria & Sreenivasan (2020) for recent overviews on the various predictions. Despite the absence of consensus on the precise form of  $F(x)$ , the following general features emerge. There exist two successive ranges:

- the near-dissipation range for  $0.2 \lesssim k\eta \lesssim 4$  where the logarithmic derivative of the spectrum is not linear and its curvature clearly indicates  $\alpha < 1$ ,
  - the far-dissipation range for  $k\eta \gtrsim 4$  where the spectrum is well described by a pure exponential decay, which corresponds to  $\gamma = 1$ ,
- irrespective of the value for  $\beta$ . These observations hold for the NS equation in the absence of thermal noise. Of course, at large wavenumbers, the thermal fluctuations become non-negligible and drastically affect the shape of the spectrum, leading to the equilibrium  $k^2$  spectrum reflecting equipartition of energy Bandak *et al.* (2021); Bell *et al.* (2022); McMullen *et al.* (2022). This crossover was shown to occur well above the mean-free path, at scales within the dissipation range. Thus, depending on the system actual scales for thermal

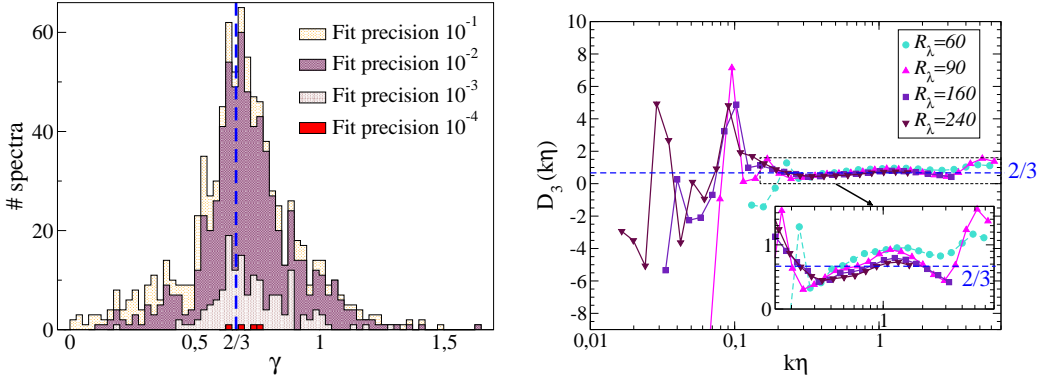


Figure 10: *Left panel*: distribution of the exponent  $\gamma$  of the stretched exponential for over 1600 spectra collected in experimental data from Modane wind tunnel, with different precision criteria for the fit of the spectrum in the dissipation range (see Gorbunova *et al.* (2020) for details). *Right panel*: Third logarithmic derivative  $D_3$  of  $E(k)$  as a function of the wavenumber from DNS at different Taylor Reynolds number. If  $E(k)$  is described by Eq. (7.8), one obtains  $D_3(k) = \gamma$  Gorbunova *et al.* (2020). The spectrum in the near-dissipation range is magnified in the inset. The local exponent approaches the blue dashed line, which indicates the FRG prediction  $\gamma = 2/3$ , as  $R_\lambda$  increases.

and turbulent fluctuations, the pure exponential decay associated with far-dissipation range may be unobservable in real turbulence and superseded by the thermal spectrum.

Leaving aside this issue, the form of the spectrum just beyond the inertial range can be deduced from FRG by taking the appropriate  $t \rightarrow 0$  limit in the expression for the two-point correlation function at large wavenumbers. If one assumes that the scaling variable  $tk^{2/3}$  saturates when  $t$  approaches the Kolmogorov time-scale  $\tau_K = \sqrt{\nu/\bar{\epsilon}}$  and  $k$  reaches  $L^{-1}$ , one obtains for the energy spectrum

$$E(k) = \lim_{t \rightarrow 0} 4\pi k^2 C^{(2)}(t, \mathbf{k}) = A\bar{\epsilon}^{2/3} (k\eta)^{-\beta} \exp(-\mu(k\eta)^\gamma) \quad (7.8)$$

with  $\gamma = 2/3$  and  $\beta = 5/3$ . The expression for  $C^{(2)}$  is obtained in the large wavenumber expansion and at the fixed-point, thus this behaviour is expected to be valid at wavenumbers large  $k \gg L^{-1}$  but still controlled by the fixed-point, which corresponds to the near-dissipation range. Let us emphasise that the result (7.8) does not have the same status as the expression for  $C^{(2)}$  (6.19). It clearly relies on an additional assumption, the saturation of the scaling variable, which is reasonable but not rigorous. In particular, if one assumes the existence of different successive scalings, associated with the emergence of quasi-singularities Dubrulle (2019), one would obtain a different result.

However, it seems reasonable to assume that the first scaling to dominate close to the inertial range is the Komogorov one, which leads to the stretched exponential (7.8) with the  $\gamma = 2/3$  exponent. This prediction has been verified in high-resolution DNS Canet *et al.* (2017); Gorbunova *et al.* (2020); Buaria & Sreenivasan (2020). It has also been observed in experimental data from von Kármán swirling flows Debue *et al.* (2018) and from the Modane wind tunnel Gorbunova *et al.* (2020). The latter yields the estimate  $\gamma \simeq 0.68 \pm 0.19$ , which is in very good agreement with the FRG prediction. Two examples of determination of  $\gamma$  are shown on Fig. 10.

## 8. Time-dependence of correlation functions in passive scalar turbulence

We now consider a passive scalar field  $\theta(t, \mathbf{x})$  which dynamics is governed by the advection-diffusion equation (2.4). In this section, we consider three cases for the carrier flow: i) the advecting field  $\mathbf{v}(t, \mathbf{x})$  is a turbulent velocity field solution of the incompressible NS equation (2.1), ii)  $\mathbf{v}(t, \mathbf{x})$  is a random vector field with a Gaussian distribution characterised by zero mean and covariance

$$\langle v_\alpha(t, \mathbf{x}) v_\beta(t', \mathbf{y}) \rangle = \delta(t - t') D_0 \int_{\mathbf{p}} \frac{e^{i\mathbf{p} \cdot (\mathbf{x} - \mathbf{y})} P_{\alpha\beta}^\perp(\mathbf{p})}{(p^2 + m^2)^{\frac{d}{2} + \frac{\varepsilon}{2}}} \quad (8.1)$$

where  $P_{\alpha\beta}^\perp(\mathbf{p})$  is the transverse projector which ensures incompressibility, and iii) the same random vector field with finite time correlations instead of  $\delta(t - t')$ . The model ii) was proposed by Kraichnan (1968, 1994), and has been thoroughly studied (we refer to Falkovich *et al.* (2001); Antonov (2006) for reviews). In this model, the parameter  $0 < \varepsilon/2 < 1$  corresponds to the Hölder exponent, describing the velocity roughness from very rough for  $\varepsilon \rightarrow 0$  to smooth for  $\varepsilon \rightarrow 2$ , and  $m$  acts as an IR cutoff.

The spatio-temporal correlations of the passive scalar in the three models for the carrier flow has been investigated within the FRG formalism in Ref. Pagani & Canet (2021). We first summarise the main results, and then present comparison with DNS for the three cases.

### 8.1. FRG results for the correlation functions of passive scalars

#### 8.1.1. Scalar field in Navier-Stokes flow

We start with the model i), *i.e.* a scalar field transported by a NS turbulent flow. We focus on the inertial-convective range, in which the energy spectrum of the scalar decays as  $E_\theta(\mathbf{p}) \sim p^{-5/3}$  as established by Obukhov and Corrsin in their seminal works Obukhov (1949); Corrsin (1951). As shown in Sec. 3.3, the action for the passive scalar possesses similar extended symmetries as the NS action. As a consequence, the structure of the related Ward identities for the vertices is the same: they all vanish upon setting one wavevector to zero, unless it is carried by a velocity field in which case it can be expressed using the  $\mathcal{D}_\alpha$  operator (3.42). Hence, the derivation of Sec. 6 can be reproduced identically in the presence of the scalar fields. We refer to Pagani & Canet (2021) for details. This yields the general expression for the time-dependence of any  $n$ -point generalised correlation function of the scalar in the limit of large wavenumbers.

In this section, we only consider two-point correlation functions, so we drop the superscript <sup>(2)</sup> on  $C$  in the following. The correlation function of the scalar, defined in time-wavevector coordinates as  $C_{\theta, \text{NS}}(t, \mathbf{p}) \equiv \langle \theta(t, \mathbf{p}) \theta(0, -\mathbf{p}) \rangle$ , is given in the FRG formalism by

$$C_{\theta, \text{NS}}(t, \mathbf{p}) = \frac{\bar{\varepsilon}_\theta \bar{\varepsilon}^{-1/3}}{p^{11/3}} \begin{cases} C_0 \exp(-\alpha_0(L/\tau)^2 p^2 t^2), & t \ll \tau \\ C_\infty \exp(-\alpha_\infty(L^2/\tau) p^2 |t|) & t \gg \tau, \end{cases} \quad (8.2)$$

where  $\bar{\varepsilon}$  and  $\bar{\varepsilon}_\theta$  denote the mean energy dissipation rates of the velocity and scalar fields respectively, and  $\tau \equiv (L^2/\bar{\varepsilon})^{-1/3}$  the eddy-turnover time at the energy injection scale. The constants  $C_{0, \infty}$  and  $\alpha_{0, \infty}$  are not universal, but  $\alpha_{0, \infty}$  are the same constants as the ones in the NS velocity correlation function Eq. (6.19). Hence, the temporal decay of the scalar correlations is determined in the inertial-convective range by the one of the carrier fluid. In particular, these constants depend on the profile of the forcing exerted on the velocity, but not on the one exerted on the scalar field.

### 8.1.2. Scalar field in white-in-time synthetic velocity flow

Let us now focus on the model ii) proposed by Kraichnan Kraichnan (1968), in which the NS velocity field is replaced by a random vector field with white-in-time Gaussian statistics. The remarkable feature of this model is that despite its extreme simplification compared to real scalar turbulence, it still retains its essential features, and in particular universal anomalous scaling exponents of the structure functions. Moreover, it is simple enough to allow for analytical calculation in suitable limits Chertkov & Falkovich (1996); Chertkov *et al.* (1995); Gawedzki & Kupiainen (1995); Bernard *et al.* (1996, 1998); Adzhemyan *et al.* (1998, 2001); Kupiainen & Muratore-Ginanneschi (2007); Pagani (2015), see Falkovich *et al.* (2001); Antonov (2006) for reviews. The temporal dependence of the scalar correlation function was analyzed in Mitra & Pandit (2005); Sankar Ray *et al.* (2008). Within the FRG framework, the large wavenumber expansion also allows in this case for the closure of the flow equations for the scalar correlation functions. Indeed, for Kraichnan model, the action for the velocity field  $\mathcal{S}_{\text{NS}}[\mathbf{v}, \bar{\mathbf{v}}, p, \bar{p}]$  is simply replaced by

$$\mathcal{S}_{\text{K}}[\mathbf{v}] = \int_{\mathbf{x}} v_{\alpha}(t, \mathbf{x}) \frac{(-\partial^2 + m^2)^{\frac{d+\varepsilon}{2}}}{2D_0} v_{\alpha}(t, \mathbf{x}). \quad (8.3)$$

Remarkably, the total action  $\mathcal{S}_{\text{K}} + \mathcal{S}_{\theta}$  still possesses the same extended symmetries, but for the time-dependent shifts of the response fields (3.34) and (3.39), which reduce to  $\bar{\theta}(t, \mathbf{x}) = \bar{\theta}(t, \mathbf{x}) + \bar{\varepsilon}(t)$ . The resulting Ward identities endow an essentially identical structure, such that the derivation of the large wavenumber expansion proceeds in the same way. The essential difference arises when computing the loop integral in the second line of Eq. (6.7), in which the velocity propagator in (6.6) is replaced by

$$\bar{G}_{v_{\alpha}v_{\beta}}(\omega, \mathbf{q}) = 2D_0 \frac{P_{\alpha\beta}^{\perp}(\mathbf{q})}{(q^2 + m^2)^{\frac{d+\varepsilon}{2}} + \mathcal{R}_{\kappa, v\nu}(\mathbf{q})}. \quad (8.4)$$

Because of the white-in-time (frequency-independent) nature of the Kraichnan propagator, the loop integral can be computed explicitly for any time delay, and yields a linear dependence in  $t$ . This implies that the decay of the scalar correlation is always exponential in time, e.g. for the two-point function

$$C_{\theta, \text{K}}(t, \mathbf{p}) = F(p) e^{-\kappa_{\text{ren}} p^2 |t|}, \quad (8.5)$$

hence there is no Gaussian regime at small times. Moreover, one obtains an explicit expression for the non-universal constant  $\kappa_{\text{ren}}$

$$\kappa_{\text{ren}} = \kappa_{\theta} + \frac{d-1}{2d} \int_{\mathbf{p}} \frac{D_0}{(p^2 + m^2)^{\frac{d+\varepsilon}{2} + \frac{\varepsilon}{2}}}. \quad (8.6)$$

The second term in the renormalised diffusivity  $\kappa_{\text{ren}}$  embodies the effect of fluctuations and can therefore be interpreted as an eddy diffusivity. The prefactor  $F(p)$  in (8.5) is given by an integral, which behaves in the inertial range as  $F(p) \sim p^{-d-2+\varepsilon}$  while in the weakly non-linear regime (*i.e.* when the convective term is perturbative), it behaves as  $F(p) \sim p^{-d-2-\varepsilon}$  Frisch & Wirth (1996); Pagani & Canet (2021).

### 8.1.3. Scalar field in time-correlated synthetic velocity flow

Let us introduce a slight extension of Kraichnan model, model iii), in which the white-in-time covariance (8.1) of the synthetic velocity field is replaced by one with tunable time-correlations  $D_{T_e}(t - t')$ , where  $T_e$  represents the typical decorrelation time of the synthetic velocity. The pure Kraichnan model is simply recovered in the limit  $T_e \rightarrow 0$  where

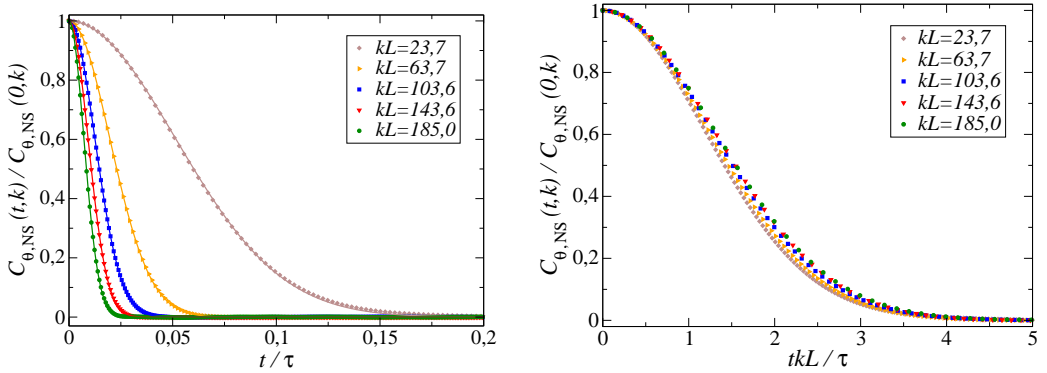


Figure 11: Time dependence of the normalised two-point correlation function  $C_{\theta,NS}(t, k)$  of the scalar in the NS flow at different wavenumbers  $k$  for  $R_\lambda = 90$ , as a function of  $t$ . (left panel) and of  $kt$  (right panel), which results in their collapse.  $L$  is the integral length scale,  $\tau$  is the eddy-turnover time scale at the integral scale.

$D_0(t-t') \equiv \delta(t-t')$ . The calculation of the scalar correlation functions within the FRG large wavenumber expansion is strictly identical to the pure Kraichnan case, except for the loop integral in Eq. (6.7). Indeed, as soon as some time dependence is introduced in the velocity covariance, hence in the velocity propagator (8.4), one restores the two time regimes. Let us focus for simplicity on the two-point scalar correlation function  $C_{\theta,KT_e}(t, \mathbf{p})$ . For small time delays  $t \ll T_e$ , the Fourier exponentials in the loop integral can be expanded and one finds the Gaussian decay in  $pt$ , whereas for large time delays  $t \gg T_e$ ,  $T_e$  can be replaced by zero in the integral and one recovers the Kraichnan exponential decay in  $p^2|t|$ .

The great advantage of this model is that the time-scale of the correlation function of the velocity field is adjustable and can be varied independently, in particular in DNS, such that it allows one to access the crossover between the two time regimes, as shown in Sec. 8.4.

## 8.2. Passive scalars in Navier-Stokes flow

The spatio-temporal behaviour of the correlation function of the scalar transported by NS flow has been studied in DNS in Ref. Gorbunova *et al.* (2021b), using similar numerical methods as for the NS case. The Schmidt number of the scalar, defined as the ratio of the fluid viscosity to the scalar diffusivity  $Sc = \nu/\kappa_\theta$  was varied from 0.7 to 36, and the two-point correlations of both the scalar and the velocity fields were recorded during the runs with similar averages as in Eq. (7.1).

The results for  $C_{\theta,NS}(t, \mathbf{k})$  are presented in Fig. 11. Each curve for a fixed wavenumber is accurately fitted by a Gaussian  $f_{\text{Gaus}}(t) = c \exp(-(t/\tau_0)^2)$ . Moreover, all curves for different wavenumbers collapse when plotted as a function of the variable  $kt$ , as expected from the FRG result (8.2). This behaviour is completely similar to the one of the NS velocity field presented in Fig. 5, as anticipated. The transported scalars behave in the inertial-convective range as the carrier fluid particles.

The decorrelation time  $\tau_0$  extracted from the Gaussian fit is displayed in Fig. 12. According to (8.2), it is related to  $\alpha_0$  as  $\tau_0/\tau = (\sqrt{\alpha_0}kL)^{-1}$ , and it is found to precisely conform to the expected  $k^{-1}$  decay. Moreover, beyond this behaviour, the FRG analysis yields that the prefactor  $\alpha_0$  is uniquely fixed by the properties of the carrier fluid, and is therefore equal for the velocity and the transported scalars. The numerical data for  $\alpha_0$  shown in Fig. 12 confirms this result, since the values of  $\alpha_0$  for the velocity correlations and for the scalar correlations are in very close agreement, and almost independent of the scalar properties. Indeed, the

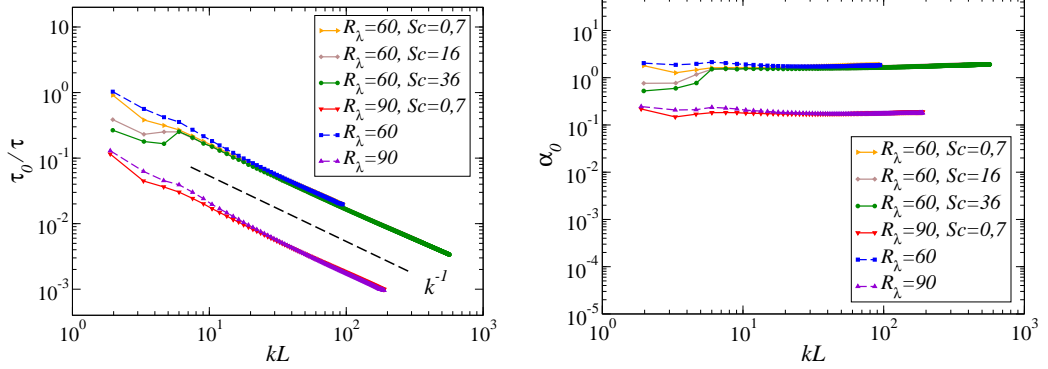


Figure 12: *Left panel*: Decorrelation time  $\tau_0$  extracted from the Gaussian fit of the scalar correlations (plain lines) and of the velocity correlations (dashed lines) as a function of the wavenumber for various  $R_\lambda$  and  $Sc$ . *Right panel*: non-universal parameter  $\alpha_0$  obtained as  $\alpha_0 = \tau^2/(\tau_0 kL)^2$ . In both panels, the data for  $R_\lambda = 90$  are shifted downward by a factor 10 for visibility.

variation of  $Sc$  from 0.7 to 36 does not lead to significant changes of  $\alpha_0$ . Hence the dynamics of the scalar field is dominated by the random advection and the sweeping effect.

At large time delays, a crossover from the Gaussian in  $kt$  to an exponential in  $k^2t$  is predicted by the FRG result (8.2). However, the Gaussian decay at small time induces a fast decrease of the correlations, such that the signal approaches zero and becomes oscillatory in the simulations before the crossover can occur. This prevents from its detection, as for the NS flow, which is not surprising since in this inertial-convective the behaviour of the scalar closely follows the one of the velocity field. It would be very interesting to study other regimes of the scalar in order to find a more favorable situation to observe the large-time regime. Meanwhile, the crossover can be evidenced in the case of synthetic flows, as we now show.

### 8.3. Passive scalars in the Kraichnan model

The correlation function of the scalar field transported in a white-in-time synthetic velocity field has also been studied in Ref. Gorbunova *et al.* (2021b). A random vector field, isotropic and divergenceless, conforming to a Gaussian distribution with the prescribed covariance (8.1) is generated. The advection-diffusion equation (2.4) with this synthetic field is then solved using DNS. The details of the procedure and parameters can be found in Gorbunova *et al.* (2021b). In order to achieve a precision test of the FRG result (8.5) and (8.6), 24 different sets of simulations were analyzed, varying the different parameters: Hölder exponent  $\varepsilon$ , amplitude  $D_0$  of the velocity covariance, and diffusivity  $\kappa_\theta$  of the scalar.

For each set, the correlation function of the scalar  $C_{\theta,\kappa}(t, \mathbf{k})$  was computed. As illustrated in Fig. 13, it always exhibits an exponential decay in time, perfectly modelled by the fitting function  $f_{\text{exp}}(t) = c \exp(-t/\tau_K)$ . The decorrelation time  $\tau_K$  depends on the wavenumber as  $\tau_K \sim k^{-2}$ , as expected from (8.5), and shown in Fig. 14.

Beyond the global exponential form of the spatio-temporal dependence of the scalar correlation function, the non-universal factor  $\kappa_{\text{ren}}$  in the exponential can be computed explicitly for the Kraichnan model within the FRG framework and is given by (8.6). Its value depends on the parameters  $\varepsilon$ ,  $D_0$  characterising the synthetic velocity and  $\kappa_\theta$  characterising the scalar. All these parameters have been varied independently in the 24 sets of simulations. For each set,  $\kappa_{\text{ren}}^{\text{num}}$  is determined from the numerical data as the plateau value of  $\tau_K k^2$ , where  $\tau_K$  is extracted from the exponential fit, as illustrated in Fig. 14. Besides, the value

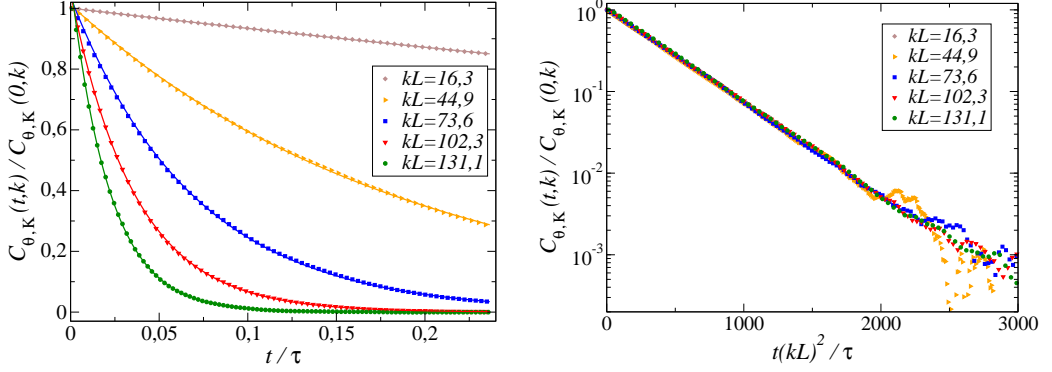


Figure 13: Time dependence of the normalised two-point correlation function of the scalar  $C_{\theta,K}(t, k)$  in Kraichnan model at different wavenumbers, as a function of time (*right panel*) and of the variable  $k^2 t$  (*left panel*) which leads to their collapse. Data from the numerical simulation, for  $\varepsilon = 1$  in this example, are denoted with dots and their exponential fits with continuous lines.

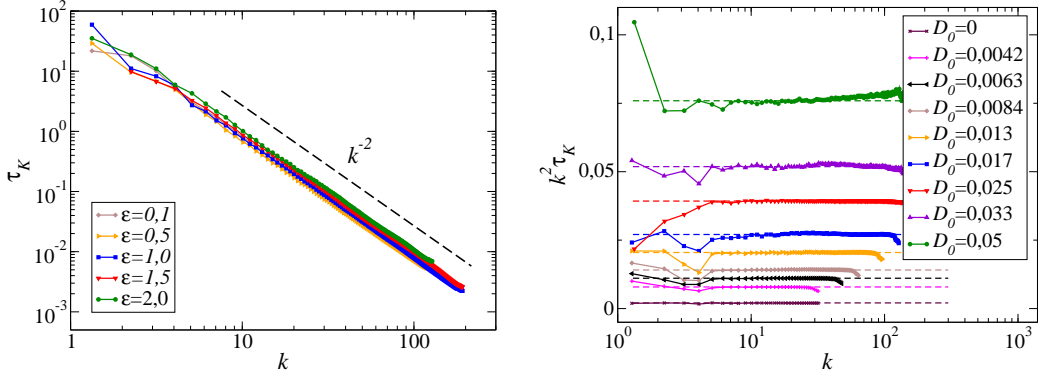


Figure 14: *Left panel*: Decorrelation time  $\tau_K$  extracted from the exponential fits for different values of the Hölder exponent  $\varepsilon$  from 0.1 to 2. *Right Panel*: Compensated decorrelation time  $k^2 \tau_K$  extracted from the exponential fits, for different values of  $D_0$  and  $\varepsilon = 1$ . The renormalised diffusivity  $\kappa_{\text{ren}}$  for each curve is determined as the fitted value of the plateau represented by dashed lines.

of  $(\kappa_{\text{ren}} - \kappa_\theta)$  depends on the synthetic velocity only and can be computed prior to any simulation as  $\kappa_{\text{ren}}^{\text{num}} - \kappa_\theta = A_\varepsilon D_0$  with  $A_\varepsilon = \frac{1}{3} \sum_p \frac{D_0}{(p^2 + m^2)^{\frac{3}{2} + \frac{\varepsilon}{2}}}$  following the FRG expression

(8.6). The comparison of the two estimations for  $\kappa_{\text{ren}}$  is displayed in Fig. 15, which shows a remarkable agreement. Let us emphasise that the numerical data presented spans values of  $\varepsilon$  up to 1.5, well beyond the perturbative regime Adzhemyan *et al.* (1998). This analysis hence provides a thorough confirmation of the FRG theory, including to the precise form of the non-universal prefactor in the exponential.

#### 8.4. Passive scalars in a time-correlated synthetic flow

Let us now turn to the extended Kraichnan model iii), *i.e.* a scalar field advected by a synthetic velocity field with finite time correlations  $D_{T_e}(t - t')$ . The simplest implementation of these finite time correlations in the DNS is to define a correlator  $D_{T_e}(t) = \frac{1}{T_e} \theta(t - T_e)$  where  $\theta(t)$  is the Heavyside step function. Hence, when  $T_e$  is negligible compared to the other

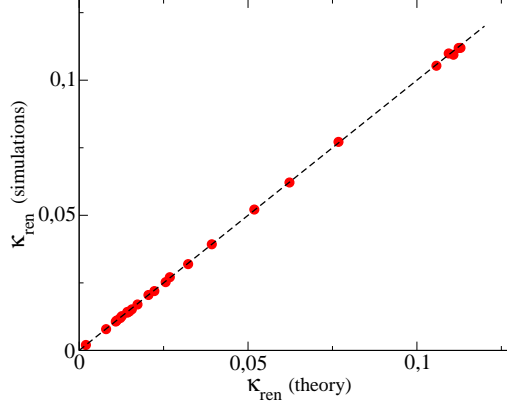


Figure 15: Renormalised scalar diffusivity:  $\kappa_{\text{ren}}$  (simulations) is obtained from the plateau values of  $k^2\tau_K$  extracted from the exponential fits of the scalar correlation function;  $\kappa_{\text{ren}}$  (theory) is calculated from its theoretical estimate based on Eq. (8.6). The data are gathered from the 24 data sets for which the parameters  $\varepsilon$ ,  $Sc$ ,  $D_0$ ,  $\kappa_\theta$  are varied independently (see Gorbunova *et al.* (2021b) for detailed parameters).

dynamical time scales of the mixing ( $\tau_A \sim \eta_B/U_{\text{rms}}$  for advection, and  $\tau_\kappa \sim \eta_B^2/\kappa_\theta$  for diffusion, with  $\eta_B$  the Batchelor scale, *i.e.* the smallest variation scale of the scalar), the velocity field can be considered as white-in-time (pure Kraichnan model). In contrast, when  $T_e$  becomes comparable with the typical decorrelation time of the scalar – say  $\tau_K$  estimated from the pure Kraichnan model at intermediate wavenumbers – then it realises a correlated synthetic velocity field.

The correlation function of the scalar  $C_{\theta, K_{T_e}}(t, \mathbf{k})$ , obtained from DNS of model iii), is shown in Fig. 16. At small time delays  $t \leq T_e$ , the different curves for each wavenumber are well fitted by Gaussian curves, whereas at large time delays, they depart from their Gaussian fits and decay much more slowly. The slower decay is precisely modelled by exponential fits. Hence, the crossover from the small-time Gaussian regime to the large-time exponential one, predicted by FRG, can be observed in this model. It can be further evidenced by computing the time derivative of  $\log C_{\theta, K_{T_e}}(t, \mathbf{k})$ . According to the FRG results, one should obtain

$$\frac{1}{k^2} \frac{\partial \log C_{\theta, K_{T_e}}(t, \mathbf{k})}{\partial t} = \begin{cases} -2\alpha_0 t & t \ll T_e \\ -\alpha_\infty & t \gg T_e \end{cases}, \quad (8.7)$$

where  $\alpha_{0, \infty}$  are the non-universal prefactors depending on the velocity characteristics only. This derivative is displayed in Fig. 16. All the curves collapse when divided by  $k^2$ , and show a linear decay with negative slope at small time, which crosses over to a negative constant at large time, in agreement with (8.7). Note that at higher wavenumbers (not shown), the large-time regime becomes indiscernible as the scalar field decorrelates fast (because of the  $\sim k^2$  dependence) down to near-zero noisy values before  $T_e$  is reached. This prevents us from resolving the crossover for these wavenumbers. This hints that a similar effect hinders the large-time regime in NS flows.

## 9. Conclusion and Perspectives

The purpose of this *JFM Perspectives* was to give an overview of what has been achieved using FRG methods in the challenging field of turbulence, and to provide the necessary technical elements for the reader to grasp the basis and the scope of these results. An important aspect is that the FRG belongs to the realm of “first-principles” approaches, in

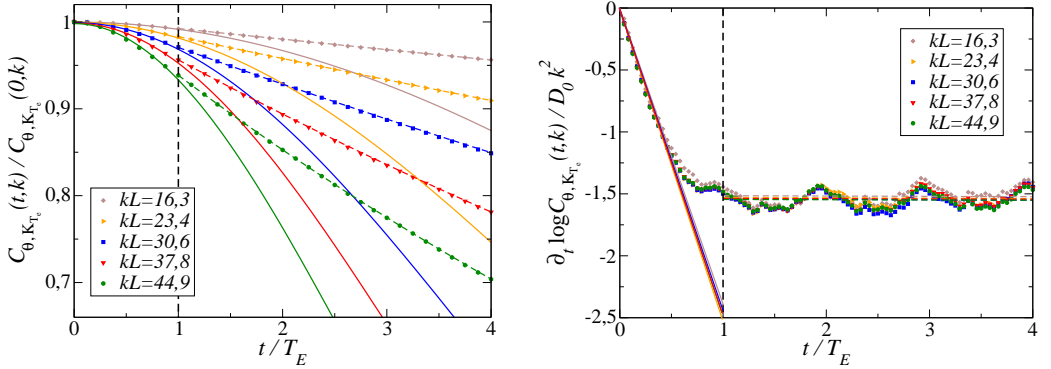


Figure 16: *Left panel:* Time dependence of the normalised two-point correlation function  $C_{\theta, \kappa_{T_e}}(t, k)$  at different wavenumbers  $k$ . Data from the numerical simulation are denoted with dots, their Gaussian fits calculated for  $t \leq T_e$  with continuous lines, their exponential fits calculated for  $t \geq T_e$  with dashed lines. *Right panel:* time derivative of the logarithm of the same data (including the fits), divided by  $D_0 k^2$ .

the sense that it is a tool to compute statistical properties of a system from its underlying microscopic or fundamental description, that is, in the case of turbulence, from the NS equations, without phenomenological inputs. An essential ingredient in this method is the symmetries, and extended symmetries, which can be fully exploited within the field-theoretical framework through exact Ward identities, that we expounded. So far, the main aspects of turbulence addressed with the FRG methods are the universal statistical properties of stationary, homogeneous and isotropic turbulence. In this context, the main achievements of this approach are twofold.

The first one is the evidence for the existence of a fixed-point of the RG flow, for physical forcing concentrated at large scales, which describes the turbulent state. This was not accessible using perturbative RG approaches, because they are restricted to long-ranged power-law forcing which changes the nature of the turbulence. The very existence of a fixed-point demonstrates two essential properties of turbulence: universality (independence of the precise forcing and dissipation mechanisms) and power-law behaviours. So far, the existence of the fixed-point was established within a simple approximation of the FRG, called LO (leading-order), which amounts to neglecting all vertices of order  $n \geq 3$  but the one present in the microscopic theory. This rather simple approximation yields the exact result for the third-order structure function, and leads to K41 scaling for the energy spectrum and the second-order structure function. It calls for further calculations, with improved approximations, in order to determine whether anomalous exponents arise when including higher-order vertices in the FRG ansatz. This is a first route to be explored, possibly coupled with the introduction of composite operators, to achieve this goal. This program is currently under investigation in shell models, which are simplified models of turbulence.

The second achievement using FRG, which is the most important one, is the obtention of the general expression, at large wavenumbers, of the spatio-temporal dependence of any  $n$ -point correlation and response function in the turbulent stationary state. The valuable feature of this expression is that it is asymptotically exact in the limit of large wavenumbers. Given the scarcity of rigorous results in 3D turbulence, this point is remarkable and worth highlighting. All the  $n$ -point correlation functions are endowed with a common structure for their temporal behaviour, which can be simply summarised, on the example of the two-point function  $C(t, \mathbf{p})$  for conciseness, as follows. At small time delays  $t$ ,  $C(t, \mathbf{p})$  exhibits a fast Gaussian decay in the variable  $pt$ , while at large time delays, it shows a crossover to

a slower exponential decay in the variable  $p^2|t|$ . The prefactors  $\alpha_0$  entering the Gaussian, and  $\alpha_\infty$  entering the exponential, respectively, are non-universal, but are equal for any  $n$ -point correlations. Similar expressions have been established in the case of passive scalars transported by turbulent flows, in the three cases where the turbulent velocity field is either the solution of the NS equations, or a synthetic random velocity field (Kraichnan model and its time-correlated extension). For the NS turbulent flow, the behaviour of the scalar follows in the inertial-convective range the one of the velocity field with fully analogous spatio-temporal correlations, including the non-universal prefactors. In the case of the white-in-time Kraichnan model, the temporal decay of the scalar correlations is purely exponential in  $p^2t$ , but a Gaussian regime opens up at small time delays when introducing a finite time-correlation in the velocity covariance.

The FRG results for the spatio-temporal correlation functions can be simply understood on phenomenological grounds, based on reasonable assumptions and on standard results for the single-particle dispersion problem. It can be argued that the two time regimes predicted by the FRG are related to the ballistic (at small times) or diffusive (at large time) motion of the Lagrangian particle in a turbulent flow. This allows one to highlight the connection with the random sweeping effect, which is well-known phenomenologically.

Moreover, the FRG results can be compared with DNS, which allows one in particular to quantify the precise range of validity of the “large wavenumber limit” which underlies the FRG calculations. Several DNS have been conducted both for NS turbulence and passive scalar turbulence with the different models for the advecting velocity field. They brought a thorough and accurate confirmation of the FRG predictions in the small-time regime, including high-precision tests in the case of the Kraichnan model. In contrast, the large-time regime has remained elusive in most DNS, due to the steepness of the Gaussian regime, which leads to a fast damping of the correlations to near-zero levels and renders very challenging its numerical detection. The crossover has been evidenced in the time-correlated synthetic velocity field, because in this case, the different time-scales are more easily adjustable in order to reach the large-time exponential decay before the signal gets too low and indiscernible from numerical noise. Although challenging, it would be very interesting to push further the DNS investigations in order to access and study the large-time regime for the NS flow. Another direction which remains unexplored so far is to test in DNS the FRG predictions for 2D turbulence, for which explicit expressions for the spatio-temporal correlations at large wavenumbers are also available Tarpin *et al.* (2019).

The temporal behaviour of the  $n$ -point correlation functions are obtained within FRG from the leading term in the large wavenumber expansion of the flow equations. Although this leading term is exact at large  $p$ , it vanishes at coinciding times  $t = 0$ , such that it does not carry any information on the structure functions, and in particular on their possible anomalous exponents. Another route in the quest for the intermittency corrections is thus to compute within the large wavenumber expansion, the first non-vanishing term at equal times. Preliminary results were obtained in this direction for 2D turbulence, but it remains to be completed and extended to study 3D turbulence.

The calculation of anomalous exponents within the FRG framework is clearly the next challenge to be addressed and probably the most significant. However, another promising line of research is the use of FRG to build effective models for the small scales. The FRG is designed by essence to construct a sequence of scale-dependent effective descriptions of a given system from the microscopic scale to the macroscopic one. In particular, if stopped at any chosen scale, the FRG flow provides the effective model at that scale, including the effect of fluctuations on all smaller (distance-)scales (larger wavenumbers). Computing such effective models from the fundamental equations, e.g. NS equations, via a controlled procedure of integration of fluctuations would be very valuable in many applications.

Probably the most relevant one is to improve current models used as a “sub-grid” description – that is model for the non-resolved scales – in many numerical schemes, such as LES, meteorological or climate models. Of course, a long path lies before arriving at competitive results, since one should first extend the FRG framework to describe more realistic situations, such as non-homogeneous, or anisotropic, or non-stationary conditions, the presence of shear, fluxes at the boundaries, etc. . . . Nonetheless, we believe that this path is worth exploring, since its outcome would be really valuable.

**Acknowledgements.** L.C. would like to sincerely thank all her collaborators involved in the works presented here, whose implication was essential to obtain all these results. She thanks in particular Bertrand Delamotte and Nicolás Wschebor, with whom the FRG approach to turbulence was initiated, and largely developed. She is also grateful to Guillaume Balarac for all the work with DNS, and Gregory Eyink and Vincent Rossetto, who greatly contributed in analysing the data and the results of DNS and experiments. Her special and warm thanks go to the PhD students, Anastasiia Gorbunova and Malo Tarpin, and postdoc Carlo Pagani, whose contributions were absolutely pivotal on FRG or DNS works. L.C. would also like to thank Mickael Bourgoïn, Nicolas Mordant, Bérengère Dubrulle and her team for their great help with experimental data.

**Funding.** This work was supported by the Agence Nationale pour la Recherche (grant ANR-18-CE92-0019 NeqFluids) and by the Institut Universitaire de France.

**Declaration of interests.** The author reports no conflict of interest.

## Appendix A. Flow equations in the LO approximation

We report in this Appendix additional details on the derivation of the flow equations, within the LO approximation presented in Sec. 5, for the functions  $f_{\kappa,\perp}^v$  and  $f_{\kappa,\perp}^D$ , and their explicit expressions. We refer to Ref. Canet *et al.* (2016) for the full derivation.

From the general form of the effective average action and of the regulator term  $\Delta\mathcal{S}_\kappa$ , one can infer the general structure of the propagator matrix, defined as the inverse of the Hessian of  $\Gamma_\kappa + \Delta\mathcal{S}_\kappa$ . It is more conveniently expressed in Fourier space where it is diagonal in wavevector and frequency, such that it is just the inverse of a matrix

$$\bar{G}_\kappa(\omega, \mathbf{p}) = \left[ \bar{\Gamma}_\kappa^{(2)} + \mathcal{R}_\kappa \right]^{-1}(\omega, \mathbf{p}). \quad (\text{A } 1)$$

As usual, because of rotational and parity invariance, any generic two-(space)index function (in Fourier space)  $F_{\alpha\beta}(\omega, \mathbf{p})$  can be decomposed into a longitudinal and a transverse part as  $F_{\alpha\beta}(\omega, \mathbf{p}) = F_{\parallel}(\omega, \mathbf{p})P_{\alpha\beta}^{\parallel}(\mathbf{p}) + F_{\perp}(\omega, \mathbf{p})P_{\alpha\beta}^{\perp}(\mathbf{p})$  where the transverse and longitudinal projectors are defined by

$$P_{\alpha\beta}^{\perp}(\mathbf{p}) = \delta_{\alpha\beta} - \frac{p_\alpha p_\beta}{p^2}, \quad \text{and} \quad P_{\alpha\beta}^{\parallel}(\mathbf{p}) = \frac{p_\alpha p_\beta}{p^2}. \quad (\text{A } 2)$$

Inverting the matrix  $\left[ \bar{\Gamma}_\kappa^{(2)} + \mathcal{R}_\kappa \right]$ , one obtains the general propagator

$$\bar{G}_{\kappa,\alpha\beta}(\omega, \mathbf{p}) = \begin{array}{c} u_\alpha \\ \bar{u}_\alpha \\ p \\ \bar{p} \end{array} \left( \begin{array}{cccc} u_\beta & \bar{u}_\beta & p & \bar{p} \\ \bar{G}_{\kappa,\alpha\beta}^{uu}(\omega, \mathbf{p}) & \bar{G}_{\kappa,\alpha\beta}^{u\bar{u}}(\omega, \mathbf{p}) & 0 & ip_\alpha \bar{G}_\kappa^{u\bar{p}}(\omega, \mathbf{p}) \\ \bar{G}_{\kappa,\alpha\beta}^{\bar{u}u}(-\omega, \mathbf{p}) & 0 & ip_\alpha \bar{G}_\kappa^{\bar{u}p}(\omega, \mathbf{p}) & 0 \\ 0 & -ip_\beta \bar{G}_\kappa^{\bar{u}p}(-\omega, \mathbf{p}) & \bar{G}_\kappa^{pp}(\omega, \mathbf{p}) & \bar{G}_\kappa^{p\bar{p}}(\omega, \mathbf{p}) \\ -ip_\beta \bar{G}_\kappa^{u\bar{p}}(-\omega, \mathbf{p}) & 0 & \bar{G}_\kappa^{p\bar{p}}(-\omega, \mathbf{p}) & 0 \end{array} \right) \quad (\text{A } 3)$$

with in the pressure sector

$$\bar{G}_\kappa^{pp}(\omega, \mathbf{p}) = -\frac{\rho}{p^2} \bar{\Gamma}_{\kappa,\parallel}^{(0,2)}(\omega, \mathbf{p}), \quad \bar{G}_\kappa^{p\bar{p}}(\omega, \mathbf{p}) = \frac{\rho}{p^2} \bar{\Gamma}_{\kappa,\parallel}^{(1,1)}(-\omega, \mathbf{p}), \quad (\text{A } 4)$$

and in the mixed velocity-pressure sector

$$\bar{G}_\kappa^{u\bar{p}}(\omega, \mathbf{p}) = -\frac{1}{p^2}, \quad \bar{G}_\kappa^{\bar{u}p}(\omega, \mathbf{p}) = \frac{\rho}{p^2}. \quad (\text{A } 5)$$

Furthermore, the components of the propagator in the velocity sector are purely transverse (that is, all the longitudinal parts vanish), as a consequence of incompressibility, and given by

$$\begin{aligned} \bar{G}_{\kappa, \alpha\beta}^{u\bar{u}}(\omega, \mathbf{q}) &= P_{\alpha\beta}^\perp(\mathbf{q}) \frac{1}{\bar{\Gamma}_{\kappa, \perp}^{(1,1)}(-\omega, \mathbf{q}) + R_\kappa(\mathbf{q})} \\ \bar{G}_{\kappa, \alpha\beta}^{uu}(\omega, \mathbf{q}) &= -P_{\alpha\beta}^\perp(\mathbf{q}) \frac{\bar{\Gamma}_{\kappa, \perp}^{(0,2)}(\omega, \mathbf{q}) - 2N_\kappa(\mathbf{q})}{\left[ \bar{\Gamma}_{\kappa, \perp}^{(1,1)}(\omega, \mathbf{q}) + R_\kappa(\mathbf{q}) \right]^2}. \end{aligned} \quad (\text{A } 6)$$

One can then insert the expression (A 3) into Eq. (5.1), and compute the matrix product and trace to obtain the flow of  $\bar{\Gamma}_\kappa^{(2)}$ . Within the LO approximation, only the bare vertex  $\bar{\Gamma}_\kappa^{(2,1)}$  remains and is given by (5.9), such that in Eq. (5.1), one may set  $\bar{\Gamma}_\kappa^{(4)} = 0$ , and only a few elements are non-zero in the matrices  $\bar{\Gamma}_{\kappa, \ell}^{(3)}$ .

According to the expressions (5.8) for  $\bar{\Gamma}_{\kappa, \alpha\beta}^{(0,2)}$  and  $\bar{\Gamma}_{\kappa, \alpha\beta}^{(1,1)}$ , the flow equations of the transverse functions  $f_{\kappa, \perp}^D$  and  $f_{\kappa, \perp}^\nu$  may be defined as

$$\begin{aligned} \partial_\kappa f_{\kappa, \perp}^\nu(\mathbf{p}) &= \frac{1}{(d-1)} P_{\alpha\beta}^\perp(\mathbf{p}) \partial_\kappa \Gamma_{\kappa, \alpha\beta}^{(1,1)}(\nu = 0, \mathbf{p}) \\ \partial_\kappa f_{\kappa, \perp}^D(\mathbf{p}) &= -\frac{1}{2(d-1)} P_{\alpha\beta}^\perp(\mathbf{p}) \partial_\kappa \Gamma_{\kappa, \alpha\beta}^{(0,2)}(\nu = 0, \mathbf{p}). \end{aligned} \quad (\text{A } 7)$$

After some calculations Canet *et al.* (2016), one deduces the following flow equations

$$\begin{aligned} \partial_s f_{\kappa, \perp}^\nu(\mathbf{p}) &= \frac{1}{(d-1)} \int_{\mathbf{q}} \left\{ \frac{\partial_s R_\kappa(\mathbf{q}) \tilde{f}_\perp^D(\mathbf{p} + \mathbf{q})}{\tilde{f}_\perp^\nu(\mathbf{p} + \mathbf{q}) (\tilde{f}_\perp^\nu(\mathbf{q}) + \tilde{f}_\perp^\nu(\mathbf{p} + \mathbf{q}))^2} \right. \\ &\times \left[ \left( -\mathbf{p}^2 + \frac{(\mathbf{p} \cdot (\mathbf{p} + \mathbf{q}))^2}{(\mathbf{p} + \mathbf{q})^2} \right) (d-1) - 2\mathbf{p} \cdot \mathbf{q} \left( 1 - \frac{(\mathbf{p} \cdot \mathbf{q})^2}{q^2 p^2} \right) \right] \\ &+ \frac{1}{\tilde{f}_\perp^\nu(\mathbf{q}) (\tilde{f}_\perp^\nu(\mathbf{q}) + \tilde{f}_\perp^\nu(\mathbf{p} + \mathbf{q}))} \left[ \partial_s R_\kappa(\mathbf{q}) \frac{\tilde{f}_\perp^D(\mathbf{q}) (2\tilde{f}_\perp^\nu(\mathbf{q}) + \tilde{f}_\perp^\nu(\mathbf{p} + \mathbf{q}))}{\tilde{f}_\perp^\nu(\mathbf{q}) (\tilde{f}_\perp^\nu(\mathbf{q}) + \tilde{f}_\perp^\nu(\mathbf{p} + \mathbf{q}))} - \partial_s N_\kappa(\mathbf{q}) \right] \\ &\times \left. \left[ \left( -\mathbf{p}^2 + \frac{(\mathbf{p} \cdot \mathbf{q})^2}{q^2} \right) (d-1) + 2 \frac{\mathbf{p} \cdot (\mathbf{p} + \mathbf{q})}{(\mathbf{q} + \mathbf{p})^2} \left( q^2 - \frac{(\mathbf{p} \cdot \mathbf{q})^2}{p^2} \right) \right] \right\} \quad (\text{A } 8) \end{aligned}$$

$$\begin{aligned} \partial_s f_{\kappa, \perp}^D(\mathbf{p}) &= -\frac{1}{2(d-1)} \int_{\mathbf{q}} \left\{ \frac{2\tilde{f}_\perp^D(\mathbf{q} + \mathbf{p})}{\tilde{f}_\perp^\nu(\mathbf{p} + \mathbf{q}) \tilde{f}_\perp^\nu(\mathbf{q}) (\tilde{f}_\perp^\nu(\mathbf{q}) + \tilde{f}_\perp^\nu(\mathbf{p} + \mathbf{q}))} \right. \\ &\times \left[ \partial_s R_\kappa(\mathbf{q}) \frac{\tilde{f}_\perp^D(\mathbf{q}) (2\tilde{f}_\perp^\nu(\mathbf{q}) + \tilde{f}_\perp^\nu(\mathbf{p} + \mathbf{q}))}{\tilde{f}_\perp^\nu(\mathbf{q}) (\tilde{f}_\perp^\nu(\mathbf{q}) + \tilde{f}_\perp^\nu(\mathbf{p} + \mathbf{q}))} - \partial_s N_\kappa(\mathbf{q}) \right] \\ &\times \left[ 2 \frac{1}{q^2 (\mathbf{p} + \mathbf{q})^2} \left( q^2 - \frac{(\mathbf{p} \cdot \mathbf{q})^2}{p^2} \right) \left( \mathbf{p}^2 \mathbf{p} \cdot \mathbf{q} + 2(\mathbf{p} \cdot \mathbf{q})^2 - \mathbf{p}^2 q^2 \right) \right. \\ &\left. \left. + \left( 2\mathbf{p}^2 - \frac{(\mathbf{p} \cdot (\mathbf{p} + \mathbf{q}))^2}{(\mathbf{p} + \mathbf{q})^2} - \frac{(\mathbf{p} \cdot \mathbf{q})^2}{q^2} \right) (d-1) \right] \right\} \quad (\text{A } 9) \end{aligned}$$

where  $\partial_s \equiv \kappa \partial_\kappa$ ,  $\tilde{f}_\perp^\gamma(\mathbf{p}) \equiv f_{\kappa,\perp}^\gamma(\mathbf{p}) + R_\kappa(\mathbf{q})$  and  $\tilde{f}_\perp^D(\mathbf{p}) \equiv f_{\kappa,\perp}^D(\mathbf{p}) + N_\kappa(\mathbf{q})$ . Note that a typo has been corrected in the last line of Eq. (A 9) compared to Ref. Canet *et al.* (2016).

## Appendix B. Next-to-leading order term in 2D Navier-Stokes equation

The large wavenumber expansion underlying the derivation of Eq. (6.7) is inspired by the BMW approximation scheme. This scheme can be in principles improved order by order. There are two possible strategies to achieve this. The first one is to increase the order at which the closure using the BMW expansion is performed. Let us consider for instance the flow equation for the two-point function  $\Gamma_\kappa^{(2)}$ . At leading order, the three- and four-point vertices entering this equation are expanded around  $\mathbf{q} = 0$ . At the next-to-leading order, one keeps the full vertices in the flow equation for  $\Gamma_\kappa^{(2)}$ , and perform the  $\mathbf{q} = 0$  expansion for the higher-order vertices entering the flow equations of  $\Gamma_\kappa^{(3)}$  and  $\Gamma_\kappa^{(4)}$ , and so on. An alternative way to improve the BMW approximation scheme is to include higher-order terms in the Taylor expansion of the vertices for a given order  $n$ , e.g.

$$\begin{aligned} \Gamma_\kappa^{(n)}(\omega, \mathbf{q}, \varpi_1, \mathbf{p}_1, \dots) &\stackrel{q \approx 0}{\simeq} \Gamma_\kappa^{(n)}(\omega, 0, \varpi_1, \mathbf{p}_1, \dots) + \frac{\partial}{\partial \mathbf{q}} \Gamma_\kappa^{(n)}(\omega, \mathbf{q}, \varpi_1, \mathbf{p}_1, \dots) \Big|_{\mathbf{q}=0} \\ &+ \frac{1}{2} \frac{\partial^2}{\partial \mathbf{q}^2} \Gamma_\kappa^{(n)}(\omega, \mathbf{q}, \varpi_1, \mathbf{p}_1, \dots) \Big|_{\mathbf{q}=0}. \end{aligned} \quad (\text{B } 1)$$

This second strategy has been implemented to study 2D turbulence in Tarpin *et al.* (2019). The reason for focusing on 2D rather than 3D turbulence is that the 2D NS action possesses additional symmetries, which can be used to control exactly the derivatives of vertices at  $\mathbf{q} = 0$ .

In 2D, the incompressibility constraint allows one to express the velocity field as the curl of a pseudo-scalar field  $\psi(t, \mathbf{x})$  called the stream function:  $v_\alpha = \varepsilon_{\alpha\beta} \partial_\beta \psi$ . Formulating the action in term of the stream function allows one to simply integrate out the pressure fields, yielding

$$\begin{aligned} \mathcal{S}_\psi[\psi, \bar{\psi}] &= \int_{t, \mathbf{x}} \partial_\alpha \bar{\psi} \left[ \partial_t \partial_\alpha \psi - \nu \nabla^2 \partial_\alpha \psi + \varepsilon_{\beta\gamma} \partial_\gamma \psi \partial_\beta \partial_\alpha \psi \right] \\ &- \int_{t, \mathbf{x}, \mathbf{x}'} \partial_\alpha \bar{\psi}(t, \mathbf{x}) N \left( \frac{|\mathbf{x} - \mathbf{x}'|}{L} \right) \partial'_\alpha \bar{\psi}(t, \mathbf{x}') \Big\}. \end{aligned} \quad (\text{B } 2)$$

This action possesses all the extended symmetries discussed in Sec. 3.3. In particular, the Galilean transformation reads in this formulation

$$\delta\psi = \varepsilon_{\alpha\beta} x_\alpha \dot{\eta}_\beta(t) + \eta_\alpha(t) \partial_\alpha \psi, \quad \delta\bar{\psi} = \eta_\alpha(t) \partial_\alpha \bar{\psi}, \quad (\text{B } 3)$$

and the time-gauged shift of the response fields now simply amounts to the transformation

$$\delta\psi = 0, \quad \delta\bar{\psi} = x_\alpha \dot{\eta}_\alpha(t), \quad (\text{B } 4)$$

where  $\eta$ ,  $\bar{\eta}$  are the time-dependent parameters of the transformations. Note that these transformations are linear in  $x$ . Thus, in Fourier space, this leads to Ward identity constraining the first derivative of a vertex at one vanishing wavevector. If the zero wavevector is carried by a response stream, one deduces from (B 4) the following Ward identity

$$\frac{\partial}{\partial q_{m+1}^\alpha} \Gamma_\kappa^{(m,n)}(\dots, \varpi_{m+1}, \mathbf{q}_{m+1}, \dots) \Big|_{\mathbf{q}_{m+1}=0} = 0. \quad (\text{B } 5)$$

which is equivalent to Eq. (3.36) in terms of the velocity. Similarly, if the zero wavevector

is carried by a stream field, the time-gauged Galilean transformation (B 3) yields a Ward identity, equivalent to Eq. (3.36), which exactly fixes the  $\partial_q$  derivative of this vertex in the stream formulation.

One can study the action (B 2) within the FRG formalism. It is clear that the same closure can be achieved in the limit of large wavenumber. In the stream formulation, the zeroth order in the large wavenumber expansion is trivial. This just reflects the fact that the stream and response stream functions are defined up to a constant function of time, and the functional integral does not fix this gauge invariance, such that the zeroth order carries no information. One thus has to consider the next term (first  $\mathbf{q}$  derivative) in the Taylor expansion of the vertices, which are precisely the ones fixed by the Ward identities. One thus obtains the exact same result as (6.7) expressed in term of the stream function. One can derive from it in a similar way the expression of the time dependence for generic  $n$ -point correlation functions in 2D turbulence. Note that they bare a different form than in 3D, due to the different scaling exponents (in particular  $z$ ). Contrary to the 3D case, this result has not been tested yet in direct numerical simulations.

As in 3D, the leading order term in the limit of large wavenumber vanishes at equal times, such than one is left with power laws in wavenumbers with exponents stemming from standard scale invariance (Kraichnan-Leith scaling). However, additional extended symmetries were unveiled for the 2D action, which can be exploited to compute the next-to-leading order term (in the second line of Eq. (B 1)). At equal times, *i.e.* integrated over all external frequencies, this term writes

$$\begin{aligned} \partial_s \int_{\varpi_\ell} \mathcal{W}_\kappa^{(n)} \Big|_{\text{next-to-leading}} &= -\frac{1}{2} \int_{\omega_1, \mathbf{q}_1, \omega_2, \mathbf{q}_2} H_{\kappa, \gamma \delta}(-\omega_1, -\mathbf{q}_1, -\omega_2, -\mathbf{q}_2) \\ &\times \int_{\varpi_\ell} \left[ \frac{q_a^\mu q_b^\nu q_c^\rho q_d^\sigma}{4!} \frac{\partial^2}{\partial q_a^\mu \partial q_b^\nu \partial q_c^\rho \partial q_d^\sigma} \frac{\delta}{\delta u_\gamma(\omega_1, \mathbf{q}_1)} \frac{\delta}{\delta u_\delta(\omega_2, \mathbf{q}_2)} \mathcal{W}_\kappa^{(n)} \right] \Big|_{\mathbf{q}_1 = \mathbf{q}_2 = 0} \end{aligned} \quad (\text{B 6})$$

where  $a, b, c, d$  take values in  $\{1, 2\}$ , and we have not used explicitly translational invariance so that the  $\mathbf{q}$  derivatives can be expressed unambiguously. One can show that the only non-vanishing contributions are the ones with two  $q_1$  and two  $q_2$ . The contributions with four  $q_1$  vanish when evaluated at  $\mathbf{q}_2 = 0$  because of the time-gauged symmetry, while the ones with three  $q_1$  and one  $q_2$  are proportional to a  $\mathcal{D}_\mu$  operator and vanish when integrated over frequencies. To go further requires to control second derivatives of vertices. This can partially be achieved in 2D because the field theory (B 2) exhibits two additional extended symmetries, which correspond to transformations quadratic in  $x$ , and thus yield Ward identities for the second  $\mathbf{q}$  derivative of vertices in Fourier space.

The first new symmetry is a quadratic in  $x$  shift of the response fields, following

$$\delta\psi = 0, \quad \delta\bar{\psi} = \frac{x^2}{2} \bar{\eta}(t). \quad (\text{B 7})$$

One deduces the following Ward identity for second derivatives of a vertex function evaluated at a vanishing wavenumber carried by a response field

$$\frac{\partial^2}{(\partial q_{\bar{\ell}}^\alpha)^2} \Gamma_\kappa^{(m,n)}(\dots, \omega_{\bar{\ell}}, \mathbf{q}_{\bar{\ell}}, \dots) \Big|_{\mathbf{q}_{\bar{\ell}}=0} = 0, \quad (\text{B 8})$$

where  $\bar{\ell}$  is a response field index. Remarkably, the transformation (B 7), which reads in the velocity formulation

$$\delta\bar{v}_\alpha = \varepsilon_{\alpha\beta\gamma} x_\beta \eta_\gamma(t), \quad \delta\bar{p} = v_\alpha \varepsilon_{\alpha\beta\gamma} x_\beta \eta_\gamma(t), \quad (\text{B 9})$$

is also an extended symmetry of the 3D NS equation, but it has not been exploited yet.

In analogy with the time-dependent Galilean transformation, which can be interpreted as a time-gauged generalisation of space translations, one can write the time-gauged extension of space rotations, which reads in the stream formulation

$$\delta\psi = -\dot{\eta}(t)\frac{x^2}{2} + \eta(t)\varepsilon_{\alpha\beta}x_\beta\partial_\alpha\psi, \quad \delta\bar{\psi} = \eta(t)\varepsilon_{\alpha\beta}x_\beta\partial_\alpha\bar{\psi}. \quad (\text{B } 10)$$

This transformation leads to a new extended symmetry of the 2D action, while it is not an extended symmetry of the 3D one. It is interesting to notice that gauged rotations are also an extended symmetry of the action corresponding to the Kraichnan model in any spatial dimension. As this transformation is also quadratic in  $x$ , it leads as well to a Ward identity for the second  $\mathbf{q}$  derivative of a vertex in Fourier space, this time when the  $\mathbf{q}$  wavevector is carried by the field itself

$$\frac{\partial^2}{(\partial q^\alpha)^2}\Gamma_\kappa^{(m+1,n)}(\omega, \mathbf{q}, \omega_1, \mathbf{q}_1, \dots)\Big|_{\mathbf{q}=0} = \mathcal{R}(\omega)\Gamma_\kappa^{(m,n)}(\omega_1, \mathbf{q}_1, \dots), \quad (\text{B } 11)$$

where  $\mathcal{R}(\omega)$  is an operator achieving finite shifts by  $\omega$  of the external frequencies of the function on which it acts, similarly to  $\mathcal{D}_\alpha(\omega)$  in (3.33), at the difference that it also involves a derivative with respect to external wavenumbers (see Tarpin *et al.* (2019) for details).

Using translation and rotation invariance of  $H_{\kappa,\gamma,\delta}$  in (B 6), one can show that there are only two remaining contributions of the form  $\frac{\partial^4}{\partial q_1^\mu \partial q_1^\mu \partial q_2^\nu \partial q_2^\nu}$  and  $\frac{\partial^4}{\partial q_1^\mu \partial q_1^\nu \partial q_2^\mu \partial q_2^\nu}$ . The first type of contributions are controlled by the Ward identities (B 8) and (B 11). Hence, either they are zero or they are proportional to a  $\mathcal{R}$  operator, and thus vanish when integrated over frequencies. However, the second type of contributions, the crossed derivatives, are not controlled by these identities. One can argue that they are nevertheless suppressed by a combinatorial factor. One thus arrives at the conclusion that most of the sub-leading terms in the large wavenumber expansion are exactly controlled by symmetries and vanish, while the remaining terms, which are not controlled by the symmetries, appear small based on combinatorics. This suggests that corrections to standard Kraichnan-Leith scaling of equal-time quantities in the large wavenumber regime, *i.e.* for the direct cascade, should be small, although it can only be argued at this stage.

## REFERENCES

- ADZHEMYAN, L.Ts., ANTONOV, N.V. & KIM, T. L. 1994 Composite operators, operator expansion, and galilean invariance in the theory of fully developed turbulence. Infrared corrections to Kolmogorov scaling. *Theor. Math. Phys.* **100**, 1086.
- ADZHEMYAN, L. Ts., ANTONOV, N. V., BARINOV, V. A., KABRITS, YU. S. & VASIL'EV, A. N. 2001 Anomalous exponents to order  $\varepsilon^3$  in the rapid-change model of passive scalar advection. *Phys. Rev. E* **63**, 025303.
- ADZHEMYAN, L. Ts., ANTONOV, N. V. & VASIL'EV, A. N. 1998 Renormalization group, operator product expansion, and anomalous scaling in a model of advected passive scalar. *Phys. Rev. E* **58**, 1823–1835.
- ADZHEMYAN, L. Ts., ANTONOV, N. V. & VASIL'EV, A. N. 1999 *The Field Theoretic Renormalization Group in Fully Developed Turbulence*. London: Gordon and Breach.
- ANTONOV, N. V. 2006 Renormalization group, operator product expansion and anomalous scaling in models of turbulent advection. *J. Phys. A: Math. Gen.* **39** (25), 7825–7865.
- ANTONOV, N. V., BORISENOK, S. V. & GIRINA, V. I. 1996 Renormalisation Group approach in the theory of fully developed turbulence. Composite operators of canonical dimension 8. *Theor. Math. Phys.* **106**, 75.
- BALOG, IVAN, CHATÉ, HUGUES, DELAMOTTE, BERTRAND, MAROHNIC, MAROJE & WSCHBOR, NICOLÁS 2019 Convergence of nonperturbative approximations to the renormalization group. *Phys. Rev. Lett.* **123**, 240604.

- BANDAK, DMYTRO, EYINK, GREGORY L., MAILYBAEV, ALEXEI & GOLDENFELD, NIGEL 2021 Thermal noise competes with turbulent fluctuations below millimeter scales.
- BARBI, DIRK & MÜNSTER, GERNOT 2013 Renormalisation group analysis of turbulent hydrodynamics. *Physics Research International* **2013**, 872796.
- BEC, JÉRÉMIE & KHANIN, KONSTANTIN 2007 Burgers turbulence. *Physics Reports* **447** (1), 1–66.
- BELL, JOHN B., NONAKA, ANDREW, GARCIA, ALEJANDRO L. & EYINK, GREGORY 2022 Thermal fluctuations in the dissipation range of homogeneous isotropic turbulence. *Journal of Fluid Mechanics* **939**, A12.
- BENITEZ, FEDERICO, MÉNDEZ-GALAIN, RAMÓN & WSCHBOR, NICOLÁS 2008 Calculations on the two-point function of the  $o(n)$  model. *Phys. Rev. B* **77** (2), 024431.
- BERGES, JURGEN, TETRADIS, NIKOLAOS & WETTERICH, CHRISTOF 2002 Non-perturbative Renormalization flow in quantum field theory and statistical physics. *Phys. Rep.* **363** (4-6), 223 – 386, arXiv: [hep-ph/0005122](https://arxiv.org/abs/hep-ph/0005122).
- BERNARD, DENIS, GAWEDZKI, K. & KUPIAINEN, A. 1996 Anomalous scaling in the N point functions of passive scalar. *Phys. Rev. E* **54**, 2564, arXiv: [chao-dyn/9601018](https://arxiv.org/abs/chao-dyn/9601018).
- BERNARD, DENIS, GAWEDZKI, K. & KUPIAINEN, A. 1998 Slow Modes in Passive Advection. *Journal of Statistical Physics* **90**, 519, arXiv: [cond-mat/9706035](https://arxiv.org/abs/cond-mat/9706035).
- BIFERALE, L., BOFFETTA, G., CELANI, A. & TOSCHI, F. 1999 Multi-time, multi-scale correlation functions in turbulence and in turbulent models. *Physica D: Nonlinear Phenomena* **127** (3), 187–197.
- BIFERALE, LUCA, CALZAVARINI, ENRICO & TOSCHI, FEDERICO 2011 Multi-time multi-scale correlation functions in hydrodynamic turbulence. *Physics of Fluids* **23** (8), 085107.
- BLAIZOT, JEAN-PAUL, MÉNDEZ-GALAIN, RAMÓN & WSCHBOR, NICOLÁS 2006 A new method to solve the non-perturbative Renormalization Group equations. *Phys. Lett. B* **632** (4), 571 – 578.
- BLAIZOT, J.-P., MÉNDEZ-GALAIN, R. & WSCHBOR, N. 2007 Non-perturbative Renormalization Group calculation of the scalar self-energy. *Eur. Phys. J. B* **58**, 297–309.
- BUARIA, DHAWAL & SREENIVASAN, KATEPALLI R. 2020 Dissipation range of the energy spectrum in high reynolds number turbulence. *Phys. Rev. Fluids* **5**, 092601.
- BUCKMASTER, TRISTAN & VICOL, VLAD 2017 Nonuniqueness of weak solutions to the navier-stokes equation. *arXiv:1709.10033* .
- CALLAN, CURTIS G. 1970 Broken scale invariance in scalar field theory. *Phys. Rev. D* **2**, 1541–1547.
- CANET, LÉONIE, CHATÉ, HUGUES & DELAMOTTE, BERTRAND 2011a General framework of the non-perturbative Renormalization Group for non-equilibrium steady states. *J. Phys. A* **44** (49), 495001.
- CANET, LÉONIE, CHATÉ, HUGUES, DELAMOTTE, BERTRAND & WSCHBOR, NICOLÁS 2010 Nonperturbative renormalization group for the Kardar-Parisi-Zhang equation. *Phys. Rev. Lett.* **104** (15), 150601.
- CANET, LÉONIE, CHATÉ, HUGUES, DELAMOTTE, BERTRAND & WSCHBOR, NICOLÁS 2011b Nonperturbative Renormalization Group for the Kardar-Parisi-Zhang equation: General framework and first applications. *Phys. Rev. E* **84**, 061128.
- CANET, LÉONIE, DELAMOTTE, BERTRAND & WSCHBOR, NICOLÁS 2015 Fully developed isotropic turbulence: Symmetries and exact identities. *Phys. Rev. E* **91**, 053004.
- CANET, LÉONIE, DELAMOTTE, BERTRAND & WSCHBOR, NICOLÁS 2016 Fully developed isotropic turbulence: Nonperturbative renormalization group formalism and fixed-point solution. *Phys. Rev. E* **93**, 063101.
- CANET, LÉONIE, ROSSETTO, VINCENT, WSCHBOR, NICOLÁS & BALARAC, GUILLAUME 2017 Spatiotemporal velocity-velocity correlation function in fully developed turbulence. *Phys. Rev. E* **95**, 023107.
- CHEN, SHIYI & KRAICHNAN, ROBERT H. 1989 Sweeping decorrelation in isotropic turbulence. *Physics of Fluids A* **1** (12), 2019–2024.
- CHEKTKOV, M. & FALKOVICH, G. 1996 Anomalous scaling exponents of a white-adveced passive scalar. *Phys. Rev. Lett.* **76**, 2706–2709.
- CHEKTKOV, M., FALKOVICH, G., KOLOKOLOV, I. & LEBEDEV, V. 1995 Normal and anomalous scaling of the fourth-order correlation function of a randomly advected passive scalar. *Phys. Rev. E* **52**, 4924–4941.
- CHEVILLARD, L., ROUX, S. G., LÉVÊQUE, E., MORDANT, N., PINTON, J.-F. & ARNÉODO, A. 2005 Intermittency of velocity time increments in turbulence. *Phys. Rev. Lett.* **95**, 064501.
- CORRSIN, STANLEY 1951 On the Spectrum of Isotropic Temperature Fluctuations in an Isotropic Turbulence. *J. Appl. Phys.* **22** (4), 469–473.
- CORRSIN, S 1959 Progress report on some turbulent diffusion research. *Advances in Geophysics* **6**, 161–164.
- CORRSIN, S. 1962 Theories of turbulent dispersion. In *Mécanique de la Turbulence* (ed. A. Favre), *Colloques Internationaux du CNRS* 108, pp. 27–52. Paris: Éditions du Centre National de la Recherche Scientifique, proceedings of the International Colloquium on Turbulence at the University of Aix-Marseille, 28 August-2 September, 1961.

- DE POLSI, GONZALO, BALOG, IVAN, TISSIER, MATTHIEU & WSCHEBOR, NICOLÁS 2020 Precision calculation of critical exponents in the  $o(n)$  universality classes with the nonperturbative renormalization group. *Phys. Rev. E* **101**, 042113.
- DE POLSI, GONZALO, HERNÁNDEZ-CHIFFLET, GUZMÁN & WSCHEBOR, NICOLÁS 2021 Precision calculation of universal amplitude ratios in  $o(n)$  universality classes: Derivative expansion results at order  $O(\partial^4)$ . *Phys. Rev. E* **104**, 064101.
- DEBUE, PAUL, KUZZAY, DENIS, SAW, EWE-WEI, DAVIAUD, FRANÇOIS, DUBRULLE, BÉRENGÈRE, CANET, LÉONIE, ROSSETTO, VINCENT & WSCHEBOR, NICOLÁS 2018 Experimental test of the crossover between the inertial and the dissipative range in a turbulent swirling flow. *Phys. Rev. Fluids* **3**, 024602.
- DEDOMINICIS, C. & MARTIN, P. C. 1979 Energy spectra of certain randomly-stirred fluids. *Phys. Rev. A* **19**, 419–422.
- DELAMOTTE, BERTRAND 2012 An Introduction to the nonperturbative renormalization group. *Lect. Notes Phys.* **852**, 49–132, arXiv: [cond-mat/0702365](https://arxiv.org/abs/cond-mat/0702365).
- DE DOMINICIS, C. 1976 Techniques de renormalisation de la théorie des champs et dynamique des phénomènes critiques. *J. Phys. (Paris) Colloq.* **37** (C1), 247–253.
- DRIVAS, THEODORE D., JOHNSON, PERRY L., LALESCU, CRISTIAN C. & WILCZEK, MICHAEL 2017 Large-scale sweeping of small-scale eddies in turbulence: A filtering approach. *Phys. Rev. Fluids* **2**, 104603.
- DUBRULLE, BÉRENGÈRE 2019 Beyond kolmogorov cascades. *Journal of Fluid Mechanics* **867**, P1.
- DUCLUT, CHARLIE & DELAMOTTE, BERTRAND 2017 Frequency regulators for the nonperturbative renormalization group: A general study and the model a as a benchmark. *Phys. Rev. E* **95**, 012107.
- DUPUIS, N., CANET, L., EICHHORN, A., METZNER, W., PAWLOWSKI, J.M., TISSIER, M. & WSCHEBOR, N. 2021 The nonperturbative functional renormalization group and its applications. *Physics Reports* **910**, 1–114, the nonperturbative functional renormalization group and its applications.
- ELLWANGER, U. 1994 Flow equations and BRS invariance for Yang-Mills theories. *Phys. Lett. B* **335**, 364.
- FALKOVICH, G., FOUXON, I. & OZ, Y. 2010 New relations for correlation functions in Navier–Stokes turbulence. *J. Fluid Mech.* **644**, 465–472.
- FALKOVICH, G., GAWĘDZKI, K. & VERGASSOLA, M. 2001 Particles and fields in fluid turbulence. *Rev. Mod. Phys.* **73** (4), 913–975, arXiv: [cond-mat/0105199](https://arxiv.org/abs/cond-mat/0105199).
- FAVIER, B., GODEFERD, F. S. & CAMBON, C. 2010 On space and time correlations of isotropic and rotating turbulence. *Physics of Fluids* **22** (1), 015101.
- FEDORENKO, ANDREI A, DOUSSAL, PIERRE LE & WIESE, KAY JÖRG 2013 Functional Renormalization Group approach to decaying turbulence. *J. Stat. Mech.: Theor. and Exp.* **2013** (04), P04014.
- FORSTER, DIETER, NELSON, DAVID R. & STEPHEN, MICHAEL J. 1977 Large-distance and long-time properties of a randomly stirred fluid. *Phys. Rev. A* **16** (2), 732–749.
- FOURNIER, J. D. & FRISCH, U. 1983 Remarks on the renormalization group in statistical fluid dynamics. *Phys. Rev. A* **28**, 1000–1002.
- FRISCH, U. 1995 *Turbulence: the legacy of A. N. Kolmogorov*. Cambridge: Cambridge University Press.
- FRISCH, U & WIRTH, A 1996 Inertial-diffusive range for a passive scalar advected by a white-in-time velocity field. *Europhysics Letters (EPL)* **35** (9), 683–688.
- GAWĘDZKI, KRZYSZTOF & KUPIAINEN, ANTTI 1995 Anomalous Scaling of the Passive Scalar. *Phys. Rev. Lett.* **75**, 3834–3837, arXiv: [chao-dyn/9506010](https://arxiv.org/abs/chao-dyn/9506010).
- GORBUNOVA, ANASTASIIA 2021 Fonctions de corrélation en turbulence : simulations numériques et comparaison avec l’analyse par le groupe de renormalisation fonctionnel. PhD thesis, thèse de doctorat dirigée par Rossetto-Giaccherino, Vincent Balarac, Guillaume et Canet, Léonie Physique théorique Université Grenoble Alpes 2021.
- GORBUNOVA, ANASTASIIA, BALARAC, GUILLAUME, BOURGOIN, MICKAËL, CANET, LÉONIE, MORDANT, NICOLAS & ROSSETTO, VINCENT 2020 Analysis of the dissipative range of the energy spectrum in grid turbulence and in direct numerical simulations. *Phys. Rev. Fluids* **5**, 044604.
- GORBUNOVA, A., BALARAC, G., CANET, L., EYINK, G. & ROSSETTO, V. 2021a Spatio-temporal correlations in three-dimensional homogeneous and isotropic turbulence. *Physics of Fluids* **33** (4), 045114, arXiv: <https://doi.org/10.1063/5.0046677>.
- GORBUNOVA, ANASTASIIA, PAGANI, CARLO, BALARAC, GUILLAUME, CANET, LÉONIE & ROSSETTO, VINCENT 2021b Eulerian spatiotemporal correlations in passive scalar turbulence. *Phys. Rev. Fluids* **6**, 124606.
- GOTOH, TOSHIYUKI, RO GALLO, ROBERT S., HERRING, JACKSON R. & KRAICHNAN, ROBERT H. 1993 Lagrangian velocity correlations in homogeneous isotropic turbulence. *Physics of Fluids A* **5** (11), 2846–2864.
- HE, GUO-WEI, WANG, MENG & LELE, SANJIVA K. 2004 On the computation of space-time correlations by large-eddy simulation. *Physics of Fluids* **16** (11), 3859–3867.

- HE, GUO-WEI & ZHANG, JIN-BAI 2006 Elliptic model for space-time correlations in turbulent shear flows. *Phys. Rev. E* **73**, 055303.
- HE, XIAOZHOU & TONG, PENG 2011 Kraichnan's random sweeping hypothesis in homogeneous turbulent convection. *Phys. Rev. E* **83**, 037302.
- HEISENBERG, W. 1948 Zur statistischen theorie der turbulenz. *Zeitschrift für Physik* **124** (7), 628–657.
- JANSSEN, HANS-KARL 1976 On a lagrangean for classical field dynamics and Renormalization Group calculations of dynamical critical properties. *Z. Phys. B* **23**, 377–380.
- KANEDA, YUKIO 1993 Lagrangian and Eulerian time correlations in turbulence. *Physics of Fluids A: Fluid Dynamics* **5** (11), 2835–2845.
- KANEDA, YUKIO, ISHIHARA, TAKASHI & GOTOH, KOJI 1999 Taylor expansions in powers of time of lagrangian and eulerian two-point two-time velocity correlations in turbulence. *Physics of Fluids* **11** (8), 2154–2166.
- KARDAR, MEHRAN, PARISI, GIORGIO & ZHANG, YI-CHENG 1986 Dynamic scaling of growing interfaces. *Phys. Rev. Lett.* **56** (9), 889–892.
- VON KÁRMÁN, THEODORE & HOWARTH, LESLIE 1938 On the statistical theory of isotropic turbulence. *Proc. R. Soc. Lond. A* **164** (917), 192–215, arXiv: <http://rspa.royalsocietypublishing.org/content/164/917/192.full.pdf>.
- KHURSHID, SUALEH, DONZIS, DIEGO A. & SREENIVASAN, K. R. 2018 Energy spectrum in the dissipation range. *Phys. Rev. Fluids* **3**, 082601.
- KLOSS, THOMAS, CANET, LÉONIE & WSCHBOR, NICOLÁS 2012 Nonperturbative Renormalization Group for the stationary Kardar-Parisi-Zhang equation: Scaling functions and amplitude ratios in 1+1, 2+1, and 3+1 dimensions. *Phys. Rev. E* **86**, 051124.
- KOPIETZ, PETER, BARTOSCH, LORENZ & SCHÜTZ, FLORIAN 2010 *Introduction to the Functional Renormalization Group, Lecture Notes in Physics*, vol. 798. Berlin: Springer.
- KRAICHNAN, R. H. 1964 Kolmogorov's hypotheses and eulerian turbulence theory. *Physics of Fluids* **7** (11), 1723.
- KRAICHNAN, ROBERT H. 1968 Small-Scale Structure of a Scalar Field Convected by Turbulence. *Phys. Fluids* **11** (5), 945.
- KRAICHNAN, ROBERT H. 1994 Anomalous scaling of a randomly advected passive scalar. *Phys. Rev. Lett.* **72**, 1016–1019.
- KUPIAINEN, A. & MURATORE-GINANNESCHI, P. 2007 Scaling, renormalization and statistical conservation laws in the Kraichnan model of turbulent advection. *J. Statist. Phys.* **126**, 669, arXiv: [nlin/0603031](https://arxiv.org/abs/nlin/0603031).
- LESIEUR, M. 2008 *Turbulence in Fluids*, 4th edn. Springer.
- LÉVÊQUE, E., CHEVILLARD, L., PINTON, J.-F., ROUX, S., ARNÉODO, A. & MORDANT, N. 2007 Lagrangian intermittencies in dynamic and static turbulent velocity fields from direct numerical simulations. *Journal of Turbulence* **8**, N3.
- L'VOV, VICTOR & PROCACCIA, ITAMAR 1995 Exact resummations in the theory of hydrodynamic turbulence. i. the ball of locality and normal scaling. *Phys. Rev. E* **52**, 3840–3857.
- L'VOV, VICTOR S., PODIVILOV, EVGENII & PROCACCIA, ITAMAR 1997 Temporal multiscaling in hydrodynamic turbulence. *Phys. Rev. E* **55**, 7030–7035.
- MARTIN, P. C., SIGGIA, E. D. & ROSE, H. A. 1973 Statistical dynamics of classical systems. *Phys. Rev. A* **8**, 423–437.
- MAZZINO, A. 1997 Effective correlation times in turbulent scalar transport. *Phys. Rev. E* **56**, 5500–5510.
- MCCOMB, W. D. & YOFFE, S. R. 2017 A formal derivation of the local energy transfer (LET) theory of homogeneous turbulence\*. *Journal of Physics A: Mathematical and Theoretical* **50** (37), 375501.
- MC MULLEN, RYAN M., KRYGIER, MICHAEL C., TORCZYNSKI, JOHN R. & GALLIS, MICHAEL A. 2022 Navier-stokes equations do not describe the smallest scales of turbulence in gases. *Phys. Rev. Lett.* **128**, 114501.
- MEJÍA-MONASTERIO, CARLOS & MURATORE-GINANNESCHI, PAOLO 2012 Nonperturbative Renormalization Group study of the stochastic Navier-Stokes equation. *Phys. Rev. E* **86**, 016315.
- MITRA, DHRUBADITYA & PANDIT, RAHUL 2005 Dynamics of Passive-Scalar Turbulence. *Phys. Rev. Lett.* **95** (14), 144501.
- MONIN, A. S. & YAGLOM, A. M. 2007 *Statistical Fluid Mechanics: Mechanics of turbulence*. Cambridge, Massachusetts and London, England: MIT Press.
- MORRIS, T. R. 1994 The exact Renormalisation Group and approximate solutions. *Int. J. Mod. Phys. A* **9**, 2411.

- NELKIN, MARK & TABOR, M. 1990 Time correlations and random sweeping in isotropic turbulence. *Phys. Fluids A* **2** (1), 81–83.
- OBUKHOV, A M 1949 Structure of Temperature Field in Turbulent Flow. *Izv. Geogr. Geophys.* **13** (1), 58–69.
- O’GORMAN, P. A. & PULLIN, D. I. 2004 On modal time correlations of turbulent velocity and scalar fields. *J. of Turbulence* **5**, N35.
- ORSZAG, STEVEN A. & PATTERSON, G. S. 1972 Numerical simulation of three-dimensional homogeneous isotropic turbulence. *Phys. Rev. Lett.* **28**, 76–79.
- PAGANI, C. 2015 Functional Renormalization Group approach to the Kraichnan model. *Phys. Rev.* **E92** (3), 033016, [Addendum: *Phys. Rev. E* **97**, 4,049902(2018)], arXiv: 1505.01293.
- PAGANI, CARLO & CANET, LÉONIE 2021 Spatio-temporal correlation functions in scalar turbulence from functional renormalization group. *Physics of Fluids* **33** (6), 065109.
- POLCHINSKI, JOSEPH 1984 Renormalization and effective lagrangians. *Nuclear Physics B* **231** (2), 269 – 295.
- POULAIN, C., MAZELLIER, N., CHEVILLARD, L., GAGNE, Y. & BAUDET, C. 2006 Dynamics of spatial fourier modes in turbulence - sweeping effect, long-time correlations and temporal intermittency. *Eur. Phys. J. B* **53** (2), 219–224.
- SANADA, T. & SHANMUGASUNDARAM, V. 1992 Random sweeping effect in isotropic numerical turbulence. *Physics of Fluids A: Fluid Dynamics* **4** (6), 1245–1250.
- SANKAR RAY, SAMRIDDI, MITRA, DHRUBADITYA & PANDIT, RAHUL 2008 The universality of dynamic multiscaling in homogeneous, isotropic Navier–Stokes and passive-scalar turbulence. *New J. Phys.* **10** (3), 033003.
- SHRAIMAN, BORIS I. & SIGGIA, ERIC D. 2000 Scalar turbulence. *Nature* **405** (6787), 639–646.
- SMITH, L.M. & WOODRUFF, S.L. 1998 Renormalization Group analysis of turbulence. *Annu. Rev. Fluid Mech.* **30**, 275.
- SREENIVASAN, KATEPALLI R. 2019 Turbulent mixing: A perspective. *PNAS* **116** (37), 18175–18183.
- SYMANZIK, K. 1970 Small distance behaviour in field theory and power counting. *Communications in Mathematical Physics* **18**.
- TARPIN, MALO 2018 Non-perturbative renormalisation group approach to some out of equilibrium systems : diffusive epidemic process and fully developed turbulence. PhD thesis, thèse de doctorat dirigée par Canet, Léonie Physique théorique Université Grenoble Alpes (ComUE) 2018.
- TARPIN, MALO, CANET, LÉONIE, PAGANI, CARLO & WSCHBOR, NICOLÁS 2019 Stationary, isotropic and homogeneous two-dimensional turbulence: a first non-perturbative renormalization group approach. *Journal of Physics A: Mathematical and Theoretical* **52** (8), 085501.
- TARPIN, MALO, CANET, LÉONIE & WSCHBOR, NICOLÁS 2018 Breaking of scale invariance in the time dependence of correlation functions in isotropic and homogeneous turbulence. *Physics of Fluids* **30** (5), 055102, arXiv: <https://doi.org/10.1063/1.5020022>.
- TAYLOR, GEOFFREY I 1922 Diffusion by continuous movements. *Proceedings of the London Mathematical Society* **2** (1), 196–212.
- TENNEKES, H. 1975 Eulerian and lagrangian time microscales in isotropic turbulence. *J. Fluid Mech.* **67**, 561–567.
- TOMASSINI, PAOLO 1997 An exact renormalization group analysis of 3d well developed turbulence. *Physics Letters B* **411** (1), 117 – 126.
- VERMA, MAHENDRA K. 2019 *Energy Transfers in Fluid Flows: Multiscale and Spectral Perspectives*. Cambridge University Press.
- WALLACE, JAMES M. 2014 Space-time correlations in turbulent flow: A review. *Theoretical and Applied Mechanics Letters* **4** (2), 022003.
- WETTERICH, CHRISTOF 1993 Exact evolution equation for the effective potential. *Phys. Lett. B* **301** (1), 90 – 94.
- WIESE, KAY JÖRG 1998 On the perturbation expansion of the KPZ equation. *J. Stat. Phys.* **93** (1-2), 143–154.
- WILCZEK, M. & NARITA, Y. 2012 Wave-number–frequency spectrum for turbulence from a random sweeping hypothesis with mean flow. *Phys. Rev. E* **86**, 066308.
- WILSON, K. G. & KOGUT, J. 1974 The Renormalization Group and the  $\epsilon$ -expansion. *Phys. Rep. C* **12**, 75.
- YAGLOM, A. M. 1949 Über die lokale Struktur des Temperaturfeldes in einer turbulenten Strömung. *Dokl. Akad. Nauk SSSR, n. Ser.* **69**, 743–746.
- YAKHOT, VICTOR, ORSZAG, STEVEN A. & SHE, ZHEN-SU 1989 Space-time correlations in turbulence: Kinematical versus dynamical effects. *Physics of Fluids A* **1** (2), 184–186.
- YEUNG, P. K. & SAWFORD, BRIAN L. 2002 Random-sweeping hypothesis for passive scalars in isotropic turbulence. *J. Fluid Mech.* **459**, 129–138.

- ZHAO, XIN & HE, GUO-WEI 2009 Space-time correlations of fluctuating velocities in turbulent shear flows. *Phys. Rev. E* **79**, 046316.
- ZHOU, YE 2010 Renormalization Group theory for fluid and plasma turbulence. *Phys. Rep.* **488** (1), 1 – 49.
- ZHOU, YE 2021 Turbulence theories and statistical closure approaches. *Physics Reports* **935**, 1–117, turbulence theories and statistical closure approaches.